Institut de Neuropatologia
Hospital Universitari de Bellvitge

Departament de Patologia i Terapèutica Experimental
Universitat de Barcelona

Vías de señalización en enfermedades priónicas

Agustín Rodríguez Fernández
2007

5- Resultados

5.1- *Metabotropic glutamate receptor/phospholipase C pathway: a vulnerable target to Creutzfeldt-Jakob disease in the cerebral cortex.*

A. Rodríguez, M. Freixes, E. Dalfó, M. Martín, B. Puig and I. Ferrer

Neuroscience 131 (2005) 825-832

El glutamato es el principal neurotransmisor en la corteza cerebral. Se ha sugerido que alteraciones en la transmisión glutamatérigica tienen un papel central en algunas enfermedades neurodegenerativas. Los mGluRs están acoplados a señales de transducción intracelular vía proteínas G. El grupo I de los mGluRs está acoplado positivamente a la PLCβ_1. La ECJ es una encefalopatía espongiforme transmisible humana asociada a una disfunción en la glicoproteína de membrana PrP que se convierte en una isoforma anormal, con una estructura predominante de hoja-β, que es patogénica y parcialmente resistente a la digestión por proteasas. Las proteínas asociadas a la transducción de señales del grupo I de los mGluRs han sido examinadas en la corteza frontal (área 8) de 12 casos con ECJ y cuatro controles por medio de electroforesis y WB de homogeneizados totales. Los análisis densitométricos de las bandas demuestran niveles de expresión disminuidos de PLCβ_1 y PLCγ, una fosfolipasa no relacionada con la señalización glutamatérgica que es sustrato de una tirosina kinasa, en los casos con ECJ comparados con controles. La nPKCδ también se encuentra disminuída significativamente en los casos ECJ. No se han encontrado modificaciones significativas en los niveles de expresión de mGluR$_1$ y cPKCα. No hay modificaciones en la solubilidad de PLCβ_1, en fracciones solubles en PBS, desoxicolato y SDS en ECJ comparado con controles. Finalmente, no hay interacciones entre la PLCβ_1 y la PrP, tal y como revelan los ensayos de inmunoprecipitación hechos en controles y ECJ. Estos resultados muestran, en primer lugar, niveles reducidos de fosfolipasas, particularmente de PLCβ_1 que puede interferir en la señalización del grupo I de los mGluRs en la corteza frontal en ECJ. Estas anormalidades no son el resultado de una solubilidad anormal o de interacciones con la PrP. La participación selectiva de los mGluRs de grupo I puede tener efectos funcionales en el procesamiento y la modulación de la transmisión glutamatérgica en ECJ.

Neuroscience 131 (2005) 825–832

METABOTROPIC GLUTAMATE RECEPTOR/PHOSPHOLIPASE C PATHWAY: A VULNERABLE TARGET TO CREUTZFELDT-JAKOB DISEASE IN THE CEREBRAL CORTEX

A. RODRÍGUEZ,[a] M. FREIXES,[a] E. DALFÓ,[a] M. MARTÍN,[c] B. PUIG[a] AND I. FERRER[a,b]*

[a]*Institut de Neuropatologia, Servei Anatomia Patològica, IDIBELL-Hospital Universitari de Bellvitge, c/ Feixa llarga sn, 08907 Hospitalet de Llobregat, Spain*

[b]*Unitat de Neuropatología Experimental, Universitat de Barcelona, 08907 Hospitalet de Llobregat, Spain*

[c]*Departamento de Química Inorgánica, Orgánica y Bioquímica, Facultad de Químicas, Centro Regional de Investigaciones Biomédicas, Universidad de Castilla-La Mancha, Ciudad Real, Spain*

Abstract—Glutamate is the main excitatory neurotransmitter in the cerebral cortex. Altered glutamatergic transmission has been suggested as having a central role in many neurodegenerative diseases. Metabotropic glutamate receptors (mGluRs) are coupled to intracellular signal transduction via G proteins, and they mediate slower responses than ionotropic glutamate receptors. Group I mGluRs are positively coupled to phospholipase C β1 ($PLC\beta_1$). Creutzfeldt-Jakob disease (CJD) is a human transmissible spongiform encephalopathy associated with a dysfunction in the membrane glycoprotein PrP which is converted into an abnormal isoform, with a predominant β-sheet structure, that is pathogenic and partially resistant to protease digestion. Proteins associated with the signal transduction of group I mGluRs were examined in the frontal cortex (area 8) of 12 cases with sCJD and four age-matched controls, by means of gel electrophoresis and Western blotting of total homogenates. Densitometric analysis of the bands demonstrated decreased expression levels of $PLC\beta_1$ and PLCγ, a non-related phospholipase which is a substrate of tyrosine kinase, in CJD cases when compared with controls. Novel protein kinase C δ (nPKCδ) has also been found to be significantly decreased in CJD cases. However, no modifications in $mGluR_1$ cPKCα expression levels are found in CJD when compared with controls. No modifications in $PLC\beta_1$ solubility in PBS-, deoxycholate- and sodium dodecylsulphate-soluble fractions have been observed in CJD when compared with controls. Finally, no interactions between PLCβ1 and PrP, as revealed by immunoprecipitation assays, have been found in CJD and controls. The present results show, for the first time, reduced expression levels of phospholipases, particularly $PLC\beta_1$, which may interfere with group I mGluR signaling in the cerebral cortex in CJD. These abnormalities are not the result of abnormal PLC solubility or interactions with PrP. Selective involvement of group I mGluRs may have functional effects on glutamatergic transmission modulation and processing in CJD. © 2005 IBRO. Published by Elsevier Ltd. All rights reserved.

Key words: metabotropic glutamate receptors, phospholipase C, protein kinase C, Creutzfeldt-Jakob disease, prion diseases.

*Correspondence to: I. Ferrer, Institut Neuropatologia, Servei Anatomia Patològica, IDIBELL-Hospital Universitari de Bellvitge, c/ Feixa llarga sn, 08907 Hospitalet de Llobregat, Spain.
E-mail address: 8082ifa@comb.es (I. Ferrer).

Abbreviations: AD, Alzheimer's disease; BSE, bovine spongiform encephalopathy; CJD, Creutzfeldt-Jakob's disease; DAG, diacylglycerol; DLBD, diffuse Lewy body disease; ER, endoplasmic reticulum; GluR, glutamate receptor; IP_3, inositol 1,4,5-trisphosphate; mGluR, metabotropic glutamate receptor; PKC, protein kinase C; PLC, phospholipase C; PrP^c, cellular prion protein; sCJD, sporadic Creutzfeldt-Jakob's disease; SDS-PAGE, sodium dodecylsulphate–polyacrylamide gel electrophoresis; TSE, transmissible spongiform encephalopathy.

Glutamate is the main excitatory neurotransmitter in the CNS whose actions are mediated by glutamate receptors (GluRs) in target cells. GluRs are classified as ionotropic and metabotropic receptors. Ionotropic GluRs are ligand-gated cation channels that mediate fast excitatory neurotransmission, whereas metabotropic GluRs (mGluRs) are coupled to intracellular transduction via G-proteins, and mediate slower responses (Conn and Pin, 1997; Michaelis, 1998; Ozawa et al., 1998).

mGluRs are divided into eight subtypes, which are categorized into three groups according to signal transduction properties. Group I, including $mGluR_1$ and $mGluR_5$, are positively coupled to phospholipase C (PLC). Three structural groups constitute the PLC system: β, γ and δ. $PLC\beta_1$, which is the most highly expressed of PLCβ isoforms in the brain, is activated by the G_q family of G-proteins, whereas non-related PLCγ is a substrate for tyrosine kinase (Hamm, 1998; Rebecchi and Pentyala, 2000; Rhee, 2001). Activation of post-synaptic $mGluR_1$ and $mGluR_5$ promotes $PLC\beta_1$ activation, which hydrolyzes a minor membrane phospholipid, phosphatidylinositol 4,5-bisphosphate, to produce a pair of intracellular messengers, diacylglycerol (DAG) and inositol 1,4,5-trisphosphate (IP_3). The interaction between IP_3 and a protein forming a calcium channel in the membrane of the endoplasmic reticulum (ER) causes a rapid efflux of Ca^{2+} accumulated in ER and an increase of free Ca^{2+} in the cytosol. DAG remaining in the plasma membrane, together with Ca^{2+}, activates protein kinase C (PKC), which regulates gene expression through phosphorylation of many target proteins, including several kinases (Hammond, 2003; Phillis and O'Regan, 2004). Group I mGluRs are implicated in synaptic plasticity and memory processing (Conn and Pin, 1997; Pin and Acher, 2002).

Prion diseases, also named transmissible spongiform encephalopathies (TSEs), are a group of neurodegenerative disorders characterized by neuronal loss, astrocytic gliosis, microgliosis, spongiform change, and abnormal

0306-4522/05$30.00+0.00
doi:10.1016/j.neuroscience.2004.12.023

prion protein production and deposition (DeArmond et al., 2003; Knight and Will, 2004). TSEs include scrapie and bovine spongiform encephalopathy (BSE) in animals, and Creutzfeldt-Jakob's disease (CJD), fatal familial insomnia, kuru and Gerstmann-Straüssler-Scheinker disease in humans (Prusiner, 1997; Aguzzi, 2003; Budka et al., 2003; DeArmond et al., 2003; Ghetti et al., 2003; Gambetti et al., 2003). PrP^{c} (cellular prion protein) is an anchored cell membrane glycoprotein related to copper metabolism and signal transduction (Prusiner, 1997; Collinge, 2001). PrP^{c} is expressed in several tissues but is particularly enriched in the CNS. According to the "protein-only" hypothesis, TSEs are caused by the conversion of PrP^{c} into an abnormal isoform, PrP^{sc}, PRP^{CJD} or PRP^{BSE} (for scrapie, CJD or BSE prion protein, respectively; Prusiner, 1997; Collinge, 2001; Aguzzi et al., 2001). This process involves a conformational transformation of an α-helical structure to a β-sheet structure. PrP^{sc}, PRP^{CJD} and PRP^{BSE}, which are also named PrP^{res} because of their resistance to proteinase K digestion, are able to recruit PrP^{c}, resulting in an autocatalytic propagation in the pathogenic conformation (Prusiner, 1997; Collinge, 2001; Aguzzi et al., 2001; Bratosiewicz-Wasik et al., 2004).

CJD occurs as a sporadic, infectious or inherited disease. Sporadic CJD (sCJD) is the most frequent type of CJD, representing about 85% of total CJD cases. A common polymorphism at codon 129 of *PRNP* (Prion protein gene) has important effects on susceptibility to the disease and on the presence of particular clinical features (Budka et al., 2003). According to their codon 129 genotype and PrP type (1 and 2), six forms of sCJD have been established (Parchi et al., 1999).

Several mechanisms are probably implicated in the degeneration of neurons in CJD (Giese and Kretzschmar, 2001). Among them, those related with synaptic transmission appear to be crucial in the pathogenesis of CJD. Decreased numbers of dendritic spines and reduced dendritic branches have been shown in pyramidal cortical neurons and in Purkinje cells (Landis et al., 1981; Ferrer et al., 1981, 1990). Moreover, reduced expression of several proteins involved in exocytosis and neurotransmission has been shown in the cerebral cortex and cerebellum in CJD (Ferrer et al., 1999, 2000). These findings demonstrate that pre- and post-synaptic structures are vulnerable to CJD. In addition, excitotoxic mechanisms of neurodegeneration have been postulated in TSEs (Scallet and Ye, 1997). Yet studies on neurotransmitters and their receptors are scanty in CJD. Previous immunohistochemical observations have shown abnormalities in the expression of ionotropic glutamate and GABA receptor subunits in the cerebral cortex and cerebellum in CJD (Ferrer and Puig, 2003). Interestingly, these changes were not merely the result of synaptic loss, as some subunits were overexpressed, thus indicating more subtle responses of neurotransmitter pathways to the effects of CJD.

In line with former studies, this work examines by gel electrophoresis and Western blot the expression levels of proteins related to group I mGluRs transduction pathways in the frontal cortex of 12 cases with sCJD. Proteins include $mGluR_1$, $PLC\beta_1$, cPKCα and nPKCδ. Control of protein degradation has been tested for every protein by processing the same material in conditions mimicking increased postmortem delay. The present results have revealed reduced $PLC\beta_1$ and nPKCδ expression levels, whereas $mGluR_1$ and cPKCα levels were similar in CJD cases and controls. These alterations are not related to changes in the solubility of $PLC\beta_1$, and they are not likely associated with abnormal interactions of $PLC\beta_1$ and PrP. Rather, the present findings support PLCs (covering PLCβ1 and PLCγ) as vulnerable targets to CJD.

EXPERIMENTAL PROCEDURES

General aspects

The brains of 12 patients with sCJD and three age-matched controls were obtained from 3 to 8 h after death and were immediately prepared for morphological and biochemical studies. The main clinical characteristics are summarized in Table 1. Criteria for the neuropathological, molecular and phenotypic diagnosis of CJD used in the present series are those currently accepted and detailed elsewhere (Parchi et al., 1999; Budka et al., 2003). For biochemical studies, samples of the frontal cortex (area 8) were frozen in liquid nitrogen and stored at −80 °C until use. Neuron loss, spongiform degeneration, astrocytic gliosis and microgliosis involving the cerebral neocortex, striatum and cerebellum, occurred in every case. Synaptic-like PrP^{res} deposits were found in the cerebral cortex and striatum in every case. In addition, PrP^{res} plaques were common in the two VV2 cases (cases 5 and 8).

In addition, samples of the frontal cortex from one control individual were obtained at 3 h postmortem and immediately frozen (time 0), or stored at 4 °C for 3 h, 6 h or 22 h, and then frozen to mimic variable postmortem delay in tissue processing and its effect on protein preservation.

Electrophoresis and Western blotting

For Western blot studies, about 0.1 g of frontal cortex was homogenized in a glass tissue grinder in 10 volumes (w/v) of cold buffer containing PBS, 0.5%, NP-40, 0.5% deoxycholic acid sodium salt, 0.1 mM phenylmethylsufonyl fluoride, 5 μg/ml aprotinin, 10 μg/ml leupeptin, 5 μg/ml pepstatin and 1 mM sodium orthovanadate, pH 7.5 to inhibit endogeneous phosphatases. After centrifugation at 3500×*g* (Eppendorf, Madison, WI, USA) for 5 min, protein concentration of total homogenate was determined with the BCA Protein Assay Kit (Pierce). Thirty micrograms of protein was mixed with loading buffer containing 0.125 M Tris (pH 6.8), 20% glycerol, 10% β-mercaptoethanol, 4% SDS and 0.002% Bromophenol Blue, and heated at 95 °C for 5 min. Sodium dodecylsulphate–polyacrylamide gel electrophoresis (10% SDS-PAGE) was carried out using a mini-protean system (Bio-Rad, Life Science, CA, USA) with molecular weight standards (Bio-Rad). Proteins were then transferred to nitrocellulose membranes using an electrophoretic transfer system (Semi-dry; Bio-Rad). The membranes were washed with TTBS containing 10 mM Tris–HCl pH 7.4, 140 mM NaCl and 0.1% Tween-20. Nonspecific blocking was performed by incubating the membranes in TTBS containing 5% skimmed milk for 20 min. Membranes were incubated with the primary antibodies at 4 °C overnight. The rabbit polyclonal antibodies to $mGluR_1$ (Upstate, CA, USA) were used at a dilution of 1:1000; the rabbit polyclonal anti-$PLC\beta_1$ (Santa Cruz Biotechnology, Santa Cruz, CA, USA) and the rabbit polyclonal anti-PLCγ (Neomarkers) antibodies were used at a dilution of 1:500; the rabbit polyclonal anti-cPKCα and nPKCδ antibodies (Santa Cruz Biotechnology) were used at a dilution of 1:1000. The

Table 1. Main clinical characteristics of CJD and control cases in the present series[a]

Case number	Age	Gender	Codon 129	14-3-3 CSF	EEG	First symptom	Survival, in months	PrP type
CJD1	60	M	MM	+	+	Dementia	3	1
CJD2	60	F	MM	+	+	Dementia	6	1
CJD3	55	M	MM	+	+	Ataxia	3	1
CJD4	74	M	?	+	+	Dementia	5	1
CJD5	66	M	VV	+	rare	Ataxia	4	2
CJD6	53	F	MM	+	+	Dementia	2	1
CJD7	85	F	MV	+	+	Dementia	14	1
CJD8	71	M	VV	+	0	Ataxia	3	2
CJD9	70	F	MM	+	+	Dementia	3	1
CJD10	59	M	MM	?	+	Dementia	8	1
CJD11	54	M	MM	+	?	Dementia	months	1
CJD12	56	M	MM	?	+	Dementia	5	1
Control1	62	M						
Control2	72	F						
Control3	73	M						

[a] EEG, typical generalized triphasic pseudoperiodic complexes; F, female; M, male; M, methionine; PrP^{res} type 1, lower band of glycosylated PrP^{res} of 21 kDa; PrP type 2, lower band of glycosylated PrP^{res} of 19 kDa. V, valine.

monoclonal anti-PrP 3F4 antibody (Dako, Carpenteria, CA, USA) was used at a dilution of 1:500. After rinsing, the membranes were incubated with the corresponding anti-rabbit or anti-mouse secondary antibodies (Dako) at a dilution of 1:1000 for 1 h at room temperature. The membranes were then washed and developed with the chemiluminescence ECL system (Amersham, Pharmacia, Bucks, UK) followed by exposure of the membranes to autoradiographic films at 4 °C. The monoclonal anti-β-actin antibody (Sigma, St. Louis, MO, USA), at a dilution of 1:5000, was used as a control of protein loading.

Protein solubility

Frozen samples of the frontal cortex (1 g) were homogenized in a glass homogenizer in 5 ml of ice-cold PBS (sodium phosphate buffer, pH 7.4, plus protease inhibitors) and centrifuged at 5800×*g* at 4 °C for 10 min. The pellet was discarded and the resulting supernatant was ultracentrifuged at 43,000×*g* at 4 °C for 1 h. The supernatant (S2) was kept as the PBS-soluble fraction. The resulting pellet was re-suspended in a solution of PBS, pH 7.4, containing 0.5% sodium deoxycholate, 1% Triton X-100 and 0.1% SDS, and it was then ultracentrifuged at 43,000×*g* at 4 °C for 1 h. The resulting supernatant (S3) was kept as the deoxycholate-soluble fraction. The corresponding pellet was re-suspended in a solution of SDS 2% in PBS and maintained at room temperature for 2 h. Immediately afterward, the samples were centrifuged at 43,000×*g* at 25 °C for 1 h and the resulting supernatant (S4) was the SDS-soluble fraction. Finally, the corresponding pellet was re-suspended in a solution of 5% SDS–urea 8 M and incubated by rotation overnight at room temperature. After centrifugation at 43,000×*g* at 25 °C for 1 h, the supernatant (S5) was kept as the urea-soluble fraction. Equal amounts (20 μl) of each fraction were mixed with reducing sample buffer and processed for 10% SDS-PAGE electrophoresis and Western blot analysis. The membranes were incubated with anti-$PLC\beta_1$ antibodies as previously. The protein bands were visualized with the ECL method.

$PLC\beta_1$ immunoprecipitation

Samples (0.1 g) of the frontal cortex were homogenized in a glass homogenizer in 1.5 ml of ice-cold lysis buffer (PBS, 1 mM sodium orthovanadate, 1 mM sodium fluoride, 10 μg/ml aprotinin and 1 mM phenylmethylsulfonyl fluoride) and centrifuged at 5800×*g* for 10 min at 4 °C. The supernatant S1 was further centrifuged at 43,000×*g* for 1 h at 4 °C to generate the supernatant S2. Protein concentrations were determined using the BCA method with bovine serum albumin as a standard. S2 fractions were diluted to roughly 1 μg/μl total protein with PBS before beginning the immunoprecipitation. Mouse monoclonal anti-$PLC\beta_1$ antibody (Upstate) (5 μg) was added to 1 mg of total protein from S2 fraction, and the mixture was gently rocked at 4 °C overnight. The immunocomplexes were captured by adding 100 μl (50 μl packed beads) of washed Protein G agarose bead slurry (Amersham Pharmacia). The reaction mixture was gently rocked at 4 °C for 2 h and the agarose beads were collected by pulsing (5 s in the microcentrifuge at 14,000×*g*), and then draining off the supernatant. The beads were washed three times with ice-cold PBS and, finally, the agarose beads were re-suspended in Laemmli buffer (25 mM Tris base pH 6.5, 10% glycerol, 6% SDS and Bromophenol Blue) and boiled for 5 min. The beads were collected using a microcentrifuge pulse, and 10% SDS–polyacrylamide gels were electrophoresed and then transferred to nitrocellulose membranes. The blotted membranes were treated with PBS containing 3% skimmed milk for 20 min at room temperature with constant agitation and then incubated with 5 μg/ml of anti-$PLC\beta_1$ (Santa Cruz Biotechnology) at a dilution of 1:100, or with the monoclonal mouse anti-PrP 3F4 antibody (Dako) used at a dilution of 1:500 in PBS containing 3% bovine serum albumin with agitation at 4 °C overnight. The protein bands were visualized using the ECL method.

PrP immunoprecipitation

Samples (0.1 g) of the frontal cortex were homogenized in a glass homogenizer in 1 ml of ice-cold lysis buffer (buffer 1) containing PBS, 50 mM Tris–HCl pH 7.5, 150 mM NaCl, 5 mM EDTA, 0.2% sarkosyl and 1 mM PMSF, and centrifuged at 12,000×*g* for 15 min at 4 °C. One hundred microliters of the supernatant were precleared with 20 μl of protein G-Sepharose beads (Amersham Pharmacia) and gently rocked for 1 h at 4 °C. The beads were previously blocked by rocking for 2 h at 4 °C in a buffer containing PBS with 10% glycerol. Protein concentrations were determined using the BCA method with bovine serum albumin as a standard. The cleaned samples were then mixed with 5 μg of the mouse anti-PrP antibody (Chemicon, Chandlers Ford, UK) and gently rocked overnight at 4 °C. The immunocomplexes were captured by adding 100 μl of washed blocked beads. The reaction mixture was rocked for 2 h at 4 °C and the beads were collected by pulsing in the microcentrifuge at 13,000×*g*. The supernatant was drained off and the beads were washed twice for 10 min each in buffer

containing 0.4% sarkosyl, and then with 50 mM Tris–HCl pH 7.5, 500 mM NaCl, 0.1% NP40 and 0.05% deoxycholate in PBS. After a pulsing centrifugation, the beads were re-suspended in Laemmli buffer containing 50 mM DTT and boiled for 5 min. The beads were collected using a microcentrifuge pulse and then loaded in SDS–polyacrylamide gels. Electrophoresed gels were transferred to nitrocellulose membranes. Blotted membranes were blocked in buffer (25 mM Tris–HCl, pH 7.3, 0.15 m NaCl, 0.1% Tween 20) containing 5% skimmed milk for 1 h at r.t. with constant agitation and then incubated with 1 μg/ml of mouse anti-PrP 3F4 antibody (Dako) used at a dilution of 1:500 containing 2% skimmed milk or with the polyclonal rabbit anti-PLCβ_1 antibody (Santa Cruz Biotechnology) with agitation at 4 °C overnight. Then, the membranes were washed for 1 h and incubated with the anti-mouse IgG (TrueBlot, San Diego, CA, USA) at a dilution of 1:1000 following the instructions of the supplier. This mouse anti-IgG does not detect the SDS-denatured forms of IgG by DTT. The blotted membranes were developed and visualized using the ECL method.

Densitometry and statistical processing of data

Protein expression levels were determined by densitometry of the bands using Total Laboratory v2.01 software. This software detects the bands obtained by Western blot and gives individual values which are dependent on the light quantification of the corresponding band. Measurements are expressed as arbitrary units. The results were normalized for β-actin. The numerical data obtained from CJD and controls were compared and statistically analyzed using STATGRAPHICS plus 5.0 software by ANOVA and the LSD statistical tests. Asterisks indicate the following P values (*) <0.05 (95% confidence level); (**) $P<0.01$ (99% confidence level); and (***) $P<0.001$ (99.9% confidence level: 0.1% risk of calling each pair of means significantly different when the actual difference equals 0).

RESULTS

Western blotting

Control of protein preservation with postmortem delay was tested by freezing a cortical sample obtained at 3 h postmortem at time 0, and at 3 h, 6 h and 22 h. The same amount of protein was loaded on each lane and Western blots to mGluR$_1$, PLCβ_1, PLCγ, cPKCα and nPKCδ were carried out in parallel for the several time-points. No differences in the expression levels of any of these proteins were detected (data not shown). Since the tissue samples in control and CJD cases were obtained between 3 and 8 h after death, possible differences in protein expression levels in the present study are likely not dependent on artifacts related with postmortem delay in tissue processing.

Western blots of frontal cortex homogenates showed no significant differences between CJD and controls in the expression levels of mGluR$_1$, although the expression levels were variable from one case to another in both control and CJD cases. In contrast, PLCβ_1 expression levels were markedly reduced in CJD when compared with age-matched controls ($P<0.01$). This was not restricted to PLCβ_1, as PLCγ was also significantly reduced in CJD ($P<0.001$; Fig. 1).

No significant differences in the expression levels of cPKCα were seen between CJD and control cases, whereas nPKCδ was only slightly reduced in CJD when compared with age-matched controls ($P<0.05$; Fig. 1).

PLCβ_1 and AC1 solubility

Three controls and three CJD cases were used to analyze protein solubility. PLCβ_1 and AC1 were recovered in the cytosolic-, deoxycholate- and SDS-soluble fractions. Both PLCβ_1 and AC1 were insoluble in urea. The patterns of solubility were similar in control and CJD cases (Fig. 2).

PLCβ_1 and PrP immunoprecipitation

Immunoprecipitation with the monoclonal anti-PLCβ1 antibody (Upstate) resulted in PLCβ1-immunoreactive bands, as recognized with the rabbit polyclonal anti-PLCβ_1 antibody (Santa Cruz Biotechnology) in the appropriate lanes. No immunoreactivity was observed in the lane corresponding to beads and antibody without sample. Blotting with anti-PrP antibody disclosed no apparent interactions between PLCβ_1 and PrP in control and CJD cases (Fig. 3A). Similarly, no PrP and PLCβ1 co-immunoprecipitation occurred in PrP immunoprecipitated samples blotted for PLCβ1 (Fig. 3B).

DISCUSSION

The present study has shown reduced expression levels of PLCβ_1 and nPKCδ in the frontal cortex of CJD when compared with age-matched controls. This is accompanied by normal levels of mGluR$_1$ and cPKCα. Alzheimer's disease (AD), tauopathies and α-synucleinopathies were absent in the present series, and no other accompanying neurological disease was observed on the neuropathological examination. Therefore, it can be assumed that the abnormalities observed here are concomitant to the prion disease. These abnormalities are selective to certain proteins, and probably not dependent on mere neuron loss, as could be inferred in case of generalized reduction levels of all the proteins analyzed. It is worth noting that PLCγ levels are also reduced in the cerebral cortex in CJD, thus suggesting that phospholipases are particularly vulnerable targets to CJD.

Studies in AD have demonstrated that G-protein-associated signaling pathways are vulnerable to AD (Yamamoto et al., 1996; Cowburn et al., 2001). The phosphoinositide hydrolysis pathway is altered in AD, as evidenced by impaired agonist and G-protein regulation of PLCβ_1, decreased PLCβ_1 levels, decreased PKC levels and activity, and reduced numbers of receptor sites (Wakabayashi et al., 1999; Bordi and Ugolini, 1999; García-Jimenez et al., 2003). Recent studies have also demonstrated abnormal mGluR expression and signaling in the cerebral cortex in diffuse Lewy body disease (DLBD) or dementia with Lewy bodies (Dalfó et al., 2004). Interestingly, glutamate binding and mGluR$_1$ levels are increased in the pure form of DLBD, which is not associated with AD pathology, when compared with age-matched controls, but not in the common form in which glutamate binding and mGluR$_1$ levels are lower than in controls (Dalfó et al., 2004). Glutamate binding and mGluR$_1$ levels are lower in DLBD common form than in controls (Dalfó et al., 2004).

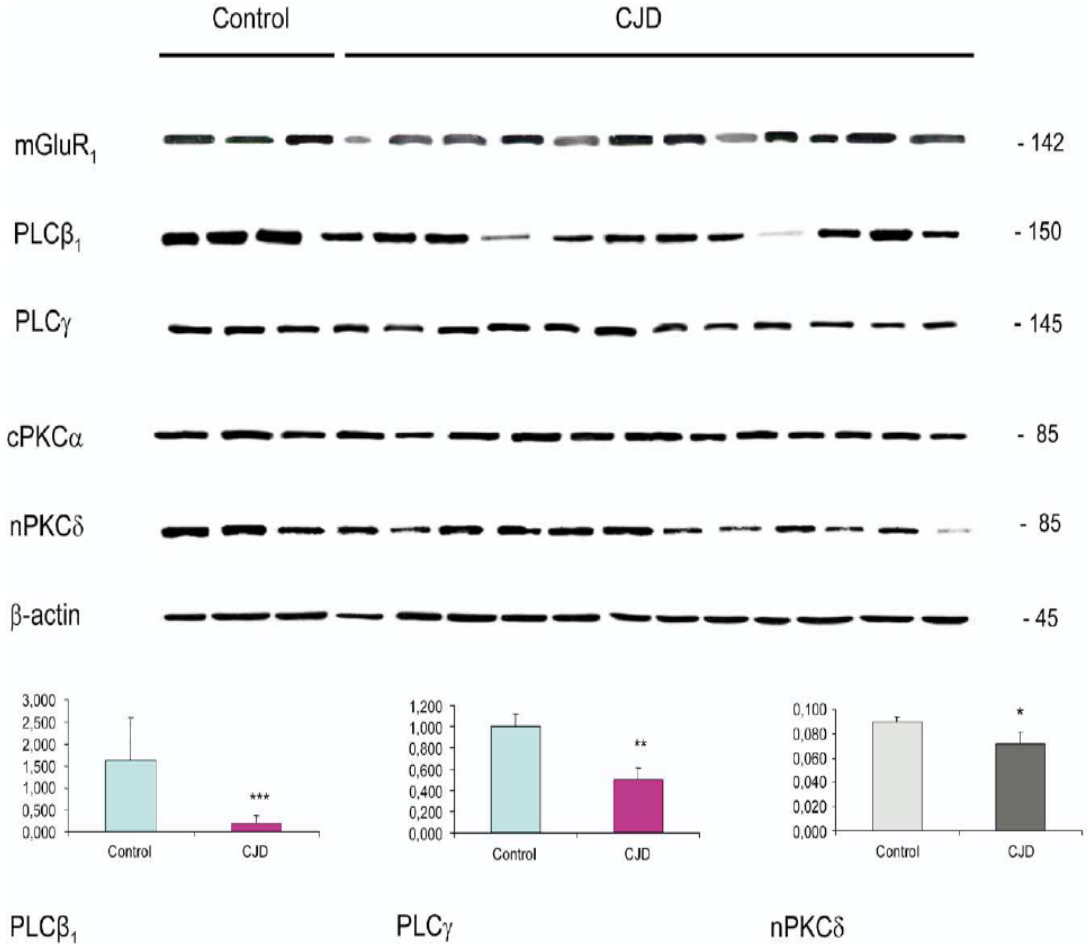

Fig. 1. mGluR1, PLCβ$_1$, PLCγ, cPKCα and nPKCδ expression levels in the frontal cortex in CJD and controls. A significant decrease ($P<0.001$) in PLCβ$_1$ expression is found in the frontal cortex in CJD when compared with age-matched controls. PLCγ was also significantly reduced in CJD ($P<0.01$). No significant differences in the expression of cPKCα are observed. Yet a moderate reduction ($P<0.05$) in nPKCδ levels is found in CJD when compared with controls.

The reasons for these differences are unclear, but it is exciting to note that PLCβ$_1$ solubility is abnormal in DLBD, and that PLCβ$_1$ interactions with abnormal α-synuclein, as revealed with immunoprecipitation assays, are reduced in DLBD when compared with controls (Dalfó et al., 2004). In contrast with DLBD, no differences in PLCβ$_1$ solubility

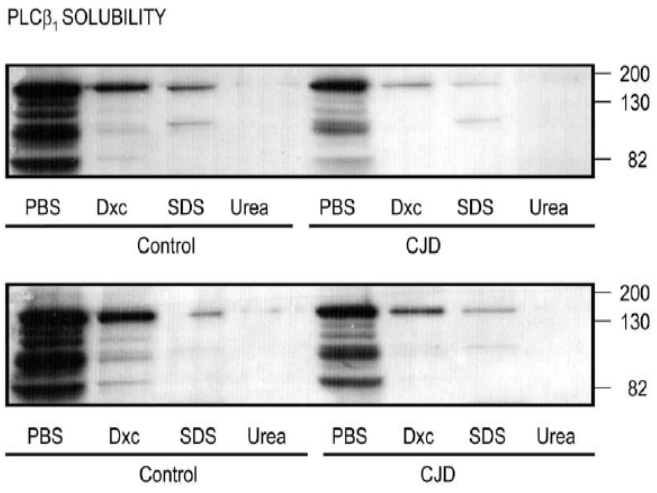

Fig. 2. PLCβ$_1$ solubility in PBS-, deoxycholate (Dxc)-, SDS- and urea-soluble fractions in two representative CJD and two representative control cases. PLCβ$_1$ is mainly recovered in the PBS-soluble fraction, and less in the Dxc- and SDS-soluble fractions in CJD and controls. No PLCβ$_1$ is recovered in the urea-soluble fraction. No differences in PLCβ$_1$ solubility are observed between CJD cases and controls.

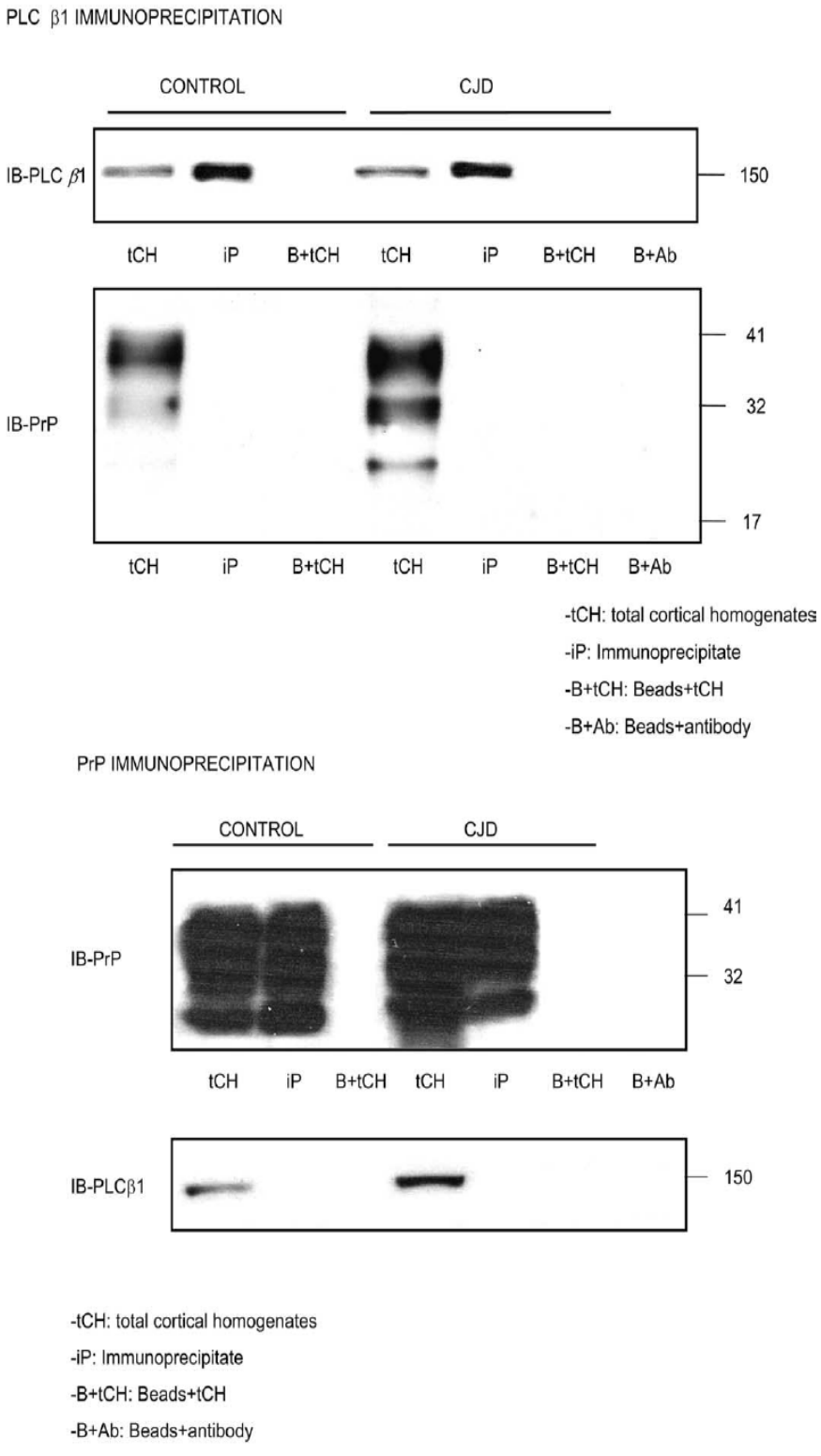

Fig. 3. (A) PLCβ_1 immunoprecipitation (Upstate antibody) immunoblotted with PLCβ_1 (Santa Cruz antibody) shows unique bands at the corresponding molecular weight (150 kDa) in total cortical homogenates (tCH) and immunoprecipiated (iP) lanes in control and CJD cases. The same membranes immunoblotted for PrP (3F4 antibody) show specific bands only in tCH but not in the iP lanes. Therefore, no interactions between PLCβ_1 and PrP are seen in PLCβ_1 immunoprecipitation assays in control and CJD cortical homogenates. Note lack of staining in the lanes containing beads and tCH without immunoprecipitation antibody (B+tCH), and in the lanes containing beads and antibody without cortical homogenate (B+Ab). (B) PrP immunoprecipitation (Chemicon antibody) imunoblotted with PrP (sF4 antibody) shows multiple bands in tCH and iP lanes in control and CJD cases. The same membranes immunoblotted PLCB$_1$ (Santa Cruz antibody) show specific bands (150 kDa) only in tCH but not in the iP lanes. Therefore, no interactions between PrP and PLCβ_1 are seen in PrP immunoprecipitation assays in control and CJD cortical homogenates. Note lack of staining in the lanes containing beads and tCH without immunoprecipitation antibody (B+tCH), and in the lanes containing beads and antibody without cortical homogenate (B+Ab).

have been observed between CJD cases and controls. Moreover, immunoprecipitation assays have shown no apparent interactions of PLCβ_1 and PrP in CJD and controls. Therefore, we can assume that mechanisms involved in PLCβ_1 abnormalities differ in DLBD and CJD.

Although no functional studies have been carried out in this series, several implications may be inferred from the present results. Decreased expression levels of PLCβ_1 may reduce cytoplasmic calcium (Ca^{2+}) concentrations and DAG levels. cPKCα requires DAG and calcium for activation, whereas nPKCδ is sensitive only to DAG (Nishizuka, 1992; Jaken, 1996; Mellor and Parker, 1998; Newton, 2001). Since DAG must be provided for PKCδ phosphorylation (Ogita et al., 1992), it is feasible that the reduced levels of PKCδ in CJD may be related to decreased PLCβ_1 expression levels and the concomitantly low DAG production rate.

Group I mGluRs are implicated in the memory process and long-term potentiation (Petersen et al., 2002; Rodrigues et al., 2002; Conn, 2003; Taccola et al., 2004). Then reduced levels of PLCβ_1 and nPKCδ may deteriorate group I mGluR signaling and function. Finally, previous investigations have suggested that reactive gliosis is associated with modifications in the activation of PLC (Floyd et al., 2004). Therefore, altered signaling pathways here observed may result in variegated deleterious consequences, including abnormal long-term potentiation, impaired memory and learning, and the characteristic neuropathological features of CJD.

Acknowledgments—This study was supported in part by grants SAF 2001-4681-E and EET 2001–3724, and by the EU Network NeuroPrion. We wish to thank T. Yohannan for editorial assistance.

REFERENCES

Aguzzi A (2003) Introduction to prion diseases. In: Neurodegeneration: the molecular pathology of dementia and movement disorders (Dickson D, ed), pp 282–286. Basel: ISN Neuropath Press.

Aguzzi A, Montrasio F, Kaeser PS (2001) Prions: health scare and biological challenge. Nat Rev Mol Cell Biol 2:118–126.

Bordi F, Ugolini A (1999) Group I metabotropic glutamate receptors: implications for brain diseases. Progr Neurobiol 59:55–79.

Bratosiewicz-Wasik J, Wasik TJ, Liberski PP (2004) Molecular approaches to mechanisms of prion diseases. Folia Neuropathol 42:S33–S46.

Budka H, Head MW, Ironside JW, Gambetti P, Parchi P, Zeidler M, Tagliavini F (2003) Sporadic Creutzfeldt-Jakob disease. In: Neurodegeneration: the molecular pathology of dementia and movement disorders (Dickson D, ed), pp 287–297. Basel: ISN Neuropath Press.

Collinge J (2001) Prion diseases of human and animals: their causes and molecular basis. Annu Rev Neurosci 24:519–550.

Conn PJ (2003) Physiological roles and therapeutic potential of metabotropic glutamate receptors. Ann NY Acad Sci 1003:12–21.

Conn P, Pin JP (1997) Pharmacology and functions of metabotropic glutamate receptors. Annu Rev Pharmacol Toxicol 37:205–237.

Cowburn RF, O'Neill C, Bonkale WL, Ohm TG, Fastbom J (2001) Receptor G-protein signaling in Alzheimer's disease. Biochem Soc Symp 67:163–175.

Dalfó E, Albasanz JL, Martín M, Ferrer I (2004) Abnormal metabotropic glutamate receptor expression and signaling in the cerebral cortex in diffuse Lewy body disease is associated with irregular α-synuclein/phospholipase C (PLCβ1) interactions. Brain Pathol 14:388–398.

DeArmond SJ, Kretzschmar HA, Prusiner SB (2003) Prion diseases. In: Greenfield's neuropathology, Vol. II (Graham DI, Lantos PL, eds), pp 273–323. London: Arnold.

Ferrer I, Costa F, Grau Veciana JM (1981) Creutzfeldt-Jakob disease: a Golgi study. Neuropathol Appl Neurobiol 7:237–242.

Ferrer I, Guionnet N, Cruz-Sánchez F, Tuñón T (1990) Neuronal alterations in patients with dementia: a Golgi study on biopsy samples. Neurosci Lett 114:11–16.

Ferrer I, Puig B (2003) GluR2/3, NMDAe1 and GABA$_A$ receptors in Creutzfeldt-Jakob disease. Acta Neuropathol 106:311–318.

Ferrer I, Puig B, Blanco R, Martí E (2000) Prion protein deposition and abnormal synaptic protein expression in the cerebellum in Creutzfeldt-Jakob disease. Neuroscience 97:715–726.

Ferrer I, Rivera R, Blanco R, Marty E (1999) Expression of proteins linked to exocytosis and neurotransmission in patients with Creutzfeldt-Jakob disease. Neurobiol Dis 6:92–100.

Floyd CL, Rzigalinski BA, Sitterding HA, Willoughby KA, Ellies EF (2004) Antagonism of group I mGluRs and PLC attenuates increases in IP-3 and reduces reactive gliosis in starving-injured astrocytes. J Neurotraum 21:205–216.

Gambetti P, Parchi P, Chen SG, Cortelli P, Lugaresi E, Montagna P (2003) Fatal insomnia: familial and sporadic. In: Neurodegeneration: the molecular pathology of dementia and movement disorders (Dickson D, ed), pp 326–332. Basel: ISN Neuropath Press.

García-Jimenez A, Fastbom J, Ohm TG, Cowburn RF (2003) G-protein α-subunit levels in the hippocampus and entorhinal cortex of brains staged for Alzheimer's disease neurofibrillary and amyloid pathologies. Neuroreport 14:1523–1527.

Ghetti B, Bugiani O, Tagliavini F, Piccardo P (2003) Gerstmann-Sträussler-Scheinker disease. In: Neurodegeneration: the molecular pathology of dementia and movement disorders (Dickson D, ed), pp 318–325. Basel: ISN Neuropath Press.

Giese A, Kretzschmar HA (2001) Prion-induced neuronal damage: the mechanisms of neuronal destruction in the subacute spongiform encephalopathies. Curr Topics Microbiol Immunol 253:203–217.

Hamm HE (1998) The many faces of G protein signaling. J Biol Chem 273:669–672.

Hammond C (2003) Cellular and molecular neurobiology. In: The metabotropic glutamate receptors, pp 314–326. Amsterdam: Academic Press.

Jaken S (1996) Protein kinase C isozymes and substrates. Curr Opin Cell Biol 8:168–173.

Knight RSG, Will RG (2004) Prion diseases. J Neurol Neurosurg Psychiat 75:S136–S142.

Landis DMD, Williams RS, Masters CL (1981) Golgi and electronmicroscopic studies of spongiform encephalopathies. Neurology 31:538–549.

Mellor H, Parker PJ (1998) The extended protein kinase C superfamily. Biochem J 332:281–292.

Michaelis EK (1998) Molecular biology of glutamate receptors in the central nervous system and their role in excitoxicity, oxidative stress and aging. Prog Neurobiol 54:369–415.

Newton AC (2001) Protein kinase C: structural and spatial regulation by phosphorylation, cofactors and macromolecular interactions. Chem Rev 101:2353–2364.

Nishizuka Y (1992) Intracellular signaling by hydrolysis of phospholipids and activation of protein kinase C. Science 258:607–614.

Ogita K, Miyamoto SI, Yamaguchi K, Koide H, Fujisawa N, Kikkawa U, Sahara S, Fukami Y, Nishizuka Y (1992) Isolation and characterization of δ-subspecies of protein kinase C from rat brain. Proc Natl Acad Sci USA 89:1592–1596.

Ozawa S, Kamiya H, Tsuzuki K (1998) Glutamate receptors in the mammalian central nervous system. Prog Neurobiol 54:518–618.

Parchi P, Giese A, Capellari S, Brown P, Schulz-Schaeffer W, Windl O, Zerr I, Budka H, Kopp N, Piccardo P, Poser S, Rojiani A,

Streichemberger N, Julien J, Vital C, Ghetti B, Gambetti P, Kretzschmar H (1999) Classification of sporadic Creutzfeldt-Jakob disease based on molecular and phenotypic analysis of 300 subjects. Ann Neurol 46:224–233.

Petersen S, Bomme C, Baastrup C, Kemp A, Christoffersen GRJ (2002) Differential effects of mGluR1 and mGluR5 antagonism on spatial learning in rats. Pharmacol Biochem Behav 73:381–389.

Phillis JW, O'Regan MH (2004) A potentially critical role of phospholipases in central nervous system ischemic, traumatic, and neurodegenerative disorders. Brain Res Rev 44:13–47.

Pin JP, Acher F (2002) The metabotropic glutamate receptors: structure, activation, mechanisms and pharmacology. Curr Drug Target CNS Neural Disord 1:297–317.

Prusiner SB (1997) The prion diseases of humans and animals. In: The molecular and genetic basis of neurological diseases (Rosenber RN, Prusiner SB, DiMauro S, Barchi RL, eds), pp 165–186. Boston: Butterworth-Heinemann.

Rebecchi MJ, Pentyala SN (2000) Structure, function, and control of phosphoinositide-specific phospholipase C. Physiol Rev 80:1291–1335.

Rhee SG (2001) Regulation of phosphoinositide-specific phospholipase C. Annu Rev Biochem 70:281–312.

Rodrigues SM, Bauer EP, Farb CR, Schafe GE, LeDoux JE (2002) The group I metabotropic glutamate receptor mGluR5 is required for fear memory formation and long-term potentiation in the lateral amygdala. J Neurosci 22:5219–5229.

Scallet AC, Ye X (1997) Excitotoxic mechanisms of neurodegeneration in transmissible spongiform encephalopathies. Ann NY Acad Sci 825:194–205.

Taccola G, Marchetti C, Nistri A (2004) Modulation of rhythmic patterns and cumulative depolarization by group I metabotropic glutamate receptors in the neonatal rats cord in vitro. Eur J Neurosci 19:533–541.

Wakabayashi K, Narisawa-Saito M, Iwakura Y, Arai T, Ikeda K, Takahashi H, Nawa H (1999) Phenotypic down-regulation of glutamate receptor subunit GluR1 in Alzheimer's disease. Neurobiol Aging 20:287–295.

Yamamoto M, Ozawa H, Saito T, Frolich L, Riederer P, Takahata N (1996) Reduced immunoreactivity of adenylyl cyclase in dementia of Alzheimer type. Neuroreport 7:2965–2970.

(Accepted 5 December 2004)

5.2- *Increased expression of water channel aquaporin 1 and aquaporin 4 in Creutzfeldt-Jakob disease and in bovine spongiform encephalopathy-infected bovine-PrP transgenic mice*

Agustín Rodríguez, Esther Pérez-Gracia, Juan Carlos Espinosa, Martí Pumarola, Juan María Torres, Isidro Ferrer

Acta Neuropathol. (Berl). 2006 Nov; 112 (5): 573-85

El cambio espongiforme es un rasgo característico de las EETs, entre las cuales se incluye a la ECJ y a la EEB. Está caracterizado por la hinchazón de los procesos neuronales y la vacuolización del neuropilo, llevando al incremento del contenido intraneuronal de agua. El estudio que se presenta examina, por electroforesis en gel y por WB, los niveles de expresión de los canales de agua AQP1 y AQP4 en homogeneizados de corteza frontal (área 8) de casos con ECJ esporádico (seis hombres, cuatro mujeres; siete casos con M/M en el codón 129 del y con PrP tipo 1; dos casos V/V en el codón 129 y PrP tipo 2, y un caso M/V en el codón 129 y PrP tipo 1) comparado con controles y casos con AD (estadío VI de Braak y Braak) y DLB. Los niveles proteicos de AQP1 y AQP4 también han sido estudiados en la corteza cerebral de ratón transgénico para la PrP bovina infectado con EEB (BoPrP-Tg110mice) examinado a 60, 150, 210 y 270 días post-inoculación (dpi) comparado con controles sanos. La densitometría cuantitativa de las bandas de AQP normalizada para β-actina se ha analizado con el programa Statgraphics plus 5.0 con los tests estadísticos ANOVA y LSD. Se han observado niveles de expresión incrementados de AQP1 (revelado por dos anticuerpos distintos) y de AQP4 en ECJ, pero no en estadíos avanzados de AD y DLB comparado con controles. Por inmunohistoquímica se ha observado que la AQP1 y la AQP4 se expresan en astrocitos en los casos afectados. No se han observado modificaciones en la expresión de AQP1 y AQP4 a 60, 150 y 210 dpi. Sí se ha encontrado aumento significativo de expresión de AQP1 y AQP4 a 270 dpi, correspondiendo al tiempo en el que aparece PrP^{res} por WB y se aprecian lesiones típicas por espongiosis en el cerebro. Estos resultados muestran, conjuntamente, un incremento de la expresión de canales de agua en el cerebro en enfermedades priónicas humanas y animales. Estas modificaciones pueden tener implicaciones en la regulación del transporte de agua en los astrocitos y puede traducirse en un desequilibrio de la homeóstasis celular en estas enfermedades.

Acta Neuropathol
DOI 10.1007/s00401-006-0117-1

ORIGINAL PAPER

Increased expression of water channel aquaporin 1 and aquaporin 4 in Creutzfeldt-Jakob disease and in bovine spongiform encephalopathy-infected bovine-PrP transgenic mice

Agustín Rodríguez · Esther Pérez-Gracia · Juan Carlos Espinosa · Martí Pumarola · Juan María Torres · Isidro Ferrer

Received: 5 June 2006 / Revised: 1 July 2006 / Accepted: 1 July 2006

Abstract Spongiform change is a cardinal feature in transmissible spongiform encephalopathies, including Creutzfeldt-Jakob disease (CJD) and bovine spongiform encephalopathy (BSE). It is characterized by swelling of the neuronal processes and vacuolization of the neuropil, leading to increased intraneuronal water content. The present study examines, by gel electrophoresis and Western blotting, the expression levels of the water channels aquaporin 1 (AQP1) and aquaporin 4 (AQP4) in the frontal cortex (area 8) homogenates of sporadic CJD cases (six men, four women; seven cases with methionine/methionine at codon 129 and PrP type 1; two cases with valine/valine at codon 129 and PrP type 2, and one case methionine/valine at codon 129 and PrP type 1) compared with age-matched controls, and cases with Alzheimer's disease (AD, stage VI of Braak and Braak) and diffuse Lewy body disease (DLB). AQP1 and AQP4 protein levels were also studied in the cerebral cortex of BSE-infected bovine-PrP transgenic mice (BoPrP-Tg110 mice) examined at 60, 150, 210 and 270 days post-inoculation (dpi) compared with healthy brain-inoculated control mice. Quantitative densitometry of AQP bands normalized for β-actin was analyzed using Statgraphics plus 5.0 software from ANOVA and LSD statistical tests. Significant increased expression levels of AQP1 (as revealed with two different antibodies) and AQP4 were seen in CJD, but not in advanced AD and DLB cases when compared with controls. Immunohistochemistry revealed that AQP1 and AQP4 were expressed in astrocytes in diseased cases. No modifications in the expression levels of AQP1 and AQP4 were observed in BSE-infected bovine-PrP transgenic mice at 60, 150 and 210 dpi. However, a significant increase in the expression levels of AQP1 and AQP4 was found in mice at 270 dpi, the time corresponding with the appearance of PrP^{res} immunoreactivity in Western blots and typical spongiform lesions in the brain. Together, these findings show increased expression of water channels in the brain in human and animal prion diseases. These modifications may have implications in the regulation of water transport in astrocytes and may account for an imbalance in water and ion homeostasis in prion diseases.

Keywords Creutzfeld-Jakob disease · Bovine spongiform encephalopathy · Prion diseases · Transmissible spongiform encephalopathies · Aquaporin · Water channels · PrP

A. Rodríguez · E. Pérez-Gracia · I. Ferrer (✉)
Institut de Neuropatologia, Servei Anatomia Patològica,
IDIBELL-Hospital Universitari de Bellvitge,
Universitat de Barcelona, carrer Feixa Llarga sn,
08907 Hospitalet de Llobregat, Barcelona, Spain
e-mail: 8082ifa@comb.es

J. C. Espinosa · J. M. Torres
Centro de Investigación en Sanidad Animal (CISA),
INIA, Valdeolomos, 28130 Madrid, Spain

M. Pumarola
Departament de Medicina Animal i Cirurgia,
Facultat de Veterinaria,
Universitat Autonoma de Barcelona, Bellaterra, Spain

Introduction

Prion diseases, also called transmissible spongiform encephalopathies (TSEs), include scrapie and bovine

Table 1 Main clinical characteristics of CJD, AD (stage VI of Braak and Braak), DLB and control cases in the present series

Case number	Age	Gender	Codon 129	14-3-3 CSF	EEG	First symptom	Survival (months)	PrP type
CJD1	60	M	MM	+	+	Dementia	3	1
CJD2	60	F	MM	+	+	Dementia	6	1
CJD3	55	M	MM	+	+	Ataxia	3	1
CJD4	74	M	MV	+	+	Dementia	5	1
CJD5	66	M	VV	+	Rare	Ataxia	4	2
CJD6	53	F	MM	+	+	Dementia	2	1
CJD7	85	F	MV	+	+	Dementia	14	1
CJD8	71	M	VV	+	0	Ataxia	3	2
CJD9	70	F	MM	+	+	Dementia	3	1
CJD10	59	M	MM	?	+	Dementia	8	1
AD1	75	M						
AD2	69	M						
AD3	86	F						
AD4	69	M						
AD5	78	F						
DLB1	71	M						
DLB2	78	M						
DLB3	78	M						
DLB4	72	F						
DLB5	77	M						
Control1	62	M						
Control2	72	F						
Control3	73	M						
Control4	58	F						

F female, *M* male, *EEG* typical generalized triphasic pseudoperiodic complexes. 14-3-3 indicates the presence (+) or absence of this protein in cerebrospinal fluid (CSF). *M* methionine, *V* valine, *PrP type* PrP^{res} type 1: lower band of glycosylated PrP^{res} of 21 kDa; type 2: lower band of glycosylated PrP^{res} of 19 kDa

spongiform encephalopathy (BSE) in animals, and Creutzfeldt-Jakob disease (CJD), fatal familial insomnia (FFI), kuru and Gerstmann-Sträussler-Scheinker disease in humans [2, 3, 22, 23, 44]. According to the "protein-only" hypothesis, TSEs are caused by the conversion of PrP^{c} into an abnormal β-sheet-enriched and partially proteinase K-resistant isoform, PrP^{res} [2, 16, 44]. PrP^{res} is able to recruit PrP^{c}, resulting in an autocatalytic propagation in the pathogenic conformation [2, 11, 16, 44].

Transmissible spongiform encephalopathies are characterized by neuronal loss, astrocytic gliosis, microgliosis, abnormal PrP^{res} production and accumulation, and spongiform change [13, 17, 27, 31]. The spongiform change, a cardinal lesion in most prion diseases, consists of the formation of rounded vacuoles within the neuropil containing, in some cases, secondary chambers. Vacuoles are swollen neuronal and astrocytic cell processes with disrupted membranes, often in contact with synaptic structures. When many of them become confluent, this results in large vacuoles distorting the cortical cytoarchitecture [29, 32, 34, 37]. Several mechanisms are probably implicated in the degeneration of neurons in prion diseases [24], but little is known about the mechanisms which participate in the vacuolization of the neuropil. However, spongiform change is likely the result of abnormal membrane homeostasis and increased water content within swollen cell processes. Furthermore, it is known that fluid-attenuated inversion recovery (FLAIR) imaging is a very helpful method in CJD and related conditions, as it reveals increased water content in selected brain areas [15, 38, 55, 56] Therefore, exploration of mechanisms regulating water homeostasis seems to be a promising step toward increased understanding of the pathogenesis of TSEs.

Aquaporins (AQPs) facilitate water flux through the plasma membrane in several cell types and play an important role in the maintenance of homeostasis [3, 19, 25, 30, 59, 60]. AQP water channels have an hourglass form, the narrowest segment of which permits the passage of water but not of protons and other cations under the control of size restriction and electrostatic repulsion [1]. AQPs are expressed differentially in tissues. Aquaporin 1 (AQP1), aquaporin 4 (AQP4) and AQP9 are AQPs present in brain. AQP1 is mainly expressed in the apical membranes of the choroid plexus, but it can be expressed by astrocytes in pathological conditions; AQP4 is particularly abundant in astrocytic end-feet bordering the endothelium and the pial surface; and AQP9 is mainly expressed in the cytoplasm of astrocytes and ependymal cells [3, 8, 21, 39–41].

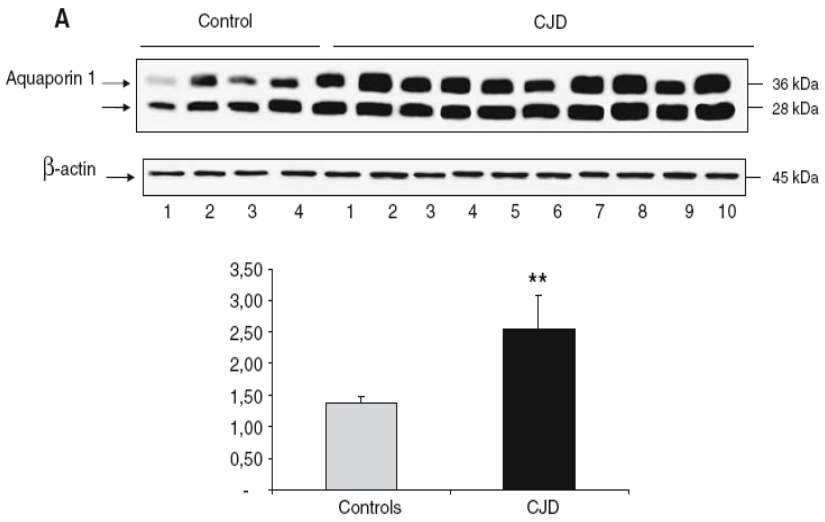

Fig. 1 **a** Western blots to AQP1 (Chemicon) of the frontal cortex in four controls and ten CJD cases show an lower band of 28 kDa and an upper (glycosylated) band of about 36 kDa. AQP1 expression is increased in every case of CJD when compared with age-matched controls. The densitometry of the bands normalized for β-actin (45 kDa) shows a significant increase of AQP1 expression in CJD cases when compared with controls. $^{**}P < 0.01$. *Numbers in the graph* correspond to arbitrary units. **b** Western blots to AQP1 (Abcam) of the frontal cortex in four controls and ten CJD cases show an lower band of 28 kDa and an upper (glycosylated) band of about 36 kDa. AQP1 expression is increased in every case of CJD when compared with age-matched controls. The densitometry of the bands normalized for β-actin (45 kDa) shows a significant increase of AQP1 expression in CJD cases when compared with controls. $^{*}P < 0.05$. *Numbers in the graph* correspond to arbitrary units

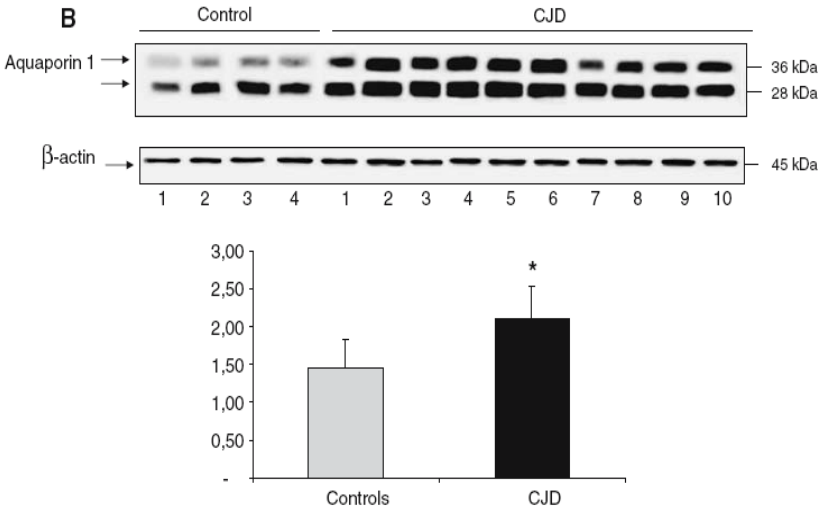

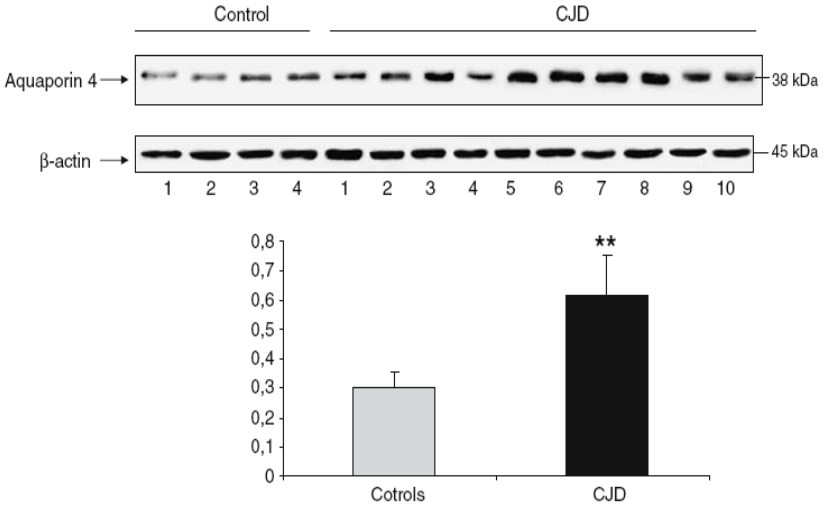

Fig. 2 Western blots of the frontal cortex in four controls and ten CJD cases show a band of 38 kDa. AQP4 expression levels are increased in every case of CJD when compared with age-matched controls. The densitometry of the bands normalized for β-actin (45 kDa) shows a significant increase of AQP4 expression in CJD cases when compared with controls. $^{**}P < 0.01$. *Numbers in the graph* correspond to arbitrary units

Previous studies based on DNA micro-array technology have shown up-regulation of AQP4 in CJD and scrapie [45, 46, 62, 63]. Yet, These findings have not been validated by other methods, and there is no description of AQPs in natural BSE and BSE murine models.

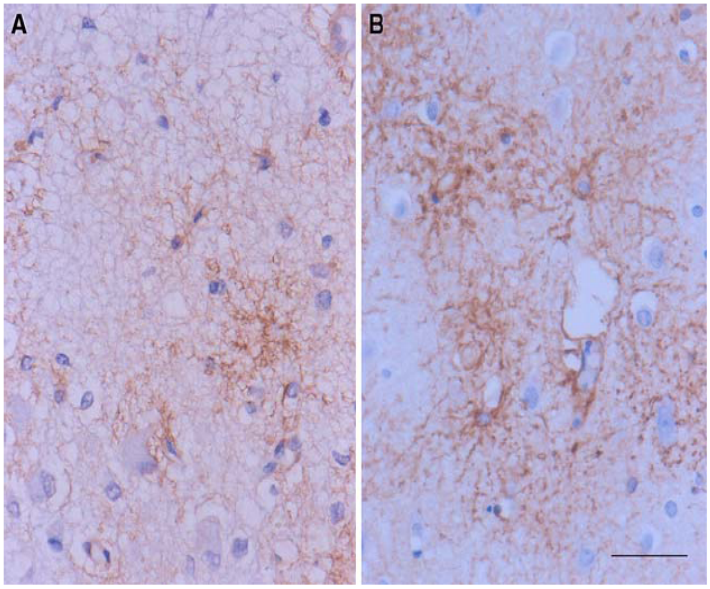

Fig. 3 AQP1 (**a**) and AQP4 (**b**) immunohistochemistry in Creutzfeldt-Jakob disease reveals AQP1 and AQP4 immunoreactivity in the cytoplasm and processes of astrocytes. Paraffin sections, slightly counterstained with haematoxylin. *Bar* = 25 µm

Based on these observations, the present study examines the expression levels of AQP1 and AQP4 by Western blotting in the frontal cortex in neuropathologically verified sporadic CJD cases obtained at short post-mortem delays compared with age-matched controls and with samples of Alzheimer's disease (AD) and Dementia with Lewy bodies (DLB). AQP9 was not examined because available antibodies were not suitable for Western blot studies. To go further into the understanding of AQPs during disease progression, AQP1 and AQP4 expressions were also examined in the brain of BSE-infected bovine-PrP transgenic mice (BoPrP-Tg110 mice) [14]. These mice can be infected with BSE without species barrier and they exhibit characteristics of the bovine disease, including positive PrP^{res} immunostaining and spongiform degeneration at about 240 days post-inoculation (dpi).

Materials and methods

Human cases

The brains of ten patients with sporadic CJD, four age-matched controls, five cases with AD and five cases with DLB were obtained from 3 to 8 h after death and were immediately prepared for morphological and biochemical studies. Criteria for the neuropathological, molecular and phenotypic diagnosis of CJD used in the present series were those accepted and detailed elsewhere [13, 43]. Criteria for clinical, pathological diagnosis and staging of AD and DLB cases used here are currently accepted [9, 10, 18, 26]. Cases of AD were categorized as stages VI of Braak and Braak [9]. Cases of DLB were categorized, on the basis of alpha-synuclein pathology, as stage 6 of Braak et al. [10]. The main clinical characteristics are summarized in Table 1. For biochemical studies, samples of the frontal cortex (area 8) were frozen in liquid nitrogen and stored at − 80°C until use. Control cases had not suffered from neurological or metabolic diseases and the neuropathological examination revealed no abnormalities.

In addition, samples of the frontal cortex from one control individual were obtained at 3 h post-mortem and immediately frozen (time 0), or stored at 4°C for 3, 6 or 22 h, and then frozen to mimic variable post-mortem delay in tissue processing and its effect on protein preservation.

BSE infection in BoPrP-Tg110 mice

The generation and characteristics of these transgenic mice, as well as the susceptibility and timing of the incubation following BSE inoculation, and the behavioral and neuropathological findings of infected mice, have been described in detail elsewhere [14]. Briefly, BoPrP-Tg110 mice express bovine PrP insert introduced in a mouse $PrP^{0/0}$ background, which confers susceptibility to BSE infection. For BSE infection, BoPrP-Tg110 mice (females, 6–7 weeks old, weighing approximately 20 g) were inoculated in the right parietal lobe using a 25 gauge disposable hypodermic syringe with 20 µl of 10% brain homogenate. TSE/08/59 inoculum, produced with a pool from the brainstem of 49 BSE infected cattle and supplied by the Veterinary Laboratory Agency (New Haw, Addlestone, Surrey, UK) was used. As negative controls, we have used the same BoPrP-Tg110 mice but inoculated with

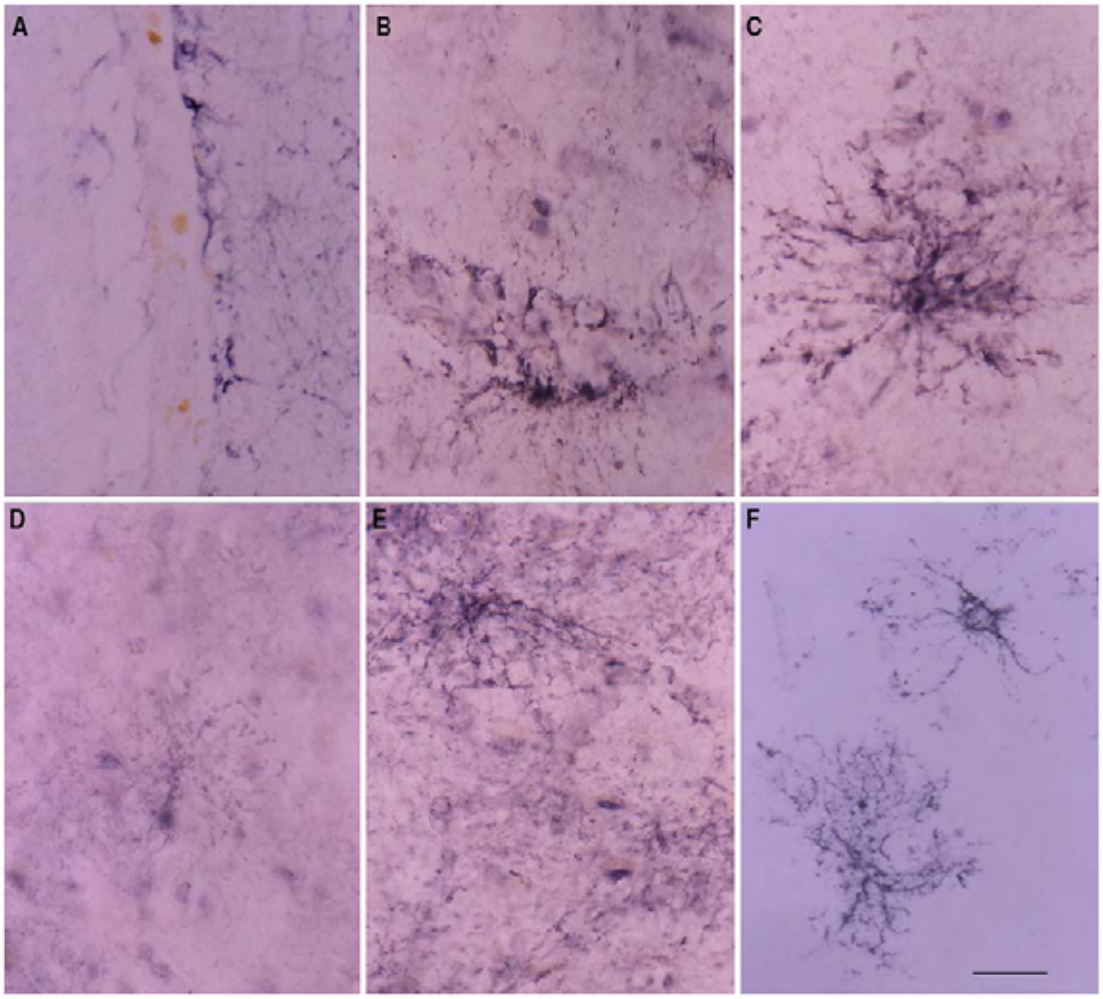

Fig. 4 AQP1 (**a–c**) and AQP4 (**d–f**) immunohistochemistry in cryostat sections processed free-floating in control (**a**, **d**) and CJD (**b**, **c**, **e**, **f**). AQP1 immunoreactivity is observed in the end-feet astrocytes surrounding blood vessels in control brains. Yet AQP1 immunoreactivity is found in the cytoplasm and processes of astrocytes in CJD. AQP4 immunostaining occurs in the cytoplasm of astrocytes in control brains, but increased immunoreactivity is observed in CJD. *Bar* = 25 μm

healthy cow brain. To minimize the risk of bacterial infection, homogenates were heated at 90°C for 10 min before inoculation. To evaluate the clinical signs appearing after inoculation, mice were observed daily and their neurological status was assessed twice a week. The presence of three signs of neurological dysfunction (using ten different items) [50, 51] was necessary for a mouse to score positive for prion disease. Animals were sacrificed at 60, 150, 210 and 270 dpi. The brains were rapidly removed from the skull and immediately prepared for neuropathological and biochemical studies.

Histopathology and immunohistochemistry in mice

Brains were prepared as previously described [14]. Tissue sections containing medulla oblongata at the level of the obex and the pontine area, cerebellum, diencephalon including thalamus, hippocampus, and cerebral cortex were processed for routine histological methods and immunohistochemistry. The avidin–biotine–peroxidase complex (ABC) method was used for the immunohistochemical detection of PrP^{res}, as previously described [40]. Briefly, tissue sections were incubated at 4°C overnight with the primary 2A11 mAb diluted 1:400 in phosphate buffer saline (PBS). This was followed by incubation with a secondary anti-mouse IgG (Dako, Madrid) diluted 1:200 in PBS. The immunoreaction was visualized with 3,3′-diaminobenzidine tetrahydrochloride (Sigma, Madrid) and 0.01% hydrogen peroxide. Finally, the sections were slightly counterstained with Mayer's haematoxylin, dehydrated and mounted on glass slides. Specific primary antibody was replaced by PBS or by non-immune

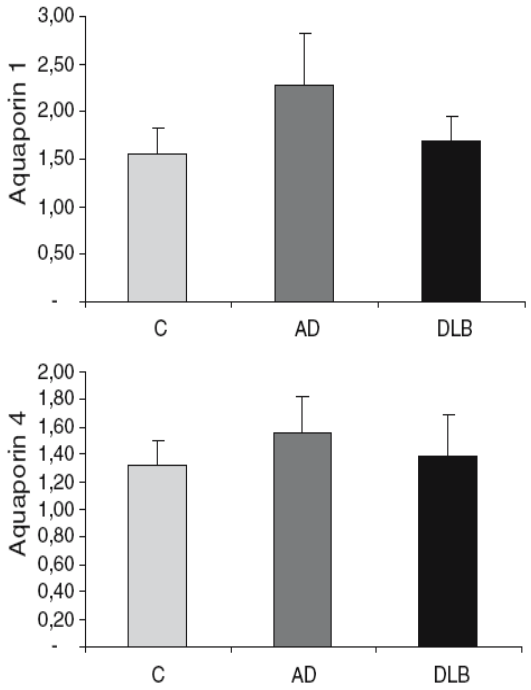

Fig. 5 No differences in the expression levels of AQP1 and AQP4 are seen in the frontal cortex of Alzheimer's disease (*AD*), Dementia with Lewy bodies (*DLB*) and control (*C*) cases

mouse serum in some tissue sections used as negative controls.

Gel electrophoresis and Western blot

For Western blot studies, about 0.1 g of frontal cortex in human cases or one cerebral hemisphere in mice was homogenized in a glass tissue grinder in 10 volumes (w/v) of cold buffer containing PBS, 0.5%, NP-40, 0.5% deoxycholic acid sodium salt, 0.1 mM phenylmethylsufonyl fluoride, 10 µg/ml aprotinin, 10 µg/ml leupeptin, 10 µg/ml pepstatin and 1 mM sodium orthovanadate, pH 7.5 to inhibit endogeneous phosphatases. Some samples were deglycosylated with N-Glycosidase F* recombinant (Roche, Barcelona) (12 U added to 20 µg) following incubation overnight at 37°C. After centrifugation at 3,500 × *g* for 5 min, protein concentration of total homogenate was determined with the BCA Protein Assay Kit (Pierce, Barcelona). Thirty micrograms of protein was mixed with loading buffer containing 0.125 M Tris (pH 6.8), 20% glycerol, 10% β-mercaptoethanol, 4% SDS and 0.002% bromophenol blue, and heated at 35°C for 5 min [35]. Sodium dodecylsulphate-polyacrylamide gel electrophoresis (10% SDS-PAGE) was carried out using a mini-protean system (Bio-Rad, Madrid) with molecular weight standards (Bio-Rad). Proteins were then transferred to nitrocellulose membranes using an electrophoretic transfer system (Semi-dry, Bio-Rad). The membranes were washed with TTBS containing 10 mM Tris–HCl pH 7.4, 140 mM NaCl and 0.1% Tween-20. Nonspecific blocking was performed by incubating the membranes in TTBS containing 5% skimmed milk for 20 min. Membranes were incubated with the primary antibodies at 4°C overnight. The rabbit polyclonal antibody anti-AQP1 (Chemicon, Barcelona) was used at a dilution of 1:1,000 in the TBST-5% skimmed milk. The rabbit polyclonal anti-AQP1 (Abcam, Cambridge) was used at a dilution of 1:500. The mouse monoclonal anti-AQP4 (Abcam) was used at a dilution of 1:500. After rinsing, the membranes were incubated with the corresponding anti-rabbit or anti-mouse secondary antibodies (Dako) at a dilution of 1:1,000 for 1 h at room temperature. The membranes were then washed and developed with the chemiluminescence ECL system (Amersham, Barcelona) followed by exposure of the membranes to autoradiographic films at 4°C. The monoclonal anti-β-actin antibody (Sigma) was used at a dilution of 1:5,000 as a control for protein loading.

Details of the AQP antibodies used are as follows. The anti-AQP1 (Abcam) antibody is raised against a 19 amino acid synthetic peptide within the carboxy terminal domain of rat AQP1 that is 100% homologous in rat, mouse, human and bovine. The anti-AQP1 (chemicon) is raised against a 19 amino acid synthetic peptide from the cytosolic carboxy terminal domain of rat AQP1. This peptide contains most of the epitopes recognized by polyclonal antibodies against the whole protein. The anti-AQP4 (Abcam) antibody is raised against a synthetic peptide corresponding to amino acids 301–318 of rat AQP4. This antibody recognizes an epitope within the cytoplasmic domain of the water-specific channel AQP4.

For PrP^{res} detection in mice, 100 µl of 10% brain homogenates (10% wt/vol) were pre-cleared by centrifugation at 2,000 × *g* for 5 min in 5% sarcosyl. Samples were treated with 20 µg/ml of proteinase K (Roche) at 37°C for 60 min, and insoluble fractions were obtained by centrifugation at 25,000 × g for 30 min. SDS sample loading buffer was added to all samples and each one was boiled for 10 min before loading on an SDS/12% polyacrylamide gel. For immunoblotting, ascites preparation of 2A11 mAb [12] was used as 1:2,000 dilution. Immunocomplexes were detected with horseradish-peroxidase conjugated anti-mouse IgG (Sigma), and developed as described above.

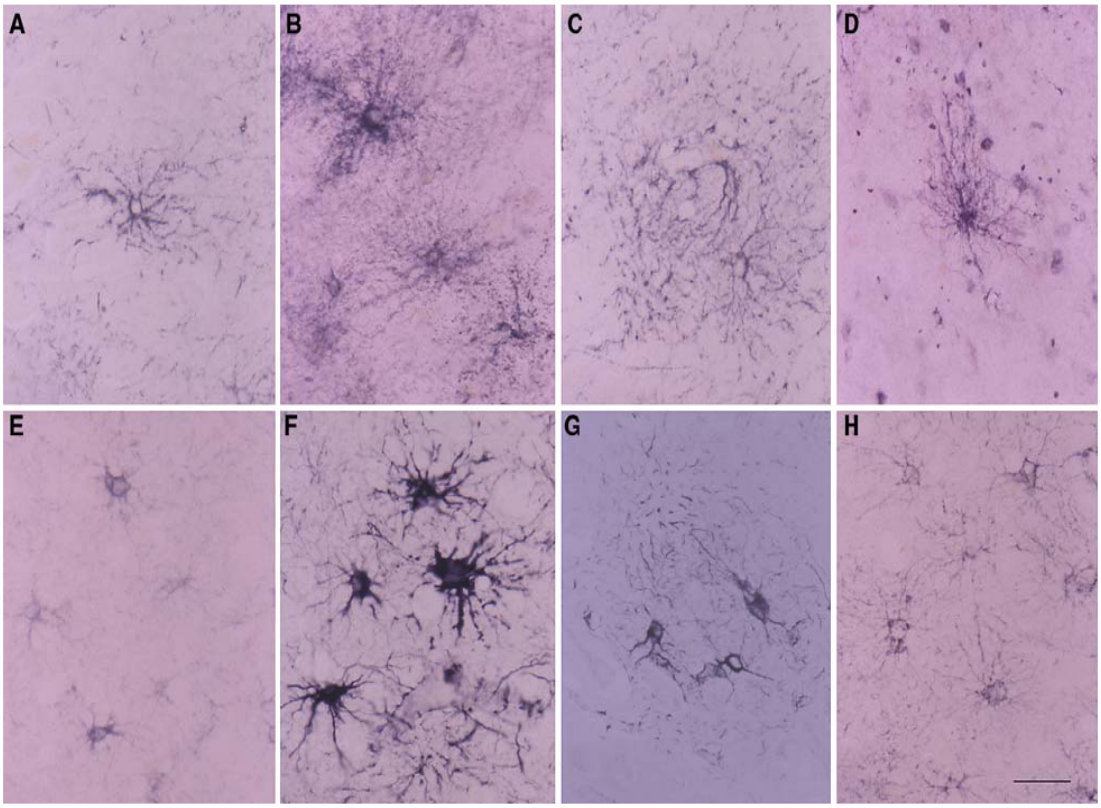

Fig. 6 Comparison of AQP4 immunoreactivity (**a–d**) and GFAP immunoreactivity (**e–h**) in the frontal cortex in control (**a**, **e**), CJD (**b**, **f**), AD (**c**, **g**) and DLB (**d**, **h**) in cryostat sections processed free-floating. Marked increase in AQP4 immunoreactivity is associated with strong GFAP immunostaining in CJD astrocytes. *Bar* = 25 μm

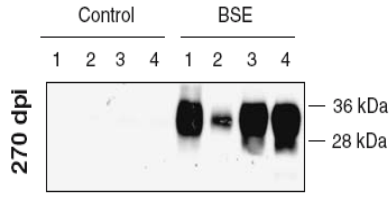

Fig. 7 Western blot analysis of PrP^{res} from brain homogenates in control and diseased mice at 270 days post inoculation (dpi). Monoclonal antibody 2A11 was used at a 1:2,000 dilution

Densitometry and statistical processing of data

Protein expression levels were determined by densitometry of the bands using Total Laboratory v2.01 software. This software detects the bands obtained by Western blot and gives individual values which are dependent on the light quantification of the corresponding band. Measurements are expressed as arbitrary units. The results were normalized for β-actin. The numerical data obtained from CJD and the corresponding controls were statistically analyzed using STATGRAPHICS plus 5.0 software from ANOVA and the LSD statistical tests. Asterisks indicate the following P values: $^{*}P < 0.05$ (95% confidence level); $^{**}P < 0.01$ (99% confidence level); and $^{***}P < 0.001$ (99.9% confidence level).

Aquaporin immunohistochemistry

Aquaporin immunohistochemistry was carried out only in human cases. No further material was available for immunohistochemistry from BoPrP-Tg110 BSE-infected mice.

Paraffin sections, 4 m thick, were processed with the EnVision + system peroxidase (DAB) procedure (Dako). The rabbit polyclonal antibody anti-AQP1 (Abcam) was used at a dilution of 1:500. The monoclonal anti-AQP4 (Abcam) was used at a dilution of 1:250. The rabbit polyclonal anti-GFAP antibody (Dako) was used at a dilution of 1:500. The sections were incubated with LSAB for 1 h at room temperature. The peroxidase reaction was visualized with 0.05% diaminobenzidine and 0.01% hydrogen peroxide (brown precipitate). Some sections were incubated without the primary antibody. No immunoreactivity was found in these samples.

Table 2 Main characteristics of BSE-infected transgenic mice

60 dpi	Controls				BSE			
	1	2	3	4	1	2	3	4
WB	–	–	–	–	–	–	–	–
IHC	–	–	–	–	–	–	–	–
HP	–	–	–	–	–	–	–	–
CS	–	–	–	–	–	–	–	–

150 dpi	Controls			BSE		
	1	2	3	1	2	3
WB	–	–	–	–	–	–
IHC	–	–	–	–	–	–
HP	–	–	–	–	–	–
CS	–	–	–	–	–	–

210 dpi	Controls			BSE		
	1	2	3	1	2	3
WB	–	–	–	–	–	–
IHC	–	–	–	–	+[a]	–
HP	–	–	–	–	+[a]	–
CS	–	–	–	–	–	–

270 dpi	Controls				BSE			
	1	2	3	4	1	2	3	4
WB	–	–	–	–	+	+	+	+
IHC	–	–	–	–	+	+	+	+
HP	–	–	–	–	+	+	+	+
CS	–	–	–	–	+	+	+	+

dpi days post-inoculation

Brain samples were analyzed by Western blot after proteinase-K treatment for PrPres detection (WB), by histopathology (HP) or by immunohistochemistry (IHC). Diseased mice were scored by clinical signs (CS) before euthanasia. HP changes are characterized by spongiform change and mild astrocytic gliosis. IHC indicates positive PrPres immunoreactivity

[a] Positive only around inoculation point

In addition, cryostat sections 7 µm thick were processed free-floating with the LSAB method. The rabbit polyclonal antibody anti-AQP1 (Abcam) was used at a dilution of 1:500. The monoclonal anti-AQP4 (Abcam) was used at a dilution of 1:250. Other sections were incubated with rabbit polyclonal anti-glial fibrillary acidic protein (GFAP) antibodies (Dako) used at a dilution of 1:250. The peroxidase reaction was visualized with NH_4NiSO_4 (0.05 M) in phosphate buffer (0.1 M), 0.05% diaminobenzidine, NH_4Cl and 0.01% hydrogen peroxide (dark blue precipitate). Some sections were incubated without the primary antibody. No immunoreactivity was found in these samples.

Results

General neuropathological findings in CJD

Neuron loss, spongiform change, astrocytic gliosis and microgliosis involving the cerebral neocortex, striatum and cerebellum, occurred in every case. Synaptic-like PrP^{res} deposits were found in the cerebral cortex and striatum in every case. In addition, PrP^{res} plaques were common in the two VV2 cases (cases 5 and 8; Table 1). Details of neuropathology and Prp^{res} immunohistochemistry in these cases can be found elsewhere [20].

General findings of AQP1 antibodies and samples

The anti-AQP1 antibodies recognized a band of 28 kDa in control and diseased cases as well as a band of about 36 kDa. Similar observations were found with the anti-AQP1 (Chemicon) and anti-AQP1 (Abcam) antibodies. The upper band was abolished following de-glycosylation at 35°C. Both bands disappeared when the sample was heated at 95°C (data not shown).

Control of protein preservation with postmortem delay was tested by freezing cortical samples obtained at 3 h postmortem (time 0), and at 3, 6 and 22 h. The same amount of protein (30 µg) was loaded on each lane and Western blots of AQP1 and AQP4 were carried out in parallel. No differences in the expression levels of any of these proteins were detected (data not shown). Since the tissue samples in control and CJD cases were obtained between 3 and 8 h after death, possible differences in protein expression levels in the present study are not likely to be dependent on artifacts related with postmortem delay in tissue processing.

AQP1 expression in CJD

Increased expression in AQP1 was seen in CJD when compared with age-matched controls. The densitometry of the bands normalized for β-actin showed a significant increase in the expression levels of AQP1 in CJD cases when compared with controls. Similar findings were observed with two different anti-AQP1 antibodies (Fig. 1a, b).

AQP4 expression in CJD

Western blots to AQP4 of frontal cortex in control and diseased cases revealed a single band of 38 kDa corresponding to the molecular weight of AQP4. Increased expression in AQP4 was seen in CJD when compared with age-matched controls. The densitometry

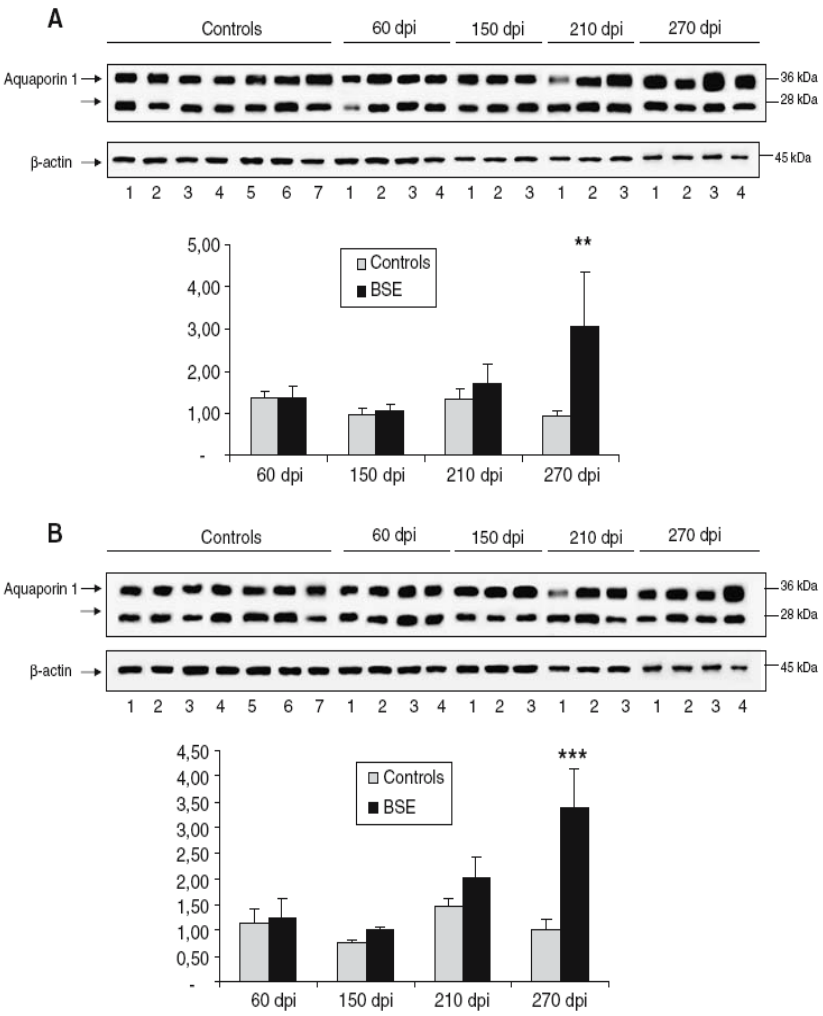

Fig. 8 **a** The densitometry of the bands to AQP1 (Chemicon) shows a significant increase in the expression levels of AQP1 at 270 dpi ($n = 4$) when compared with the corresponding controls. $^{**}P < 0.01$. Yet no differences between BSE-infected mice and controls ($n = 7$) are seen at 60 ($n = 4$), 150 ($n = 3$) and 210 ($n = 3$) dpi. *The numbers in the graphs* correspond to arbitrary units. **b** The densitometry of the bands to AQP1 (Abcam) shows a significant increase in the expression levels of AQP1 at 270 dpi ($n = 4$) when compared with the corresponding controls. $^{***}P < 0.001$. Yet no differences between BSE-infected mice and controls ($n = 7$) are seen at 60 ($n = 4$), 150 ($n = 3$) and 210 ($n = 3$) dpi. *The numbers in the graphs* correspond to arbitrary units

of the bands normalized for β-actin showed a significant increase in the expression levels of AQP4 in CJD cases when compared with controls ($P < 0.01$) (Fig. 2).

AQP1 and AQP4 immunohistochemistry in CJD

In paraffin sections, AQP4 immunoreactivity was found in the end-feet of astrocytes surrounding blood vessels and in the pial surface in control cases. No AQP1 immunoreactivity was found in the cerebral cortex in control brains (not shown). Differences between these results and basal expression levels of AQP1 in control brains as revealed with Western blot are probably due to the lower sensitivity of immunohistochemistry in paraffin sections (or loss of antigenicity due to partial AQP destruction during tissue processing) when compared with western blots of fresh samples from brain homogenates. However, AQP1 immunoreactivity was found in the cytoplasm of astrocytes in CJD. Similarly, strong AQP4 immunoreactivity was observed in the cytoplasm of astrocytes in cases with CJD (Fig. 3).

Cryostat sections processed free-floating showed AQP1 immunoreactivity in the end-feet of astrocytes surrounding blood vessels in control brains. AQP1 immunoreactivity extended to the cytoplasm and cell processes of astrocytes in CJD cases (Fig. 4a–c). AQP4 immunoreactivity was also better visualized in cryostat sections processed free-floating. AQP4 immunoreactivity decorated the cytoplasm and cell processes of protoplasmic astrocytes and fibrillar astrocytes in controls. Increased immunoreactivity was found in astrocytes in the cerebral cortex and white matter in CJD (Fig. 4d–f).

AQP1 and AQP4 expression in AD and DLB

No differences were seen in the expression levels of AQP1 and AQP4 in the frontal cortex of AD, DLB

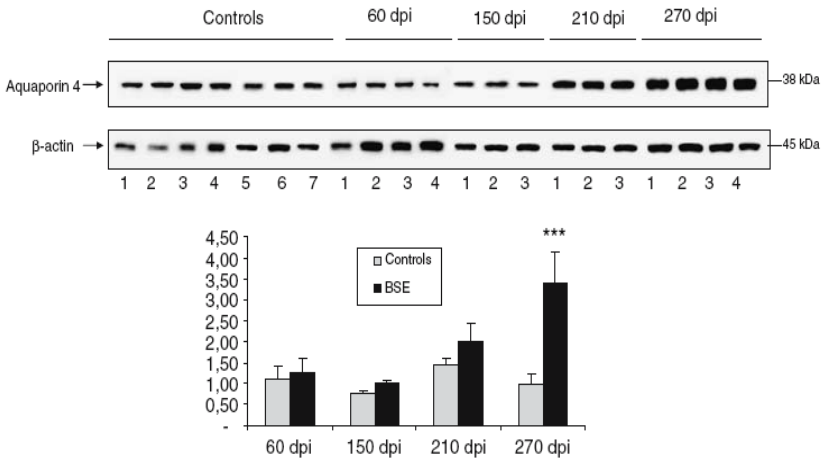

Fig. 9 Western blots to AQP4 (Abcam) of brain homogenates in control and diseased mice normalized for β-actin shows a significant increase in the expression levels of AQP1 and AQP4 at 270 dpi ($n = 4$) when compared with the corresponding controls. ***$P < 0.001$. Yet no differences between BSE-infected mice and controls ($n = 7$) are seen at 60 ($n = 4$), 150 ($n = 3$) and 210 ($n = 3$) dpi. *The numbers in the graphs* correspond to arbitrary units

and control cases. Similar findings were observed with the two anti-AQP1 antibodies (Fig. 5).

Comparative AQP4 and GFAP immunohistochemistry in control, CJD, AD and DLB

AQP4 immunoreactivity in CJD cases was higher than AQP4 immunoreactivity in controls, and in AD and DLB cases (Fig. 6a–d). Similar sections stained with anti-GFAP disclosed positive astrocytes in control and diseased cases. However, the number and size, and the amount of GFAP per cell were more pronounced in CJD than in other disease states (Fig. 6e–h).

General aspects of BSE-infected Bo-PrP transgenic mice

At 270 dpi, PrP^{res} was detected in all BSE-infected mice by both immunohistochemistry and Western blotting (Fig. 7 and Table 2). These animals also scored positively for the presence of clinical signs: hunched position, and rough coat were the prominent signs; neuropathological changes: mainly vacuolization of the neuropil mostly in the brain stem, hippocampus and cerebellar white matter. PrP^{res} deposition was most common in fine granular and punctuate neuropil and stellate foci, but also granular staining in neuron cytoplasms and around the neurons (occasionally as plaque-like deposits) was observed, resembling those patterns reported for classical BSE in cattle [14]. At 210 dpi, only one out of three animals was scored as positive by immunohistochemistry and histopathology, but it was negative for clinical scores and PrP^{res} detection by Western blot (Table 2). No positive animals were detected at 60 and 150 dpi. As expected, all control animals were scored negative for all analysis (Table 2).

AQP1 expression in BSE-infected Bo-PrP transgenic mice

Western blots to AQP1 of brain homogenates in control and diseased mice revealed two bands of 28 and 36 kDa. No significant differences between BSE-infected mice and controls were seen at 60, 150 and 210 dpi. However, increased expression of AQP1 was seen at 270 dpi when compared with the corresponding controls. The densitometry of the bands normalized for β-actin (45 kDa) showed a slight variable significant increase in the expression levels of AQP1 at this time point (Fig. 8a, b).

AQP4 expression in BSE-infected Bo-PrP transgenic mice

Western blots to AQP4 of brain homogenates in control and BSE-infected mice revealed a single band of 38 kDa. No differences in the expression levels of AQP4 were observed at 60, 150 and 210 post-inoculation. However, a significant increase in the expression levels of AQP4 was seen at 270 dpi when compared with corresponding controls (Fig 9).

Discussion

The present study shows increased AQP1 and AQP4 expression levels in the frontal cortex of patients with CJD when compared with age-matched controls. Yet no modifications in the expression levels of AQP1 and AQP4 have been observed in advanced stages of AD and DLB, thus suggesting that these changes are not

the mere result of non-specific aspects in advanced stages of diseases with dementia and degeneration of the cerebral cortex. Moreover, increased AQP1 and AQP4 levels have also been found in the cerebral cortex of BSE-infected BoPrP-Tg110 mice at 270 dpi, thus demonstrating abnormal expression of water channels in these mice with disease progression. These findings validate previous observations showing AQP4 up-regulation in CJD and natural scrapie, by using DNA micro-array technology [45, 46, 62, 63], and demonstrate that up-regulation translates to increased protein expression not restricted to AQP4 but also involving other genes of the AQP family, including AQP1. In addition to CJD and scrapie, the present findings show increased expression of AQP1 and AQP4 in advanced stages of murine BSE.

Previous studies have shown that AQPs are regulated in brain edema following traumatic injury [28, 53], cerebral ischemia [7, 47, 54, 64] and hyponatremia [58], as well as in brain tumors [42, 47, 48]. Interestingly, redistribution of AQP-4 differs in low- and high-grade human brain tumors [61]. The expression of AQP4 mRNA is decreased in the core of infarction following cerebral ischemia [49], whereas it is increased in the peri-infarcted area maximally on day 3 after focal cerebral ischemia in the rat, and in parallel to the generation of brain edema monitored by MRI [54]. Similar findings have been reported in the human brain: AQP4 immunoreactivity is decreased in the core, but increased in astrocytes at the periphery of the infarction [6]. Global ischemia is also accompanied by AQP4 up-regulation [64]. Finally, AQP4 is increased in high-grade gliomas and in reactive astrocytes surrounding malignant tumors [47]. Regarding AQP1, AQP1 is expressed in neoplastic astrocytes, and in reactive astrocytes in metastatic carcinomas [46]. AQP1 expression is also increased in glioblastomas [42]. Modifications in the expression levels of AQP may have functional implications. Thus, the use of genetically manipulated mice has been extremely helpful in increasing our understanding of brain AQPs. AQP4 deletion in mice reduces edema formation after water intoxication and after focal cerebral ischemia, thus indicating that AQP4 participates in the development of osmotic and cytotoxic edema [4, 5, 35, 36, 52, 57]. Recent studies have also shown enhanced expression of AQP4 in human brain with inflammatory diseases [6]. Moreover, AQP4 is increased in the sclerotic hippocampus in human temporal lobe epilepsy [33]. These findings suggest more subtle roles of AQPs in disease. More particularly, abnormal expression of AQP4 has been suggested to facilitate seizures in sclerotic hippocampus [33].

AQP1 and AQP4 are expressed in astrocytes in CJD thus indicating that up-regulation of AQPs occurs in astrocytes whereas no apparent AQP expression occurs in neurons. This is an interesting observation, as spongiform changes in prion diseases are related with swollen neuronal and astrocytic processes. The relationship between abnormal PrP deposition, spongiform degeneration and possible AQP up-regulation in astrocytes is still obscure, albeit that the study of the BSE murine model indicates that the three abnormalities are closely related in time with disease progression. Moreover, AQP1 is not normally expressed in astrocytes but the expression of AQP1 in these cells is related with pathology.

Whether increased levels of AQP1 and AQP4 in CJD result from increased number of astrocytes might be a matter of discussion. Yet increased AQP1 and AQP4 correlates with increased expression of GFAP rather than with the number of astrocytes in CJD when compared with other disease states. Therefore, increased expression of AQPs in prion diseases seems to be an additional equipment of certain reactive astrocytes to cope with water homeostasis. It is clear that AQPs are probably not the contributory agent of the spongiform change, but rather a response of astrocytes to abnormal water fluxes in human and animal prion diseases. Additional studies in BSE-infected mice with AQP4 deletion would be necessary to understand whether increased levels of AQPs are involved in the pathogenesis of the disease.

Disclosure statement

There is no actual or potential conflicts of interest including any financial, personal or other relationships with other people or organizations within 3 years of beginning this work that could inappropriately influence this work. Appropriate approval and procedures used in this work by the local Ethic Committee of the Hospital Universitari de Bellvitge are disclosed in the section of Materials and methods.

Acknowledgments This work was supported in part by the Ministerio de Ciencia y Tecnología: EET 2001-3724 and EET2002-05168, and CAL01-018 NoE Neuroprion CT-2004-506579. We wish to thank T. Yohannan for editorial assistance.

References

1. Agre P, Kozono D (2003) Aquaporin water channels: molecular mechanisms for human diseases. FEBS Lett 555:72–78
2. Aguzzi A (2003) Introduction to prion diseases. In: Dickson D (ed) Neurodegeneration: the molecular pathology of

dementia and movement disorders. ISN Neuropath Press, Basel, pp 282–286
3. Amiry-Moghaddam M, Ottersen OP (2003) The molecular basis of water transport in the brain. Nat Rev Neurosci 4:991–1001
4. Amiry-Moghaddam M, Williamson A, Palomba M, Eid T, de Lanerolle NC, Naglehus EA, Adams ME, Froehner SC, Agre P, Ottersen OP (2003) Delayed K+ clearance associated with aquaporin-4 mislocalization: phenotypic defects in brains of alpha-syntrophin-null mice. Proc Natl Acad Sci USA 100:13615–13620
5. Amiry-Moghaddam M, Xue R, Haug FM, Neely JD, Bhardwaj A, Agre P, Adams ME, Froehner SC, Mori S, Ottersen OP (2004) Alpha-syntrophin deletion removes the perivascular but endothelial pool of aquaporin-4 at the blood-brain barrier and delays the development of brain edema in an experimental model of acute hyponatremia. FASEB J 18:542–544
6. Aoki-Yoshimo K, Uchihara T, Duyckaerts C, Nakamura A, Haw JJ, Wakayama Y (2005) Enhanced expression of aquaporin 4 in human brain with inflammatory diseases. Acta Neuropathol 110:281–288
7. Aoki K, Uchihara T, Tsuchiya K, Nakamura A, Ikeda K, Wakayama Y (2003) Enhanced expression of aquaporin 4 in human brain with infarction. Acta Neuropathol 106:121–124
8. Badaut J, Lasbennes F, Magistretti PJ, Regli L (2002) Aquaporins in brain: distribution, physiology, and pathophysiology. J Cereb Blood Flow Metab 22:367–378
9. Braak H, Braak E (1999) Temporal sequence of Alzheimer's disease related pathology. In: Peters A, Morrison JH (eds) Cerebral cortex. Neurodegenerative and age-related changes in structure and function of cerebral cortex, vol 14. Kluwer/Plenum, New York, Dordrecht, pp 475–512
10. Braak H, Ghebremedhin E, Rub U, Bratzke H, del Tredici K (2004) Stages in the development of Parkinson's disease-related pathology. Cell Tiss Res 318:121–34
11. Bratosiewicz-Wasik J, Wasik TJ, Liberski PP (2004) Molecular approaches to mechanisms of prion diseases. Folia Neuropathol 42:S33–S46
12. Brun A, Castilla J, Ramirez MA, Prager K, Parra B, Salguero FJ, Shiveral D, Sanchez C, Sanchez-Vizcaino JM, Douglas A, Torres JM (2004) Proteinase K enhanced immunoreactivity of the prion protein-specific monoclonal antibody 2A11. Neurosci Res 48:75–83
13. Budka H, Head MW, Ironside JW, Gambetti P, Parchi P, Zeidler M, Tagliavini F (2003) Sporadic Creutzfeldt-Jakob disease. In: Dickson D (ed) Neurodegeneration: the molecular pathology of dementia and movement disorders. ISN Neuropath Press, Basel, pp 287–297
14. Castilla J, Gutierrez-Adan A, Brun A, Pintado B, Ramirez MA, Parra B, Doyle D, Rogers M, Salguero FJ, Sanchez C, Sanchez-Vizcaino JM, Torres JM (2003) Early detection of PrP(res) in BSE-infected bovine PrP transgenic mice. Arch Virol 148:677–691
15. Collie DA, Summers DM, Sellar RJ, Ironside JW, Cooper S, Zeidler M, Knight R, Will RG (2003) Diagnosing variant Creutzfeldt-Jakob disease with the pulvinar sign: MR imaging findings in 86 neuropathologically-verified cases. Am J Neuroradiol 24:1560–1569
16. Collinge J (2001) Prion diseases of human and animals: their causes and molecular basis. Annu Rev Neurosci 24:519–550
17. DeArmond SJ, Kretzschmar HA, Prusiner SB (2003) Prion diseases. In: Graham DI, Lantos PL (eds) Greenfield's neuropathology, vol II. Arnold, London, pp 273–323
18. Duyckaerts C, Dickson DW (2003) Neuropathology of Alzheimer's disease. In: Dickson D (ed) Neurodegeneration: the molecular pathology of dementia and movement disorders. ISN Neuropath Press, Basel, pp 47–65
19. Ferrer I (2005) Pathology of brain edema and brain swelling. In: Kalimo H (ed) Pathology and genetics of cerebrovascular diseases. ISN Neuropath Press, Basel, pp 32–38
20. Freixes M, Rodríguez A, Dalfó E, Ferrer I (2006) Oxidation, glycoxidation, lipoxidation, nitration, and responses to oxidative stress in the cerebral cortex in Creutzfeldt-Jakob disease. Neurobiol Aging (in press)
21. Frigeri A, Gropper MA, Turck CW, Verkman AS (1995) Immunolocalization of the mercurial-insensitive water channel and glycerol intrinsic protein in epithelial cell plasma membranes. Proc Natl Acad Sci USA 92:4328–4331
22. Gambetti P, Parchi P, Chen SG, Cortelli P, Lugaresi E, Montagna P (2003) Fatal insomnia: familial and sporadic. In: Dickson D (ed) Neurodegeneration: the molecular pathology of dementia and movement disorders. ISN Neuropath Press, Basel, pp 326–332
23. Ghetti B, Bugiani O, Tagliavini F, Piccardo P (2003) Gerstmann-Sträussler-Scheinker disease. In: Dickson D (ed) Neurodegeneration: the molecular pathology of dementia and movement disorders. ISN Neuropath Press, Basel, pp 318–325
24. Giese A, Kretzschmar HA (2001) Prion-induced neuronal damage: the mechanisms of neuronal destruction in the subacute spongiform encephalopathies. Curr Topics Microbiol Immunol 253:203–217
25. Gunnarson E, Zelenina M, Aperia A (2004) Regulation of brain aquaporins. Neuroscience 129:947–955
26. Ince PG, McKeith IG (2003) Dementia with Lewy bodies. In: Dickson D (ed) Neurodegeneration: the molecular pathology of dementia and movement disorders. ISN Neuropath Press, Basel, pp 188–197
27. Ironside JW (1998) Prion diseases in man. J Pathol 86:27–34
28. Kiening KL, van Landeghem FK, Schreiber S, Thomale UW, von Deimling A, Unterberg AW, Stover JF (2002) Decreased hemispheric aquaporin-4 is linked to evolving brain edema following controlled cortical impact injury in rats. Neurosci Lett 324:105–108
29. Kim JH, Manuelidis EE (1986) Serial ultrastructural study of experimental Creutzfeldt-Jakob disease in guinea pigs. Acta Neuropathol 69:81–90
30. Kimelberg HK (2004) Water homeostasis in the brain: basic concepts. Neuroscience 129:851–860
31. Knight RSG, Will RG (2004) Prion diseases. J Neurol Neurosurg Psychiatr 75:S136–S42
32. Landis DMD, Williams RS, Masters CL (1981) Golgi and electron microscopic studies of spongiform encephalopathies. Neurology 31:538–549
33. Lee TS, Eid T, Mane S, Kim JH, Spencer DD, Ottersen OP, de Lanerolle NC (2004) Aquaporin-4 is increased in the sclerotic hippocampus in human temporal lobe epilepsy. Acta Neuropathol 108:493–502
34. Liberski PP, Streichenberger N, Giraud P, Sotrenon M, Meyronnet D, Sikorska B, Kopp N (2005) Ultrastructural pathology of prion diseases revisited: brain biopsy studies. Neuropathol Appl Neurobiol 31:88–96
35. Manley GT, Binder DK, Papadopoulos MC, Verkman AS (2004) New insights into water transport and edema in the central nervous system from phenotype analysis of aquaporin-4 null mice. Neuroscience 129:983–991
36. Manley GT, Fujimura M, Ma T, Noshita N, Filiz F, Bollen AW, Chan P, Verkman AS (2000) Aquaporin-4 deletion in mice reduces brain edema after acute water intoxication and ischemic stroke. Nat Med 6:159–163

37. Miyakawa T, Katsuragi S, Koga Y, Moriyama S (1986) Status spongiosus in Creutzfeldt-Jakob disease. Clin Neuropathol 5:146–152
38. Murata T, Shiga Y, Higano S, Takahashi S, Mugikura S (2002) Conspicuity and evolution of lesions in Creutzfeldt-Jakob disease at diffusion-weighted imaging. Am J Neuroradiol 23:1164–1172
39. Neely JD, Christensen BM, Nilesen S, Agre P (1999) Heterotetrameric composition of aquaporin-4 water channels. Biochemistry 38:11156–11163
40. Nielsen S, Nagelhus EA, Amiry-Moghaddam M, Bourque C, Agre P, Ottersen OP (1997) Specialized membrane domains for water transport in glial cells: high-resolution immunogold cytochemistry of aquaporin-4 in rat brain. J Neurosci 17:171–180
41. Nielsen S, Smith BL, Christensen EI, Agre P (1993) Distribution of the aquaporin CHIP in secretory and resorptive epithelia and capillary endothelia. Proc Natl Acad Sci USA 90:7275–7279
42. Oshio K, Binder DK, Liang Y, Bollen A, Feuerstein B, Berger MS, Manley GT (2005) Expression of the aquaporin-1 water channel in human glial tumors. Neurosurgery 56:375–381
43. Parchi P, Giese A, Capellari S, Brown P, Schulz-Schaeffer W, Windl O, Zerr I, Budka H, Kopp N, Piccardo P, Poser S, Rojiani A, Streichemberger N, Julien J, Vital C, Ghetti B, Gambetti P, Kretzschmar H (1999) Classification of sporadic Creutzfeldt-Jakob disease based on molecular and phenotypic analysis of 300 subjects. Ann Neurol 46:224–233
44. Prusiner SB (1997) The prion diseases of humans and animals. In: Rosenber RN, Prusiner SB, DiMauro S, Barchi RL (eds) The molecular and genetic basis of neurological diseases. Butterworth-Heinemann, Boston, pp 165–186
45. Riemer C, Neidhold S, Burwinkel M, Schwartz A, Schultz J, Krätzschmar J, Mönning U, Baier M (2004) Gene expression profiling of scrapie-infected brain tissue. Biochem Biophys Res Commun 323:556–564
46. Riemer C, Queck I, Simon D, Kurth R, Baier M (2000) Identification of upregulated genes in scrapie-infected brain tissue. J Virol 74:10245–10248
47. Saadoun S, Papadopuolos MC, Davies DC, Bell BA, Krishna S (2002) Increased aquaporin 1 water channel expression in human brain tumours. Br J Cancer 87:621–623
48. Saadoun S, Papadopuolos MC, Davies DC, Krishna S, Bell BA (2002) Aquaporin-4 expression is increased in oedematous human brain tumours. J Neurol Neurosurg Psychiatr 72:262–265
49. Sato S, Umenishi F, Inamasu G, Sato M, Ishikawa M, Nishizawa M, Oizumi T (2000) Expression of water channel mRNA following cerebral ischemia. Acta Neurochir Suppl 76:239–241
50. Scott M, Foster D, Mirenda C, Serban D, Coufal F, Walchli M, Torchia M, Groth D, Carlson G, DeArmond SJ, Prusiner SB (1989) Transgenic mice expressing hamster prion protein produce species-specific scrapie infectivity and amyloid plaques. Cell 59:847–857
51. Scott MD. Groth D, Foster D, Torchia M, Yang SL, DeArmond SJ, Prusiner SB (1993) Propagation of prions with artificial properties in transgenic mice expressing chimeric PrP genes. Cell 73:979–988
52. Solenov EI, Vetrivel L, Oshio K, Manley GT, Verkman AS (2002) Optical measurement of swelling and water transport in spinal cord slices from aquaporin null mice. J Neurosci Meth 113:85–90
53. Sun MC, Honey CR, Berk C, Wong NL, Tsui JK (2003) Regulation of aquaporin-4 in a traumatic brain injury model in rats. J Neurosurg 98:565–569
54. Taniguchi M, Yamashita T, Kumura E, Tamatani M, Kobayashi A, Yokawa T, Maruno M, Kato A, Ohnishi T, Kohmura E, Tohyama M, Yoshimine T (2000) Induction of aquaporin-4 water channel mRNA after focal cerebral ischemia in rat. Mol Brain Res 78:131–137
55. Tsuboi Y, Baba Y, Don-ura K, Imamura A, Fujioka S, Yamada T (2005) Diffusion-weighted MRI in familial Creutzfeldt-Jakob disease with the codon 200 mutation in the prion protein gene. J Neurol Sci 232:45–49
56. Ukisu R, Kushihashi T, Kitanosono T, Fujisawa H, Takenaka H, Ohgiya Y, Gokan T, Munechika H (2005) Serial diffusion-weighted MRI of Creutzfeldt-Jakob disease. Am J Roentgenol 184:560–566
57. Vajda Z, Pedersen M, Fuchtbauer EM, Wertz K, Stodkilde-Jorgensen H, Sulyok E, Dóczi T, Neely JD, Agre P, Frokiaer J, Nielsen S (2002) Delayed onset of brain edema and mislocalization of aquaporin-4 in dystrophin-null transgenic mice. Proc Natl Acad Sci USA 99:13131–13136
58. Vajda Z, Promeneur D, Dóczi T, Sulyok E, Frokiaer J, Ottersen OP, Nielsen S (2000) Increased aquaporin immunoreactivity in rat brain in response to systemic hyponatremia. Biochem Biophys Res Commun 270:495–503
59. Venero JL, Machado A, Cano J (2004) Importance of aquaporins in the physiopathology of brain edema. Curr Phar Des 10:2153–2161
60. Verkman AS (2002) Physiological importance of aquaporin water channels. Ann Med 34:192–200
61. Warth A, Mittelbronn M, Wolburg H (2005) Redistribution of the water channel protein aquaporin-4 and the K+ channel protein Kir4.1 differs in low- and high-grade human brain tumors. Acta Neuropathol 109:418–426
62. Xiang W, Windl O, Westner IM, Neumann M, Zerr I, Lederer RM, Kretzschmar HA (2005) Cerebral gene expression profiles in sporadic Creutzfeldt-Jakob disease. Ann Neurol 58:242–257
63. Xiang W, Windl O, Wünsch, Dugas M, Kohlmann A, Dierkes N, Westner IM, Kretzschmar HA (2004) Identification of differentially expressed genes in scrapie-infected mouse brains by using global gene expression technology. J Virol 78:11051–11060
64. Xiao F, Arnold TC, Zhang S, Brown C, Alexander JS, Carden DL, Conrad SA (2004) Cerebral cortical aquaporin-4 expression in brain edema following cardiac arrest in rats. Acad Emerg Med 11:1001–1007

5.3- *Adenosine A_1 receptor expression and activity is increased in the cerebral cortex in Creutzfeldt-Jakob disease and in bovine spongiform encephalopathy-infected bovine-PrP mice (2006)*

Agustin Rodríguez, Mairena Martin, Jose Luis Albasanz, Marta Barrachina, Juan María Torres, Juan Carlos Espinosa, Isidro Ferrer

J. Neuropathol. Exp. Neurol. 2006 Oct; 65 (10): 964-75

Las enfermedades por prión están caracterizadas por pérdida neuronal, gliosis astrocítica, cambio espongiforme y deposición PrP^{res}. La ECJ es la enfermedad priónica humana más prevalente, mientras que el *Scrapie* y la EEB son las enfermedades por prión animales más comunes. Se han propuesto varios candidatos como mediadores de la degeneración en las enfemedades por prión, uno de ellos el glutamato. Estudios recientes han mostrado una disminución de receptores de glutamato asi como de la vía de señalización de la PLC en la corteza cerebral en ECJ, sugiriendo que esta importante vía neuromoduladora y neuroprotectora está atenuada en ECJ. La adenosina está involucrada en la regulación de distintos procesos metabólicos bajo condiciones fisiológicas y patológicas. La función de la adenosina está mediada por los ARs, que están divididos en cuatro tipos: A_1, A_{2A}, A_{2B} y A_3. Los A_1Rs son receptores acoplados a proteína-G que inducen la inhibición de la actividad AC. La acción inhibidora más dramática de los ARs se produce en el sistema glutamatérgico. Por esos motivos, en este trabajo hemos examinado los niveles de los A_1Rs en la corteza frontal de 12 pacientes con ECJ y 6 controles y en ratones transgénicos para la PrP bovina infectados con EEB (BoPrP-Tg110 mice) a diferentes tiempos de incubación para estudiar las modificaciones en los A_1Rs con la progresión de la enfermedad. Se han encontrado niveles de proteína incrementados de A_1Rs en la corteza frontal en ECJ y en estadíos avanzados de la enfermedad en el modelo murino de EEB coincidentes con la aparición de expresión de PrP^{res}. Además, se ha analizado la actividad de los A_1Rs por ensayos *in vitro* con membranas celulares de corteza frontal en ECJ. Se ha observado un aumento de la actividad del receptor en ECJ comparado con controles, considerando la disminución de la producción de cAMP, inducido por estimulación con forskolina en respuesta a los agonistas del receptor A_1R (CHA y CPA). Finalmente, los niveles de mRNA del A_1R son similares en los casos ECJ y controles, lo cual sugiere un reciclado de A_1R anormal o una deregulación de las vías de señalización asociadas a los *raft* en ECJ. Estos resultados muestran, en primera instancia, una sensibilización de los A_1Rs en las enfermedades priónicas.

J Neuropathol Exp Neurol

Vol. 65, No. 10
October 2006
pp. 964–975

ORIGINAL ARTICLE

Adenosine A_1 Receptor Protein Levels and Activity Is Increased in the Cerebral Cortex in Creutzfeldt-Jakob Disease and in Bovine Spongiform Encephalopathy-Infected Bovine-PrP Mice

Agustín Rodríguez, Mairena Martín, PhD, José Luís Albasanz, Marta Barrachina, PhD, Juan Carlos Espinosa, PhD, Juan María Torres, PhD, and Isidro Ferrer, MD, PhD

Abstract

Prion diseases are characterized by neuronal loss, astrocytic gliosis, spongiform change, and abnormal protease-resistant prion protein (PrP^{res}) deposition. Creutzfeldt-Jakob disease (CJD) is the most prevalent human prion disease, whereas scrapie and bovine spongiform encephalopathy (BSE) are the most common animal prion diseases. Several candidates have been proposed as mediators of degeneration in prion diseases, one of them glutamate. Recent studies have shown reduced metabotropic glutamate receptor/phospholipase C signaling in the cerebral cortex in CJD, suggesting that this important neuromodulator and neuroprotector pathway is attenuated in CJD. Adenosine is involved in the regulation of different metabolic processes under physiological and pathologic conditions. Adenosine function is mediated by adenosine receptors, which are categorized into 4 types: A_1, A_{2A}, A_{2B}, and A_3. A_1Rs are G-protein-coupled receptors that induce the inhibition of adenylyl cyclase activity. The most dramatic inhibitory actions of adenosine receptors are on the glutamatergic system. For these reasons, we examined the levels of A_1Rs in the frontal cortex of 12 patients with CJD and 6 age-matched controls and in BSE-infected bovine-PrP transgenic mice (BoPrP-Tg110 mice) at different postincubation times to address modifications in A_1Rs with disease progression. A significant increase in the protein levels of A_1Rs was found in the cerebral cortex in CJD and in the murine BSE model at advanced stages of the disease and coincidental with the appearance of PrP^{res} expression. In addition, the activity of A_1Rs was analyzed by in vitro assays with isolated membranes of the frontal cortex in CJD. Increased activity of the receptor, as revealed by the decreased forskolin-stimulated cAMP production in response to the A_1R agonists cyclohexyl adenosine and cyclopentyl adenosine, was observed in CJD cases when compared with controls. Finally, mRNA A_1R levels were similar in CJD and control cases, thus suggesting abnormal A_1R turnover or dysregulation of raft-associated signaling pathways in CJD. These results show, for the first time, sensitization of A_1Rs in prion diseases.

Key Words: Adenosine receptor, Bovine-PrP transgenic mice, Bovine spongiform encephalopathy, Creutzfeldt-Jakob disease, Prion.

INTRODUCTION

Prion diseases are characterized by neuronal loss, astrocytic gliosis, spongiform change, and abnormal protease-resistant prion protein (PrP^{res}) deposition. Prion diseases are caused by the conversion of cellular prion protein (PrP^{C}) into an abnormal β-sheet-enriched and partially proteinase K-resistant isoform (PrP^{res}) (1–3). PrP^{res} is able, in turn, to recruit PrP^{C}, resulting in an autocatalytic propagation in the pathogenic conformation of the protein (1–4). PrP^{C} is an anchored cell membrane glycoprotein that is expressed in several tissues but enriched in brain. Creutzfeldt-Jakob disease (CJD), fatal familial insomnia, Kuru, and Gerstmann-Straüssler-Scheinker disease are human prion diseases, whereas scrapie and bovine spongiform encephalopathy (BSE) are the most common animal prion diseases (1, 5–7). The sporadic form of CJD is the most frequent type, representing approximately 85% of total CJD cases. A common polymorphism at codon 129 of *PRNP* has important effects on clinical features, transmissibility, and susceptibility to the disease (5). PrP^{C} is involved in copper metabolism, signal transduction, and oxidative stress (1, 2, 8). However, mechanisms leading to neurodegeneration in prion diseases are not merely related with loss of PrP^{C} function, but also to other mechanisms involved in neurodegeneration and cell death. Among these, glutamate may play a cardinal role as a pivotal excitotoxic factor. In this line, PrP-induced cellular damage is markedly reduced after N-methyl-d-aspartate (NMDA) receptor inhibition in vitro (9). Despite this working hypothesis, little is known about neurotransmitter receptors in the cerebral cortex in CJD and related prion diseases (10). Yet recent studies have shown reduced metabotropic glutamate receptor/phospholipase C signaling in the cerebral

From the Institut de Neuropatologia (AR, MB, IF), Servei Anatomia Patològica, IDIBELL-Hospital Universitari de Bellvitge; Facultat de Medicina (IF), Universitat de Barcelona, 08907 Hospitalet de Llobregat; Departamento de Química Inorgánica (MM, JLA), Orgánica y Bioquímica, Facultad de Químicas, Centro Regional de Investigaciones Biomédicas, Universidad de Castilla-La Mancha, Ciudad Real; and Centro de Investigación en Sanidad Animal (CISA) (JCE, JMT), INIA, 28130 Valdeolmos, Madrid, Spain.

Send correspondence and reprint requests to: Dr. Isidro Ferrer, Institut Neuropatologia, Servei Anatomia Patològica, IDIBELL-Hospital Universitari de Bellvitge, c/Feixa Llarga sn, 08907 Hospitalet de Llobregat, Spain; E-mail: 8082ifa@comb.es

This study was supported by the Ministerio de Ciencia y Tecnología: EET 2001-3724 and EET2002-05168 and CAL01-018 NoE Neuroprion CT-2004-506579, Ministerio de Sanidad: FIS grants G03/167 and 05/1631, and grants 04/301-01 and 04/301-02 from Fundació "La Caixa".

cortex in CJD (11), suggesting that this important neuromodulator and neuroprotector pathway is attenuated in CJD.

Adenosine is involved in the regulation of different metabolic processes under physiological and pathologic conditions and mediates its function through the adenosine receptors (12–14). These are a group of G-protein-coupled receptors that are classified into 4 groups: A_1, A_{2a}, A_{2b}, and A_3. A_1Rs and A_3Rs mediate inhibition of adenylyl cyclase (AC) activity through Gαi-proteins, and A_{2a}As and A_{2b}s mediate stimulation of AC activity through Gαs proteins (15, 16). In addition, stimulation of A_1Rs activates phospholipase C, phospholipase D, and several types of K^+ channels and inhibits Ca^{2+} currents (12, 16). A_1 receptors are found in several tissues (17, 18), but they are enriched in the central nervous system, where they are expressed in the cerebral cortex, hippocampus, cerebellum, thalamus, and brainstem (17–19). In the brain, adenosine modulates neuronal activity by decreasing presynaptic release of various neurotransmitters (14, 20, 21). The most dramatic inhibitory actions are on the glutamatergic system (13, 22, 23). Molecular and functional interactions between A_1Rs and $mGluR_1$ have been reported (24). In the same line, several studies have shown that presynaptic A_1Rs can mediate the neuroprotective effects of adenosine in neurons and glial cells by limiting the opening of voltage-dependent Ca^{2+} channels, attenuating the neuronal Ca^{2+} influx, and then decreasing glutamate release (25, 26). Similarly, adenosine can inhibit glutamate-induced calcium influx and voltage-gated calcium currents through activation of A_1Rs in rat ganglion cells (27). In addition, adenosine acting through postsynaptic A_1Rs may activate K^+ channels, leading to hyperpolarization of postsynaptic neurons and promoting NMDA receptor inhibition (19).

Based on these findings and in an attempt to learn about adenosine receptors in prion diseases, the present work uses Western blotting to study the expression of A_1Rs in the frontal cortex in CJD and in the cerebral cortex of BSE-infected bovine-PrP transgenic mice (BoPrP-Tg110 mice). We also analyzed A_1R gene expression by TaqMan polymerase chain reaction (PCR) in CJD compared with age-matched controls. To test whether modifications were specific to A_1Rs, expression levels of A_2Rs were also examined in human and mouse brains. Protein studies have been accompanied with in vitro assays of AC activity in human frontal cortex using A_1R agonists cyclohexyl adenosine (CHA) and cyclopentyl adenosine (CPA). Together, the present observations show for the first time abnormal regulation and activity of A_1Rs in the cerebral cortex in prion diseases.

MATERIALS AND METHODS

General Aspects of Creutzfeldt-Jakob Disease Cases and Age-Matched Controls

The brains of 12 patients with sporadic CJD and 6 age-matched controls were obtained from 3 to 8 hours after death and were immediately prepared for biochemical studies. The main clinical characteristics are summarized in Table 1. Criteria for the neuropathologic, molecular, and phenotypic diagnosis of CJD used in the present series are those currently accepted and detailed elsewhere (5, 28). The majority of cases used in the present series are those used in a previous work focused on metabotropic glutamate receptors in CJD (11). For morphologic studies, formalin-fixed, dewaxed paraffin sections were stained with hematoxylin and eosin, Klüver-Barrera, and periodic acid-Schiff

TABLE 1. Main Clinical Characteristics of Creutzfeldt-Jakob Disease and Control Cases

Case	Age	Gender	Codon 129	14-3-3	EEG	First Symptom	Survival in Months	PrP Type
CJD1	60	M	MM	+	+	Dementia	3	1
CJD2	60	F	MM	+	+	Dementia	6	1
CJD3	55	M	MM	+	+	Ataxia	3	1
CJD4	74	M	MM	+	+	Dementia	5	1
CJD5	66	M	VV	+	+	Ataxia	4	2
CJD6	53	F	MM	+	+	Dementia	2	1
CJD7	85	F	MV	+	+	Dementia	14	1
CJD8	71	M	VV	+	–	Ataxia	3	2
CJD9	70	F	MM	+	+	Dementia	3	1
CJD10	59	M	MM	?	+	Dementia	8	1
CJD 11	60	M	MM	+	–	Ataxia	8	2
CJD 12	68	F	MM	+	+	Dementia	4	1
C1	62	M						
C2	72	F						
C3	73	M						
C4	58	F						
C5	68	M						
C6	69	M						

EEG, typical generalized triphasic pseudoperiodic complexes; 14-3-3, the presence (+) or absence of this protein in the cerebrospinal fluid; M, methionine; V, valine; PrP type, PrP^{res} type 1, lower band of nonglycosylated PrP^{res} of 21 kDa; type 2, lower band of nonglycosylated PrP^{res} of 19 kDa.

and processed for immunohistochemistry to glial fibrillary acidic protein, CD68 and *Licopericum esculentum* lectin (for microglia), α-synuclein, tau (phospho-specific antibodies), β-amyloid, α-B crystallin, and PrP. For biochemical studies, samples of the frontal cortex (area 8) were frozen in liquid nitrogen and stored at −80°C until use. Neuron loss, spongiform degeneration, astrocytic gliosis, and microgliosis involving the cerebral neocortex, striatum, and cerebellum occurred in every case. Synaptic-like PrP^{res} deposits were found in the cerebral cortex and striatum in every case. Small plaque-like PrP^{res} were rarely observed in the frontal cortex. Special care was taken to exclude CJD cases with associated β-amyloid deposition or Alzheimer disease pathology. Therefore, none of the CJD cases in the present series had concomitant diffuse or neuritic plaques. In addition, samples from 2 cases with cerebral infarction of 48, 73, and 68 hours (perinecrotic areas) and samples from subacute plaques from one patient with multiple sclerosis were processed for comparative purposes. Also for comparative purposes, the frontal cortex of 4 cases with Alzheimer disease (AD) limbic stage (III/IVB) and 4 cases with isocortical involvement (stages V/VIC of Braak and Braak [29]) were processed in parallel with frontal samples from 6 additional age-matched controls. Finally, samples of the frontal cortex from one control individual were obtained 3 hours postmortem and immediately frozen (time 0) or stored at 4°C for 3 hours, 6 hours, or 22 hours and then frozen to mimic variable postmortem delay in tissue processing and its effect on protein preservation.

Bovine Spongiform Encephalopathy Infection in BoPrP-Tg110 Mice

The generation and characteristics of these transgenic mice, as well as the susceptibility and timing of the incubation after BSE inoculation and the behavioral and neuropathologic findings of infected mice, have been described in detail elsewhere (30). Briefly, BoPrP-Tg110 mice express bovine PrP insert introduced in a mouse with $PrP^{0/0}$ background that confers susceptibility to BSE infection. BoPrP-Tg110 mice express bovine PrP instead of murine-PrP. These transgenic mice do not develop any alteration in their gene/protein expression when compared with wild-type mice. As far as we know, Tg mice have identical biologic properties as wild-type mice except for their susceptibility to BSE infection (30). For BSE infection, BoPrP-Tg110 mice (females, 6–7 weeks old, weighing approximately 20 g) were inoculated in the right parietal lobe using a 25-gauge disposable hypodermic syringe with 20 μL of 10% brain homogenate. TSE/08/59 inoculum, produced with a pool from the brainstem of 49 BSE-infected cattle and supplied by the Veterinary Laboratory Agency (New Haw, Addlestone, Surrey, U.K.), was used. As negative controls, we used the same BoPrP-Tg110 mice but inoculated with healthy cow brain. To minimize the risk of bacterial infection, homogenates were heated at 70°C for 10 minutes before inoculation. To evaluate the clinical signs appearing after inoculation, mice were observed daily and their neurologic status was assessed twice a week. The presence of 3 signs of neurologic dysfunction (using 10 different items) (31, 32) was required for a mouse to score positive for prion disease. Animals were killed at 60 (n = 4), 150 (n = 3), 210 (n = 3), and 270 (n = 4) days postinoculation (dpi). The brains were rapidly removed from the skulls and immediately prepared for neuropathologic and biochemical studies.

Histopathology and Immunohistochemistry in Mice

Tissue sections containing medulla oblongata at the level of the obex and the pontine area, cerebellum, and diencephalon, including thalamus, hippocampus, and cerebral cortex, were processed for routine histologic methods and immunohistochemistry. The avidin–biotin–peroxidase complex (ABC) method was used for the immunohistochemical detection of PrP^{res} as previously described (30). Briefly, tissue sections were incubated at 4°C overnight with the primary 2A11 mAb diluted 1:400 in phosphate buffer saline (PBS). This was followed by incubation with a secondary anti-mouse IgG (Dako, Madrid, Spain) diluted 1:20 in PBS. The immunoreaction was visualized with 3,3′-diaminobenzidine tetrahydrochloride (Sigma, Madrid, Spain) and 0.01% hydrogen peroxide. Finally, the sections were slightly counterstained with Mayer's hematoxylin, dehydrated, and mounted on glass slides. The specific primary antibody was replaced by PBS or by nonimmune mouse serum in some tissue sections used as negative controls. The

TABLE 2. Main Characteristics of Bovine Spongiform Encephalopathy (BSE)-Infected Bovine-PrP Transgenic Mice

	Controls				BSE			
	1	2	3	4	1	2	3	4
				60 dpi				
WB	–	–	–	–	–	–	–	–
IHC	–	–	–	–	–	–	–	–
HP	–	–	–	–	–	–	–	–
CS	–	–	–	–	–	–	–	–
				150 dpi				
WB	–	–	–		–	–	–	
IHC	–	–	–		–	–	–	
HP	–	–	–		–	–	–	
CS	–	–	–		–	–	–	
				210 dpi				
WB	–	–	–		–	–	–	
IHC	–	–	–		–	+	–	
HP	–	–	–		–	+	–	
CS	–	–	–		–	–	–	
				270 dpi				
WB	–	–	–	–	+	+	+	+
IHC	–	–	–	–	+	+	+	+
HP	–	–	–	–	+	+	+	+
CS	–	–	–	–	+	+	+	+

dpi, days postinoculation. Brain samples were analyzed by Western blot after proteinase-K treatment for PrP^{res} detection (WB), by histopathology (HP), or by immunohistochemistry (IHC).

Diseased mice were scored by clinical signs (CS) before euthanasia. HP changes are characterized by spongiform change and mild astrocytic gliosis. IHC indicates positive PrP^{res} immunoreactivity. Note that only one animal showed the presence of PrP^{res} at 210 days postinoculation.

main characteristics of BSE-infected bovine-PrP transgenic mice are summarized in Table 2.

Plasma Membrane Isolation

Frontal cortex (0.5 g) from controls and CJD cases was homogenized in a glass tissue grinder in 20 volumes (w/v) of isolation cold buffer containing 50 mM Tris-HCl (pH 7.4) and 10 mM $MgCl_2/6H_20$ plus 0.1 mM phenylmethylsufonyl fluoride, 5 μg/mL aprotinin, 10 μg/mL leupeptin, 5 μg/mL pepstatin, and 1 mM sodium orthovanadate to inhibit endogenous phosphatases. After a first centrifugation at 1,000 × *g* for 5 minutes, the supernatant was discarded and the pellet was resuspended with the addition of 1.5 mL of isolation cold buffer and then centrifuged at 27,000 × *g* for 30 minutes. The corresponding supernatant was discarded and the pellet was resuspended in 200 μL of isolation cold buffer and stored at −20°C. Protein concentration was measured by the BCA method.

Western Blotting

Thirty micrograms of protein were mixed with loading buffer containing 0.125 M Tris (pH 6.8), 20% glycerol, 10% β-mercaptoethanol, 4% SDS, and 0.002% bromophenol blue and heated at 95°C for 5 minutes. Sodium dodecyl sulphate–polyacrylamide gel electrophoresis (10% SDS-PAGE) was carried out using a miniprotean system (Bio-Rad, Madrid, Spain) with molecular-weight standards (Bio-Rad). Proteins were then transferred to nitrocellulose membranes using an electrophoretic transfer system (semidry; Bio-Rad). The membranes were washed with TTBS containing 10 mM Tris-HCl pH 7.4, 140 mM NaCl, and 0.1% Tween-20. Nonspecific blocking was performed by incubating the membranes in TTBS containing 5% skim milk for 20 minutes. Membranes were incubated with the primary antibodies at 4°C overnight. The rabbit polyclonal anti-A_1R antibody (Oncogene, Barcelona, Spain) was used at a dilution of 1:500. The rabbit polyclonal anti-A_{2A}R antibody (Santa Cruz Biotechnology, Madrid, Spain) was used at a dilution of 1:300. The rabbit polyclonal anti-AC1 antibody mapping at the C-terminus of AC1 of human origin (Santa Cruz Biotechnology) was used at a dilution of 1:300. The anti-A_1R antibody (Oncogene) was raised against a synthetic peptide (CQPKPPIDEDLPEEKAED) corresponding to amino acids 309–326 of rat adenosine receptor subtype A1 (A1AR). The anti-A_{2A}R antibody (Santa Cruz) is a rabbit polyclonal antibody raised against amino acids 331–412 mapping within the C-terminal cytoplasmic domain of adenosine A_{2A}R of human origin. The AC1 antibody (Santa Cruz) is an affinity-purified rabbit polyclonal antibody raised against a peptide mapping at the C-terminus of A cyclase 1 of human origin. After rinsing, the membranes were incubated with the corresponding anti-rabbit secondary antibody (Dako) at a dilution of 1:1,000 for 1 hour at room temperature. The membranes were then washed and developed with the chemiluminescence ECL system (Amersham, Madrid, Spain) followed by exposure of the membranes to autoradiographic films at 4°C. The monoclonal anti-β-actin antibody (Sigma) was used at a dilution of 1:5,000 as a control of protein loading.

A_1R Immunohistochemistry

Control and disease cases were fixed, treated with formic acid, and embedded in paraffin in the same way. Paraffin sections, 4-μm thick, were processed with the EnVision + system peroxidase (DAB) procedure (Dako). The rabbit polyclonal anti-A_1R antibody (Oncogene) was used at a dilution of 1:500. The rabbit polyclonal anti-A_{2A}R antibody (Santa Cruz Biotechnology) was used at a dilution of 1:300.

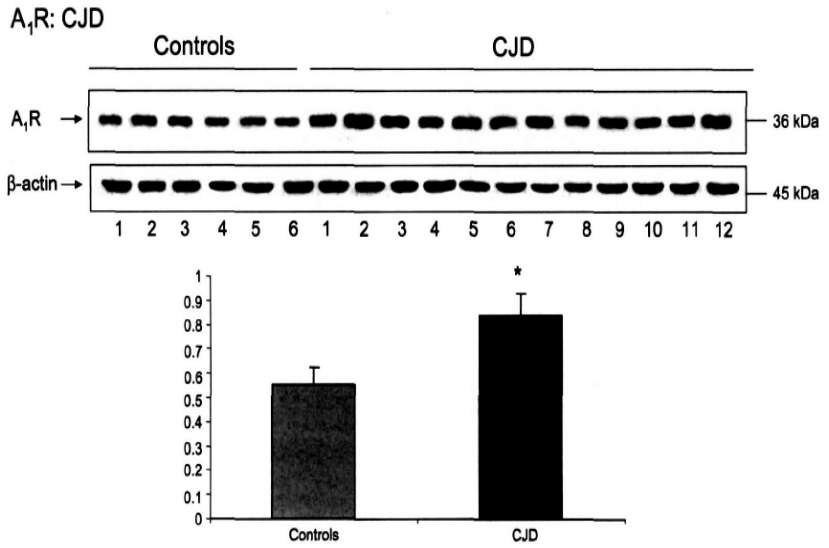

FIGURE 1. Increased A_1Rs protein levels in the frontal cortex in Creutzfeldt-Jakob disease when compared with age-matched controls. β-actin is used as a control of protein loading. Numbers in the graph are arbitrary units. Data are means ± standard deviation. Student *t*-test, $p < 0.05$.

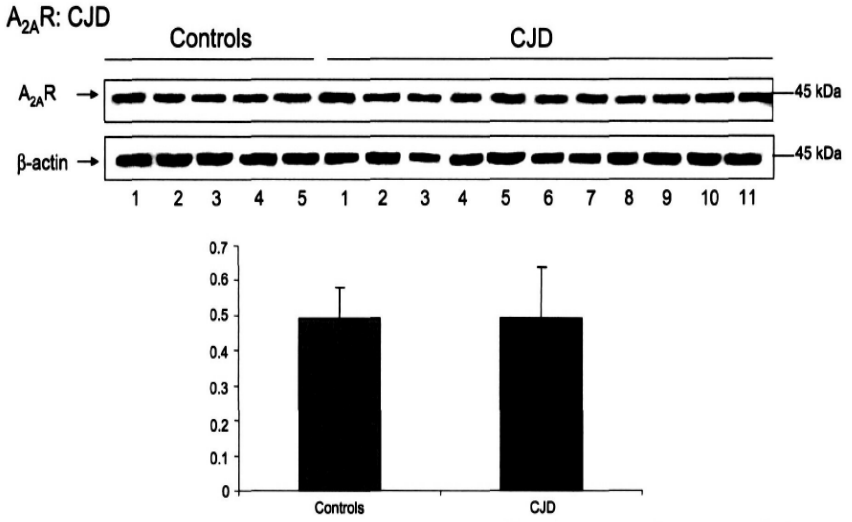

FIGURE 2. No modifications in the protein levels of A_2Rs are seen in Creutzfeldt-Jakob disease when compared with age-matched controls. β-actin is used as a control of protein loading. Numbers in the graph are arbitrary units.

The peroxidase reaction was visualized with 0.05% diaminobenzidine and 0.01% hydrogen peroxide (brown precipitate). Some sections were incubated without the primary antibody. No immunoreactivity was found in these samples.

Preliminary studies have shown that this antibody is not suitable for immunogold–electron microscopy studies. Therefore, no further attempts were made to localize A_1R receptors by electron microscopy.

mRNA Isolation

mRNA isolation was carried out in 2 steps as previously described (33). Total RNA was isolated using TRizol Reagent (Life Technologies, Barcelona, Spain) followed by the RNeasy Midi Kit (Qiagen, Barcelona, Spain). Absence of genomic DNA in RNA samples was confirmed by the Agilent bioanalyzer. Frozen human frontal cortex samples were directly homogenized in 1 mL of TRizol Reagent per 100 mg tissue and left for 5 minutes at room temperature. Next, 200 μL of chloroform was added and mixed vigorously. After 3 minutes at room temperature, the samples were centrifuged (12,000 × *g*, 15 minutes, ACD. The resulting supernatants were mixed with 0.5 mL of isopropanol, left at room temperature for 10 minutes, and then centrifuged (12,000 × *g*, 10 minutes, 4°C). After this step, the pellets were washed with 1 mL of ethanol 70% and centrifuged at 7500 × *g* for 5 minutes at 4°C. Then, the pellets were dried at room temperature for 10 minutes and resuspended in 100 μL of RNase-free water and incubated in a water bath at 55°C to 60°C for 10 minutes. Purified total RNA was mixed with 350 μL of RTL buffer (containing mercaptoethanol) provided with the RNeasy Midi Kit and 250 μL of ethanol 96%. The resulting solution was poured into an RNeasy column and centrifuged at 8000 × *g* for 15 seconds. Next, 500 μL of RPE buffer (provided with the RNeasy Midi Kit) was also poured into the column and centrifuged at 8000 × *g* for 15 seconds. This step was done twice followed by a centrifugation at 8000 × *g* for 2 minutes to completely elute the RPE buffer. Finally, the RNA was eluted by adding 30 to 40 μL of

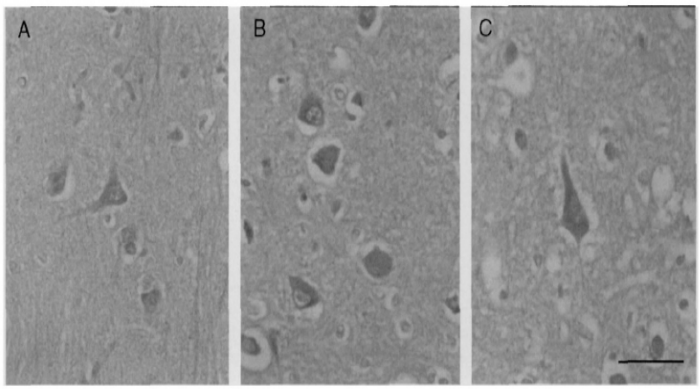

FIGURE 3. A_1R immunohistochemistry in **(A)** control and **(B, C)** Creutzfeldt-Jakob disease (CJD). A_1R immunoreactivity is found in the cytoplasm of neurons and in the neuropil in control and diseased cases. Moderate increased immunoreactivity is found in CJD when compared with controls. Paraffin sections lightly counterstained with hematoxylin. Scale bar = 25 μm.

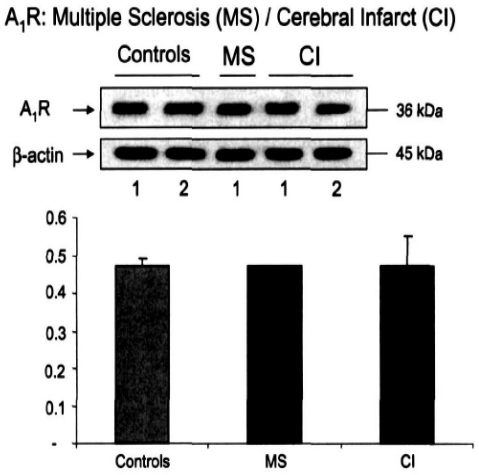

FIGURE 4. No modifications in the protein levels of A_1Rs are seen in subacute plaques in one case of multiple sclerosis (MS) and in the perinecrotic area in 2 cases with cerebral infarct when compared with age-matched controls. β-actin is used as a control of protein loading. Numbers in the graph are arbitrary units.

RNase-free water and centrifuging the column at 8000 × *g* for 1 minute. The columns used exclude tRNA, 5S, and 5.8S ribosomal RNA. The concentration of each sample was obtained from A260 measurements. RNA integrity was confirmed by using the Agilent 2100 BioAnalyzer (Agilent, Barcelona, Spain).

cDNA Synthesis

For each 100 μL reverse transcription reaction, 2 μg human RNA was mixed with 2.5 μM random hexamers, 1x TaqMan reverse transcriptase buffer, 5.5 mM $MgCl_2$, 500 μM each dATP, dTTP, dCTP and dGTP, 0.4 U/μL RNase inhibitor, and 1.25 U/μL MultiScribe reverse transcriptase (Applied Biosystems, Barcelona, Spain). Reactions were carried out at 25°C for 10 minutes to maximize primer-RNA template binding followed by 30 minutes at 48°C and then by incubation for 5 minutes at 95°C to deactivate reverse transcriptase. Parallel reactions for each RNA sample were run in the absence of MultiScribe reverse transcriptase to assess the degree of contaminating genomic DNA.

TaqMan Probes

Human β-glucuronidase (GUS) (Hs99999908_m1, TaqMan probe 5′-GACTGAACAGTCACCGACGA GAGTG-3′), human β-actin (Hs99999903_m1, TaqMan probe 5′-TCGCCTTTGCCGATCCGCCGCCCGT-3′), and human A_1R (Hs00379752_m1, TaqMan probe 5′-GAT CCCTCTCCGGTACAAGATGGTG-3′) were examined in the present study. The TaqMan assay for GUS is located between 11 and 12 exon boundary at position 1816 of NM_000181.1 transcript sequence. The predicted amplicon size is approximately 81 base pairs. The TaqMan assay for β-actin is located in the 5′ UTR region at position 36 of NM_001101.2 transcript generating an amplicon of 171 base pairs. The TaqMan assay for A_1R is located between 5 and 6 exon boundary, at position 752 of NM_000674.1 transcript, generating an amplicon of 111 base pairs.

TaqMan Polymerase Chain Reaction

TaqMan PCR assays for A_1R were performed in duplicate on cDNA samples in 96-well optical plates using an ABI Prism 7700 Sequence Detection system (Applied Biosystems). The plates were capped using optical caps (Applied Biosystems). The ABI Prism 7700 measures the

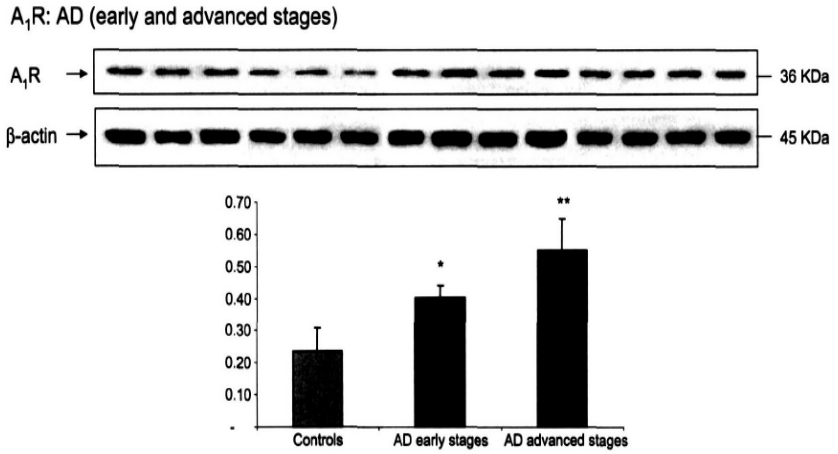

FIGURE 5. Increased A_1Rs protein levels in the frontal cortex in 4 cases with stage III/IVB (lanes 7–10) and in 4 cases of Alzheimer disease stages V/VIC of Braak and Braak (lanes 11–14) compared with A_1Rs protein levels in 6 age-matched controls (lanes 1–6). β-actin is used as a control of protein loading. Numbers in the graph are arbitrary units. Data are means ± standard deviation. Student *t*-test, $p < 0.05$ (*) and $p < 0.01$ (**).

fluorescent accumulation of the PCR product by continuously monitoring cycle threshold (Ct), which is an arbitrary value assigned manually to a level somewhere above the baseline but in the exponential phase of PCR where there are no rate-limiting components. The Ct value sets the point at which the sample amplification plot crosses the threshold. The Ct values correlate with the initial amount of specific template. For each 20 μL TaqMan reaction, 9 μL cDNA (diluted 1/50, which corresponds approximately to the cDNA from 4 ng of RNA) was mixed with 1 μL 20x TaqMan Gene Expression Assays and 10 μL of 2x TaqMan Universal PCR Master Mix (Applied Biosystems). Parallel assays for each sample were carried out using primers and probes with β-actin and GUS for normalization. The reactions were carried out using the following parameters: 50°C for 2 minutes, 95°C for 10 minutes, 40 cycles of 95°C for 15 seconds, and 60°C for 1 minute. Standard curves were prepared for ADORA1 (A_1R), β-actin, and GUS using serial dilutions of control human brain RNA. Finally, all TaqMan PCR data were captured using the Sequence Detector Software (SDS version 1.9; Applied Biosystems). The TaqMan probe for β-actin does not recognize DNA because it matches to exon–exon boundary. In this line, the gene expression ID suffix indicates the assay placement: "_m" indicates an assay whose probe spans an exon junction and does not detect genomic DNA. "_g" indicates an assay that may detect genomic DNA. In our study, the TaqMan probe for β-actin has an assay ID hs99999903_m1 indicating that this probe only recognizes cDNA.

Determination of Adenylyl Cyclase Activity

Adenylyl cyclase activity was determined in plasma membranes as previously described (34, 35) with minor modifications. Plasma membranes were first incubated with adenosine deaminase (ADA, 5 U/mg protein) at 37°C for 30 minutes to remove endogenous adenosine. Assay was performed with 20 μg of protein in a final volume of 250 μL of 50 mM Tris-HCl (pH 7.4) containing 5 mM $MgCl_2$, 1 mM DTT, 1 mg/mL BSA, 1 mg/mL creatine kinase, 10 mM creatine phosphate, and 0.1 mM Ro 20-1724 (a phosphodiesterase inhibitor). Plasma membranes were incubated at 37°C for 6 minutes in the absence (basal activity) or in the presence of 5 μM GTPγS and 50 μM or 100 μM forskolin. A1R/AC functionality was determined in the presence of 1 mM CPA

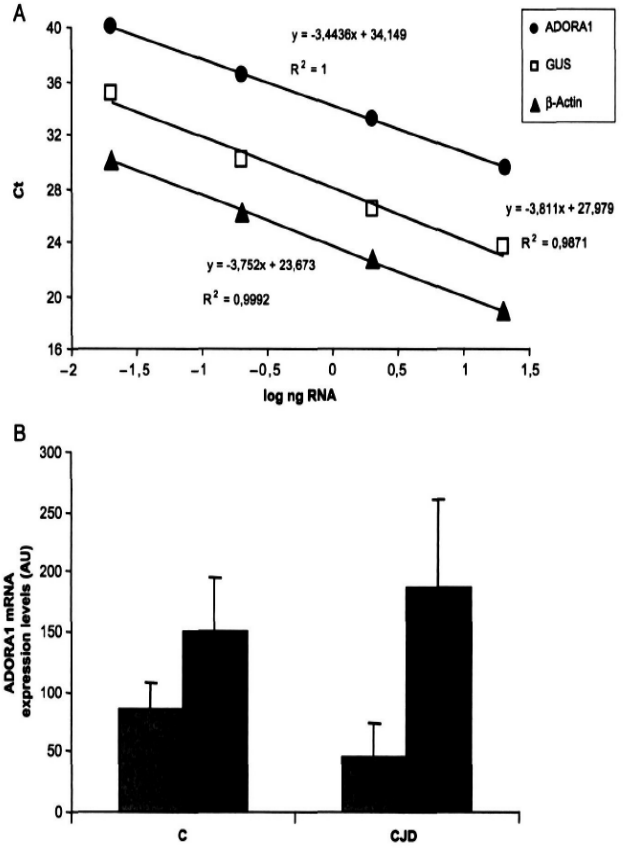

FIGURE 6. (A) Representative standard curves for ADORA1, GUS, and β-actin constructed from several concentrations of control human brain RNA. Cycle threshold (CT) values (y-axis) versus log of several RNA concentrations of control samples (x-axis) show a reverse linear correlation. **(B)** ADORA1 mRNA expression levels normalized (arbitrary units) by GUS (grey) or β-actin (black) in Creutzfeldt-Jakob disease (CJD) and age-matched controls (C) No significant differences in mRNA expression levels are seen between CJD cases and controls.

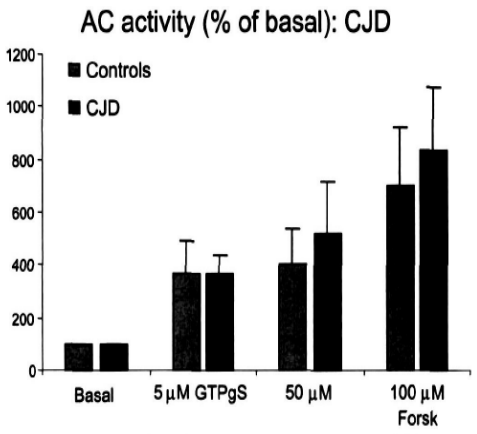

FIGURE 7. Adenyl cyclase (AC) activity in Creutzfeldt-Jakob disease (CJD). cAMP levels detected by the cAMP enzyme immunoassay kit in vitro are expressed as the percentage of AC basal activity in the presence of 5 μM GTPγS, 50 μM forskolin, and 100 μM forskolin (forsk). No significant differences in AC activity are seen between CJD and control cases in the different paradigms. Data are means ± standard deviation. Student *t*-test, $p < 0.05$.

(N^6-cyclopentyladenosine) and 1 mM CHA (cyclohexyl adenosine) used as specific A_1Rs agonists (15). The reaction was started by adding 200 μM ATP and continued with incubation at 37°C for 10 minutes while shaking. The reaction was stopped by boiling the samples. This was followed by centrifugation at 12,000 × *g* for 5 minutes. Fifty microliters of the supernatant was used to determine cAMP accumulation. cAMP concentration was determined by using the cAMP enzyme immunoassay kit (Assay Designs, Inc., Bionova, Madrid, Spain) following the instructions of the supplier. The resulting plates were examined with a plate reader at 405 nm and the results analyzed using Microsoft Excel. Microsoft Excel was used with GraphPad Prism to analyze the numeric data obtained from the reader plate using a weighed 4-parameter logistic curve. Excel was also used for the graphic representation of these results. All the experiments were carried out in triplicate.

Densitometry and Statistical Processing of Data

Protein expression levels were determined by densitometry of the bands using Total Laboratory v2.01 software. This software detects the bands obtained in Western blots and gives individual values that are dependent on the light quantification of the corresponding band. Measurements are expressed as arbitrary units. The results were normalized for β-actin. The numeric data obtained from Western blotting and AC activity assays in diseased and control cases were statistically analyzed using the Student *t*-test with Prism 4 program (GraphPad Software, San Diego, CA). Differences were considered statistically significant with the following p values: < 0.05 (*) and < 0.01 (**).

RESULTS

A_1R and A_2R in Creutzfeldt-Jacob Disease

No modifications in the protein levels of A_1R and AC were seen in tissue samples with artificial postmortem delay up to 22 hours (data not shown). Because the postmortem intervals of the samples used in the present series were less than 8 hours, possible modifications in the expression levels were not attributable to postmortem delay.

The levels of A_1R were markedly increased in the frontal cortex in CJD when compared with age-matched controls (Fig. 1). Densitometric analysis of the A_1R bands corrected for β-actin showed significant differences between CJD cases and controls ($p < 0.05$) with the increase in CJD being approximately 190%. In contrast, no differences in A_2R levels were seen in CJD when compared with age-matched controls (Fig. 2).

Immunohistochemical studies showed A_1R immunoreactivity in the cytoplasm of neurons and in the neuropil in control and diseased brains. A_1R immunoreactivity was moderately increased in CJD when compared with controls (Fig. 3). No other cells, including astrocytes and microglia, were recognized with anti-A_1R antibodies.

Although the predominant pattern of PrP^{res} deposition in the frontal cortex was synaptic in the majority of CJD cases, small plaque-like PrP^{res} deposits were seldom present. Increased A_1R immunoreactivity in neurons was not related with plaque-like PrP^{res} deposition, but, rather, increased A_1R immunoreactivity was generalized in the frontal cortex.

A_1R and A_2R in Multiple Sclerosis, Brain Infarcts, and Alzheimer Disease

No modifications in the protein levels of A_1R were observed in the perinecrotic area in 3 cases with cerebral

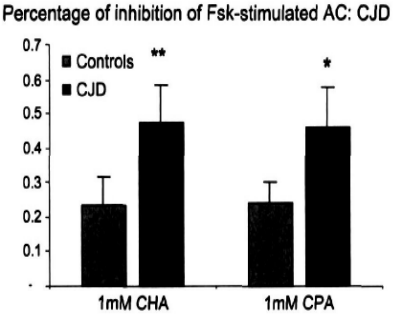

FIGURE 8. Inhibitory effects on adenylyl cyclase (AC) activity in the presence of the A_1Rs agonists CHA (cyclohexyl adenosine) or CPA (N6-cyclopentyladenosine) on 50 μM forskolin (forsk)-stimulated AC activity. Results are expressed as the percentage of AC inhibition. Significant increased AC inhibition is observed in the presence of 1 mM CHA (Student *t*-test, $p < 0.01$) or in the presence of 1 mM CPA (Student *t*-test, $p < 0.05$) in Creutzfeldt-Jakob disease compared with age-matched controls. Data are means ± standard deviation.

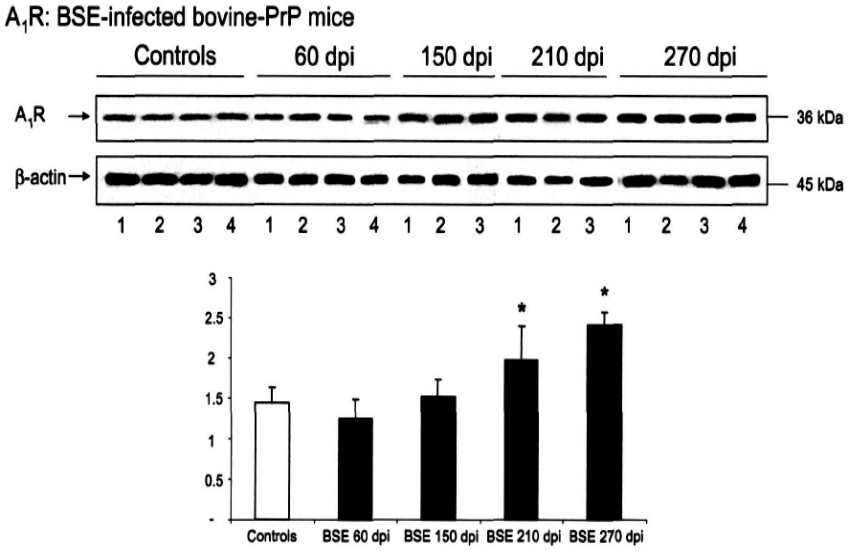

FIGURE 9. A_1Rs expression levels in bovine spongiform encephalopathy-infected bovine-PrP transgenic mice (BoPrP-Tg110) at 60, 150, 210, and 270 days postinoculation (dpi) compared with controls. Significant differences between infected mice and controls are seen at 210 and 270 dpi. Numbers in the graph are arbitrary units. Data are means ± standard deviation. Student *t*-test, $p < 0.05$.

infarcts and in subacute plaques in one case with multiple sclerosis (Fig. 4).

Finally, increased A_1R levels were observed in the frontal cortex in AD cases. Interestingly, significant differences were already observed in limbic stages (III/IVB) ($p < 0.05$), which increased in isocortical stages (V/VIC) ($p < 0.01$) (Fig. 5). As described in detail elsewhere, increased A_1R immunoreactivity in AD was found in neurons as well as in aberrant neurites in senile plaques (36).

Reverse Transcriptase–Polymerase Chain Reaction

Results obtained by the ABI Prism 7700 for ADORA1 gene were normalized by β-actin and GUS. The final results

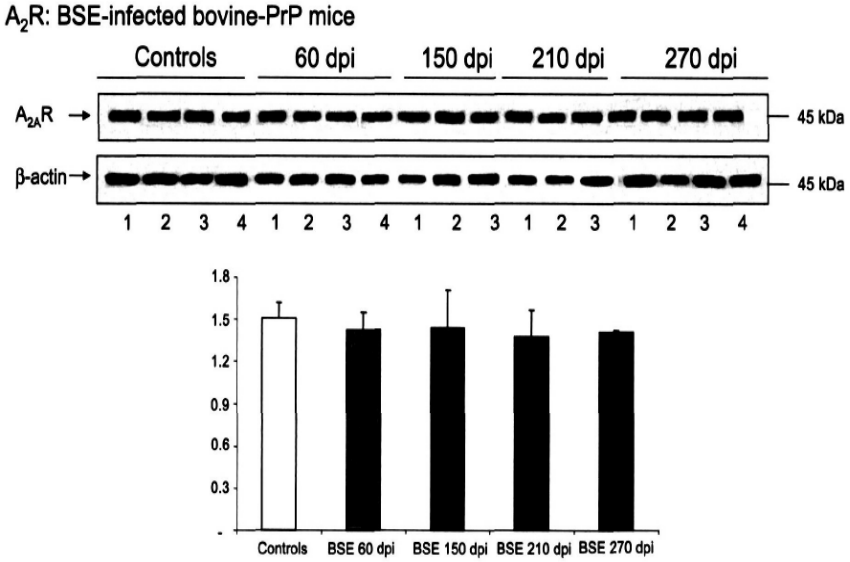

FIGURE 10. No modifications in the expression levels of A_2Rs are seen in bovine spongiform encephalopathy-infected bovine-PrP transgenic mice (BoPrP-Tg110) at 60, 150, 210, and 270 days postinoculation (dpi) compared with controls. β-actin is used as a control of protein loading. Numbers in the graph are arbitrary units.

(expressed in arbitrary units [AU]) revealed no significant differences in A_1R mRNA expression in CJD when compared with controls (Fig. 6).

Adenylyl Cyclase Expression and Activity in Creutzfeldt-Jakob Disease

Western blots to AC in the frontal cortex did not show differences between control and CJD cases (data not shown). In vitro assays were carried out with isolated membranes of the frontal cortex from CJD cases and controls. Basal AC activity was approximately of the same order (133 pmol/mg of protein/min) in CJD and controls (Fig. 7). However, significant differences were seen following the addition of the A_1Rs agonists CHA or CPA on the cAMP production in a forskolin-stimulated AC system.

Significant increased inhibition of forskolin (50 μM)-stimulated AC was found in the presence of 1 mM CHA ($p < 0.01$). This represented increased A_1Rs levels of 207%. Similarly, significant increased inhibition of forskolin (50 μM)-stimulated AC was found in the presence of 1 mM CPA ($p < 0.05$). This increased inhibition represented increased A_1Rs levels of approximately 191% in CJD compared with controls (Fig. 8).

A_1R and A_2R Western Blotting in Bovine Spongiform Encephalopathy-Infected Bovine-PrP Transgenic Mice

No differences in the protein levels of A_1Rs were seen in BSE-infected bovine-PrP transgenic mice at 60 dpi and 150 dpi when compared with age-matched controls. Yet, a significant increase was observed at 210 dpi ($p < 0.05$) and 270 dpi ($p < 0.05$) (Fig. 9). Interestingly, PrP^{res} was not detected by Western blotting until 270 dpi, although PrP^{res} was detected by immunohistochemistry in some animals at 210 dpi but not at earlier postinjection stages (Table 2). In contrast, no modification in the expression levels of A_2Rs was observed in BSE-infected bovine-PrP transgenic mice throughout the same period (Fig. 10).

DISCUSSION

The present results have shown increased A_1R protein levels in the frontal cortex in CJD compared with age-matched controls and in the cerebral cortex in BSE-infected PrP-bovine mice (BoPrP-Tg110) with disease progression. Western blots to AC and basal AC activity were similar in control and CJD cases. However, in vitro assays carried out in human samples demonstrated a marked increase in the percentage of inhibition of 50 μM forskolin-stimulated AC in the presence of the A_1R agonist ligands CPA (N6-cyclopentyladenosine) and CHA (cyclohexyl adenosine), thus indicating a sensitization of the system. Moreover, there is a strong correlation between the increased A_1R levels (186%) detected by Western blotting and the increased AC inhibition (199%) predicted by in vitro assays. These results seem to be specific for A_1Rs because the protein levels of A_2Rs are not modified in the cerebral cortex in CJD and in BSE-infected PrP-bovine mice. Because increased amount and activity of A_1Rs are accompanied by preserved levels of A_2Rs and reduced group 1 mGluR/PLCβ_1/PKCδ signaling pathway (11) in the same cases, it is reasonable to assume that increased A_1R is likely not the result of aberrant regulation of the ubiquitin–proteasome system (37). Similar findings have been observed in all CJD cases, suggesting no effect of the proteinase K-resistant PrP type or the genotype at codon 129 in the A_1R response in CJD.

It can be argued that increased levels of A_1R may be secondary to macrophage infiltration (38). Yet, results in multiple sclerosis are contradictory (39, 40), whereas we have been unable to show modifications in the levels of A_1Rs in subacute plaques in multiple sclerosis and in the perinecrotic areas in cerebral infarcts. Furthermore, immunohistochemical studies have shown A_1R immunoreactivity in neurons, which is increased in CJD cases. No other cells, including astrocytes and microglia, have been recognized with anti-A_1R antibodies.

Results of the TaqMan PCR assay have shown no changes in A_1R mRNA induction in CJD cases when compared with controls. This result indicates that increased A_1R protein levels and increased A_1R activity are not linked to an upregulation of A_1R mRNA. Rather, increased A_1R levels and activity might be related with increase rates of mRNA translation or with a longer turnover of the receptor in the cytoplasmic membrane. Another possibility is the dysregulation of A_1R or AC in membrane caveolae or in raft-associated signaling pathways (41, 42). Ligand-induced, activated A_1R receptors are internalized by caveolae (41, 42), the turnover of recycling probably depending on several factors mainly the structure of plasma cell membranes at specific sites (42). In this line, it is worth stressing that rafts are altered in prion diseases (43) and lipid and protein changes at lipidic rafts and caveolae may interfere with the normal function of these cell membrane specializations.

Studies on cortical A_1Rs in psychiatric and neurodegenerative diseases are not abundant (26, 44). Yet, previous studies in neurodegenerative diseases have shown a change in the pattern of expression and distribution of A_1Rs in the cerebral cortex in AD (36, 45). Reduction in the intensity of the radioligand binding suggested reduced A_1R function in AD (36). Other studies have shown A_1Rs redistribution and A_1Rs overexpression in neurons and in dystrophic neurites of senile plaques in AD (36). The present findings further support our previous observations showing increased A_1R protein levels in the frontal cortex in AD (36). Moreover, increased A_1R expression occurs at stages of the disease in regions (frontal cortex) with moderate amyloid burden but no morphologic evidence of hyperphosphorylated tau pathology (limbic stages III/IVB). Despite these findings, basal and stimulated AC activity is reduced in the cerebral cortex in AD (46, 47).

It is tempting to speculate about the role of abnormal PrP^{res} and β-amyloid deposition in the regulation of A_1R signaling pathway in CJD and AD, respectively. Previous studies in AD have shown increased A_1R immunoreactivity in association with senile plaques (36), and the present findings in AD cases have revealed increased A_1R protein levels in the frontal cortex of AD cases in regions with no tau pathology but with β-amyloid plaques (stage 2 of Braak and Braak).

However, increased A_1R immunoreactivity in frontal neurons in AD and CJD is generalized and not merely related with large, specific protein aggregates. In this line, it is worth considering that β-amyloid and PrP^{res} protofibrils, as well as other fibrils deposited in neurodegenerative diseases with abnormal protein aggregates, may function as pathogenic pores (48). Whether it is the presence of PrP^{res} aggregates or PrP protofibrils a principal cause of abnormal A_1R signaling needs further study.

Over expression of A_1Rs in transgenic mice results in protection from ischemia–reperfusion injury (49–51). Conversely, disruption of A_1 receptors in mice results in elimination of the effect of adenosine on excitatory neurotransmission and in reduced responses to hypoxia (52, 53). A_1Rs agonists mediate neuroprotection at presynaptic and postsynaptic levels. A_1Rs block Ca^{2+} influx, which results in the inhibition of glutamate release and reduction of its postsynaptic excitatory effects (19, 54). Furthermore, activation of presynaptic A_1Rs decreases NMDA receptor-mediated excitatory potentials during hypoxia (55, 56). Adenosine kinase inhibitors, and novel A_1Rs agonists and antagonists, are currently proposed as putative therapeutic agents in neurodegenerative diseases and other brain disorders (26, 54). Insights gained from studies on genetically modified mice with respect to the function of adenosine receptors and their potential as therapeutic targets have been reviewed elsewhere (57).

Finally, A_1Rs are accessible for in vivo imaging using selective A_1R ligands [^{18}F]CPFPX (58) and 8-dicyclopropylmethyl-1-(^{11})C-methyl-3-propylxanthine (59) and positron emission tomography (PET). Therefore, selective A_1R ligands in combination with other markers may serve to further delineate A_1R modifications by PET imaging in CJD and in other neurodegenerative disorders with disease progression.

ACKNOWLEDGMENT

The authors thank T. Yohannan for editorial assistance.

REFERENCES

1. Prusiner SB. The prion diseases of humans and animals. In: Rosenber RN, Prusiner SB, Di Mauro S, Barchi RL, eds. *The Molecular and Genetic Basis of Neurological Diseases.* Boston: Butterworth-Heinemann, 1997:165–86
2. Collinge J. Prion diseases of human and animals: Their causes and molecular basis. Annu Rev Neurosci 2001;24:519–50
3. Aguzzi A, Montrasio F, Kaeser PS. Prions: Health scare and biological challenge. Nat Rev Mol Cell Biol 2001;2:118–26
4. Bratosiewicz-Wasik J, Wasik TJ, Liberski PP. Molecular approaches to mechanisms of prion diseases. Folia Neuropathol 2004;42:S33–46
5. Budka H, Head MW, Ironside JW, et al. Sporadic Creutzfeldt-Jakob disease. In: Dickson D, ed. *Neurodegeneration: The Molecular Pathology of Dementia and Movement Disorders.* Basel: ISN Neuropath Press, 2003:287–97
6. De Armond SJ, Kretzschmar HA, Prusiner SB. Prion diseases. In: Graham DI, Lantos PL, eds. *Greenfield's Neuropathology*, vol II. London: Arnold, 2003:273–323
7. Knight RSG, Will RG. Prion diseases. J Neurol Neurosurg Psychiatry 2004;75:S136–42
8. Sakudo A, Lee D, Yoshimura E, et al. Prion protein suppress perturbation of cellular copper homeostasis under oxidative conditions. Biochem Biophys Res Commun 2004;313:850–55
9. Brown DR, Herms JW, Schmidt B, et al. PrP and beta-amyloid fragments activate different neurotoxic mechanisms in cultured mouse cells. Eur J Neurosci 1997;9:1162–69
10. Ferrer I, Puig B. GluR2/3, NMDA1 and GABAA receptors in Creutzfeldt-Jakob disease. Acta Neuropathol 2003;106:311–18
11. Rodríguez A, Freixes M, Dalfó E, et al. Metabotropic glutamate receptor/phospholipase C pathway: A vulnerable target to Creutzfeldt-Jakob disease in the cerebral cortex. Neuroscience 2005;131:825–32
12. Ralevic V, Burnstock G. Receptors for purines and pyrimidines. Pharmacol Rev 1998;50:413–92
13. Dunwiddie TV, Masino SA. The role and regulation of adenosine in the central nervous system. Annu Rev Neurosci 2001;24:31–55
14. Wittendorp MC, Von Frijtag Drabbe Künzel J, Ijzerman AP, et al. The mouse brain adenosine A1 receptor: Functional expression and pharmacology. Eur J Pharmacol 2004;487:73–79
15. Fredholm BB, Ijzerman AP, Jacobson KA, et al. International union of pharmacology. XXV. Nomenclature and classification of adenosine receptors. Pharmacol Rev 2001;53:527–52
16. Yaar R, Jones MR, Chen J-F, et al. Animal models for the study of adenosine receptor function. J Cell Physiol 2005;202:9–20
17. Reppert SM, Weaver DR, Stehle JH, et al. Molecular cloning and characterization of a rat A1-adenosine receptor that is widely expressed in brain and spinal cord. Mol Endocrinol 1991;5:1037– 48
18. Dixon AK, Gubitz AK, Sirinathsinghji DJ, et al. Tissue distribution of adenosine receptor mRNAs in the rat. Br J Pharmacol 1996;118: 461–68
19. Wardas J. Neuroprotective role of adenosine in the CNS. Pol J Pharmacol 2002;54:313–16
20. Fredholm BB, Dunwiddie TV. How does adenosine inhibit transmitter release? Trends Pharmacol Sci 1988;9:130–34
21. Arrigoni E, Rainnie DG, McCarley RW, et al. Adenosine-mediated presynaptic modulation of glutamatergic transmission in the laterodorsal tegmentum. J Neurosci 2001;21:1076–85
22. Dunwiddie TV, Hoffer BJ. Adenine nucleotides and synaptic transmission in the in vitro rat hippocampus. Br J Pharmacol 1980;69:59–68
23. Kocsis JD, Eng DL, Bjhisitkul RB. Adenosine selectively blocks parallel-fiber-mediated synaptic potentials in rat cerebellar cortex. Proc Natl Acad Sci U S A 1984;81:6531–34
24. Ciruela F, Escriche M, Burgueno J, et al. Metabotropic glutamate 1a and adenosine A1 receptors assemble into functionally interacting complexes. J Biol Chem 2001;276:18345–51
25. Schubert P, Ogata T, Ferroni S, et al. Protective mechanisms of adenosine in neurons and glials cells. Ann NY Acad Sci 1997;825: 1–10
26. Zalewska-Kaszubska J. Neuroprotective mechanisms of adenosine action in CNS neurons. Neurol Neurochir Pol 2002;36:329–36
27. Hartwick AT, Lalonde MR, Barnes S, et al. Adenosine A1-receptor modulation of glutamate-induced calcium influx in rat retinal ganglion cells. Invest Ophthalmol Vis Sci 2004;45:3740–48
28. Parchi P, Giese A, Capellari S, et al. Classification of sporadic Creutzfeldt-Jakob disease based on molecular and phenotypic analysis of 300 subjects. Ann Neurol 1999;46:224– 33
29. Braak H, Braak E. Temporal sequence of Alzheimer's disease related pathology. In: Peters A, Morrison JH, eds. Cerebral Cortex, vol. 14, Neurodegenerative and Age-Related Changes in Structure and Function of Cerebral Cortex. New York, Boston, Dordrecht, London, Moscow: Kluwer Academic/Plenum Publishers, 1999:475– 512
30. Castilla J, Gutierrez-Adan A, Brun A, et al. Early detection of PrP(res) in BSE-infected bovine PrP transgenic mice. Arch Virol 2003;148: 677– 91
31. Scott MD, Groth D, Foster D, et al. Propagation of prions with artificial properties in transgenic mice expressing chimeric PrP genes. Cell 1993; 73:979– 88
32. Scott M, Foster D, Mirenda C, et al. Transgenic mice expressing hamster prion protein produce species-specific scrapie infectivity and amyloid plaques. Cell 1989;59:847–57
33. Barrachina M, Castano E, Ferrer I. TaqMan PCR assay in the control of RNA normalization in human post-mortem brain tissue. Neurochem Int 2006;49:276– 84
34. Ruiz MA, Albasanz JL, León D, et al. Different modulation of inhibitory and stimulatory pathways mediated by adenosine after chronic in vivo agonist exposure. Brain Res 2005;1031:211–21
35. Ruíz A, Sanz JM, Gonzalez-Calero G, et al. Desensitization and internalization of adenosine A1 receptors in rat brain by in vivo treatment with

However, increased A_1R immunoreactivity in frontal neurons in AD and CJD is generalized and not merely related with large, specific protein aggregates. In this line, it is worth considering that β-amyloid and PrP^{res} protofibrils, as well as other fibrils deposited in neurodegenerative diseases with abnormal protein aggregates, may function as pathogenic pores (48). Whether it is the presence of PrP^{res} aggregates or PrP protofibrils a principal cause of abnormal A_1R signaling needs further study.

Over expression of A_1Rs in transgenic mice results in protection from ischemia–reperfusion injury (49–51). Conversely, disruption of A_1 receptors in mice results in elimination of the effect of adenosine on excitatory neurotransmission and in reduced responses to hypoxia (52, 53). A_1Rs agonists mediate neuroprotection at presynaptic and postsynaptic levels. A_1Rs block Ca^{2+} influx, which results in the inhibition of glutamate release and reduction of its postsynaptic excitatory effects (19, 54). Furthermore, activation of presynaptic A_1Rs decreases NMDA receptor-mediated excitatory potentials during hypoxia (55, 56). Adenosine kinase inhibitors, and novel A_1Rs agonists and antagonists, are currently proposed as putative therapeutic agents in neurodegenerative diseases and other brain disorders (26, 54). Insights gained from studies on genetically modified mice with respect to the function of adenosine receptors and their potential as therapeutic targets have been reviewed elsewhere (57).

Finally, A_1Rs are accessible for in vivo imaging using selective A_1R ligands [^{18}F]CPFPX (58) and 8-dicyclopropylmethyl-1-(^{11})C-methyl-3-propylxanthine (59) and positron emission tomography (PET). Therefore, selective A_1R ligands in combination with other markers may serve to further delineate A_1R modifications by PET imaging in CJD and in other neurodegenerative disorders with disease progression.

ACKNOWLEDGMENT

The authors thank T. Yohannan for editorial assistance.

REFERENCES

1. Prusiner SB. The prion diseases of humans and animals. In: Rosenber RN, Prusiner SB, Di Mauro S, Barchi RL, eds. *The Molecular and Genetic Basis of Neurological Diseases.* Boston: Butterworth-Heinemann, 1997:165–86
2. Collinge J. Prion diseases of human and animals: Their causes and molecular basis. Annu Rev Neurosci 2001;24:519–50
3. Aguzzi A, Montrasio F, Kaeser PS. Prions: Health scare and biological challenge. Nat Rev Mol Cell Biol 2001;2:118–26
4. Bratosiewicz-Wasik J, Wasik TJ, Liberski PP. Molecular approaches to mechanisms of prion diseases. Folia Neuropathol 2004;42:S33–46
5. Budka H, Head MW, Ironside JW, et al. Sporadic Creutzfeldt-Jakob disease. In: Dickson D, ed. *Neurodegeneration: The Molecular Pathology of Dementia and Movement Disorders.* Basel: ISN Neuropath Press, 2003:287–97
6. De Armond SJ, Kretzschmar HA, Prusiner SB. Prion diseases. In: Graham DI, Lantos PL, eds. *Greenfield's Neuropathology*, vol II. London: Arnold, 2003:273–323
7. Knight RSG, Will RG. Prion diseases. J Neurol Neurosurg Psychiatry 2004;75:S136–42
8. Sakudo A, Lee D, Yoshimura E, et al. Prion protein suppress perturbation of cellular copper homeostasis under oxidative conditions. Biochem Biophys Res Commun 2004;313:850–55
9. Brown DR, Herms JW, Schmidt B, et al. PrP and beta-amyloid fragments activate different neurotoxic mechanisms in cultured mouse cells. Eur J Neurosci 1997;9:1162–69
10. Ferrer I, Puig B. GluR2/3, NMDA1 and GABAA receptors in Creutzfeldt-Jakob disease. Acta Neuropathol 2003;106:311–18
11. Rodríguez A, Freixes M, Dalfó E, et al. Metabotropic glutamate receptor/phospholipase C pathway: A vulnerable target to Creutzfeldt-Jakob disease in the cerebral cortex. Neuroscience 2005;131:825–32
12. Ralevic V, Burnstock G. Receptors for purines and pyrimidines. Pharmacol Rev 1998;50:413–92
13. Dunwiddie TV, Masino SA. The role and regulation of adenosine in the central nervous system. Annu Rev Neurosci 2001;24:31–55
14. Wittendorp MC, Von Frijtag Drabbe Künzel J, Ijzerman AP, et al. The mouse brain adenosine A1 receptor: Functional expression and pharmacology. Eur J Pharmacol 2004;487:73–79
15. Fredholm BB, Ijzerman AP, Jacobson KA, et al. International union of pharmacology. XXV. Nomenclature and classification of adenosine receptors. Pharmacol Rev 2001;53:527–52
16. Yaar R, Jones MR, Chen J-F, et al. Animal models for the study of adenosine receptor function. J Cell Physiol 2005;202:9–20
17. Reppert SM, Weaver DR, Stehle JH, et al. Molecular cloning and characterization of a rat A1-adenosine receptor that is widely expressed in brain and spinal cord. Mol Endocrinol 1991;5:1037– 48
18. Dixon AK, Gubitz AK, Sirinathsinghji DJ, et al. Tissue distribution of adenosine receptor mRNAs in the rat. Br J Pharmacol 1996;118: 461–68
19. Wardas J. Neuroprotective role of adenosine in the CNS. Pol J Pharmacol 2002;54:313–16
20. Fredholm BB, Dunwiddie TV. How does adenosine inhibit transmitter release? Trends Pharmacol Sci 1988;9:130–34
21. Arrigoni E, Rainnie DG, McCarley RW, et al. Adenosine-mediated presynaptic modulation of glutamatergic transmission in the laterodorsal tegmentum. J Neurosci 2001;21:1076–85
22. Dunwiddie TV, Hoffer BJ. Adenine nucleotides and synaptic transmission in the in vitro rat hippocampus. Br J Pharmacol 1980;69:59–68
23. Kocsis JD, Eng DL, Bjhisitkul RB. Adenosine selectively blocks parallel-fiber-mediated synaptic potentials in rat cerebellar cortex. Proc Natl Acad Sci U S A 1984;81:6531–34
24. Ciruela F, Escriche M, Burgueno J, et al. Metabotropic glutamate 1a and adenosine A1 receptors assemble into functionally interacting complexes. J Biol Chem 2001;276:18345–51
25. Schubert P, Ogata T, Ferroni S, et al. Protective mechanisms of adenosine in neurons and glials cells. Ann NY Acad Sci 1997;825: 1–10
26. Zalewska-Kaszubska J. Neuroprotective mechanisms of adenosine action in CNS neurons. Neurol Neurochir Pol 2002;36:329–36
27. Hartwick AT, Lalonde MR, Barnes S, et al. Adenosine A1-receptor modulation of glutamate-induced calcium influx in rat retinal ganglion cells. Invest Ophthalmol Vis Sci 2004;45:3740–48
28. Parchi P, Giese A, Capellari S, et al. Classification of sporadic Creutzfeldt-Jakob disease based on molecular and phenotypic analysis of 300 subjects. Ann Neurol 1999;46:224– 33
29. Braak H, Braak E. Temporal sequence of Alzheimer's disease related pathology. In: Peters A, Morrison JH, eds. Cerebral Cortex, vol. 14, Neurodegenerative and Age-Related Changes in Structure and Function of Cerebral Cortex. New York, Boston, Dordrecht, London, Moscow: Kluwer Academic/Plenum Publishers, 1999:475– 512
30. Castilla J, Gutierrez-Adan A, Brun A, et al. Early detection of PrP(res) in BSE-infected bovine PrP transgenic mice. Arch Virol 2003;148: 677– 91
31. Scott MD, Groth D, Foster D, et al. Propagation of prions with artificial properties in transgenic mice expressing chimeric PrP genes. Cell 1993; 73:979– 88
32. Scott M, Foster D, Mirenda C, et al. Transgenic mice expressing hamster prion protein produce species-specific scrapie infectivity and amyloid plaques. Cell 1989;59:847–57
33. Barrachina M, Castano E, Ferrer I. TaqMan PCR assay in the control of RNA normalization in human post-mortem brain tissue. Neurochem Int 2006;49:276– 84
34. Ruiz MA, Albasanz JL, León D, et al. Different modulation of inhibitory and stimulatory pathways mediated by adenosine after chronic in vivo agonist exposure. Brain Res 2005;1031:211–21
35. Ruiz A, Sanz JM, Gonzalez-Calero G, et al. Desensitization and internalization of adenosine A1 receptors in rat brain by in vivo treatment with

5.4- *Group I mGluR signaling in EEB-infected bovine-PrP transgenic mice*

Agustin Rodríguez, Mairena Martin, Jose Luis Albasanz, Marta Barrachina, Juan Carlos Espinosa, Juan Maria Torres, Isidre Ferrer

Neurosci Lett. 2006 Dec 20; 410 (2): 115-20

Las anormalidades en la sinapsis y el fallo de la transmisión sináptica parecen ser cruciales en la patogénesis de las enfermedades priónicas. Los mecanismos excitotóxicos han sido postulados como una de las causas más importantes de la neurodegeneración en estas condiciones. En esta línea, estudios previos han mostrado una señalización anormal de los mGluRs en la ECJ. En este estudio hemos examinado esta vía por WB en la corteza cerebral de ratones transgénicos para la PrP bovina infectados con EEB a diferentes dpi. La activación del receptor $mGluR_1$ promueve la activación de la $PLC\beta_1$ que puede activar, al mismo tiempo, a la PKC, que regula la expresión génica. La densitometría de las bandas de los WB revelan que no hay diferencias significativas en los niveles de proteína de $mGluR_1$ a través del tiempo, pero muestra niveles disminuidos de $PLC\beta_1$ y de PKCδ a 270 dpi, en el mismo estadío en el que se manifiestan déficits neurológicos acompañados por cambios neuropatológicos y deposición de PrP^{res} en el cerebro. Los resultados que se presentan muestran un deterioro de la cascada $mGluR_1/PLC\beta_1$/ PKCδ con el progreso de la enfermedad en el modelo murino de EEB.

Available online at www.sciencedirect.com
ScienceDirect
Neuroscience Letters 410 (2006) 115–120
Neuroscience Letters
www.elsevier.com/locate/neulet

Group I mGluR signaling in BSE-infected bovine-PrP transgenic mice

Agustín Rodríguez[a], Mairena Martín[c], José Luís Albasanz[c], Marta Barrachina[a], Juan Carlos Espinosa[d], Juan María Torres[d], Isidre Ferrer[a,b,*]

[a] Institut de Neuropatologia, Servei Anatomia Patològica, IDIBELL-Hospital Universitari de Bellvitge, Spain
[b] Facultat de Medicina, Universitat de Barcelona, 08907 Hospitalet de Llobregat, Spain
[c] Departamento de Química Inorgánica, Orgánica y Bioquímica, Facultad de Químicas, Centro Regional de Investigaciones Biomédicas, Universidad de Castilla-La Mancha, Ciudad Real, Spain
[d] Centro de Investigación en Sanidad Animal (CISA), INIA, 28130 Valdeolmos, Madrid, Spain

Received 6 July 2006; received in revised form 22 September 2006; accepted 22 September 2006

Abstract

Abnormalities of synapses and impaired synaptic transmission appear to be crucial in the pathogenesis of prion diseases. Excitotoxic mechanisms have been postulated as a major cause of neurodegeneration in these conditions. In this line, previous studies have shown abnormal group 1 metabotropic glutamate receptor signaling in Creutzfeldt-Jakob disease (CJD). In the present study, we have examined this pathway by western blotting in the cerebral cortex of bovine-spongiform encephalopathy (BSE)-infected bovine-PrP transgenic mice at different days post-inoculation (dpi). Activation of post-synaptic metabotropic glutamate receptor 1 (mGluR1) promotes phospholipase Cβ1 (PLCβ1) activation which may activate, in turn, protein kinase C (PKC), which regulates gene expression. Densitometric analysis of the western blot bands revealed no differences in the protein levels of (mGluR1) through time, but demonstrated decreased levels of PLCβ1 and protein kinase C delta (nPKCδ) at 270 dpi, at the time when mice showed neurological deficits accompanied by neuropathological changes and PrPres deposition in the brain. The present results show, for the first time impairment of the mGluR1/PLCβ1/PKCδ pathway signaling with disease-progression in a murine model of BSE.

Keywords: Prion; Bovine spongiform encephalopathy; Metabotropic glutamate; Receptors; Phospholipase C; Protein kinase C

Prion diseases are characterized by neuronal loss, astrocytic gliosis, spongiform change and abnormal protease-resistant prion protein deposition, and they are associated with the conversion of cellular prion protein (PrPC) into an abnormal β-sheet enriched and partially proteinase K-resistant isoform (PrPres). PrPres is able, in turn, to recruit PrPC, resulting in an autocatalytic propagation in the pathogenic conformation of the protein [1,4,19]. Prion diseases include scrapie and bovine spongiform encephalopathy (BSE) in animals, and Creutzfeldt-Jakob's disease (CJD), fatal familial insomnia, kuru and Gerstmann-Straüssler-Scheinker disease in humans [1,2,19]. Several mechanisms are probably implicated in the degeneration of neurons in prion diseases [7]. Among them, those related with synaptic transmission appear to be crucial in their pathogenesis. Moreover, excitotoxic mechanisms of neurodegeneration have been postulated in prion diseases [23].

Glutamate is the main excitatory neurotransmitter in the CNS whose actions are mediated by glutamate receptors (GluRs) in target cells. GluRs are classified as ionotropic and metabotropic receptors. Ionotropic glutamate receptors (iGluRs) are ligand-gated cation channels that mediate fast excitatory neurotransmission, whereas metabotropic glutamate receptors (mGluRs) are coupled to intracellular transduction via G-proteins, and mediate slower responses [6,5,12,16,18]. mGluRs are divided into eight subtypes, which are categorized into three groups according to signal transduction properties. Group I, including mGluR1 and mGluR5, are positively coupled to phospholipase C (PLC). Three structural groups constitute the PLC system: β, γ and δ. PLCβ1, which is the most highly expressed of PLCβ isoforms in the brain, is activated by the Gq family of G-proteins, whereas non-related PLCγ is a substrate for tyrosine kinase [8,20,21]. Activation of post-synaptic mGluR1 and mGluR5 promotes PLCβ1 activation, which hydrolyzes a minor membrane

* Corresponding author at: Institut de Neuropatologia, Servei Anatomia Patològica, IDIBELL-Hospital Universitari de Bellvitge, c/Feixa Llarga sn, 08907 Hospitalet de Llobregat, Spain. Tel.: +34 93 260 7452; fax: +34 93 260 7503.
E-mail address: 8082ifa@comb.es (I. Ferrer).

0304-3940/$ – see front matter © 2006 Elsevier Ireland Ltd. All rights reserved.
doi:10.1016/j.neulet.2006.09.084

phospholipid, phosphatidylinositol 4,5-bisphosphate, to produce a pair of intracellular messengers, diacylglycerol (DAG) and inositol 1,4,5-trisphosphate (IP3). The interaction between IP3 and a protein forming a calcium channel in the membrane of the endoplasmic reticulum (ER) causes a rapid efflux of Ca^{2+} accumulated in ER and an increase of free Ca^{2+} in the cytosol. DAG remaining in the plasma membrane, together with Ca^{2+}, activates protein kinase C (PKC), which regulates gene expression through phosphorylation of many target proteins, including several kinases [9,17]. Previous studies in our lab have demonstrated reduced group I metabotropic glutamate receptor/phospholipase Cβ1 (mGluR1/PLCβ1) pathway in CJD [22]. We have herein extended the study of mGluR1/PLCβ1 and its effector protein kinase Cδ (PKCδ) in the cerebral cortex of BSE-infected bovine-PrP transgenic mice.

The generation and characteristics of these transgenic mice, as well as the susceptibility and timing of the incubation following BSE inoculation and the behavioral and neuropathological findings of infected mice, have been described in detail elsewhere [3]. Briefly, BoPrP-Tg110 mice express bovine PrP insert introduced in a mouse PrP0/0 background that confers susceptibility to BSE infection. BoPrP-Tg110 mice express bovine PrP instead of murine-PrP. These transgenic mice do not develop any alteration in their gene/protein expression when compared with wild mice. As far as we know, Tg mice has identical biological properties as wild type mice except for their susceptibility to BSE infection [3]. For BSE infection, BoPrP-Tg110 mice (females, 6–7 weeks old, weighing approximately 20 g) were inoculated in the right parietal lobe using a 25 gauge disposable hypodermic syringe with 20 μl of 10% brain homogenate. TSE/08/59 inoculum, produced with a pool from the brainstem of 49 BSE-infected cattle and supplied by the Veterinary Laboratory Agency (New Haw, Addlestone, Surrey, UK), was used. As negative controls, we used the same BoPrPTg110 mice but inoculated with healthy cow brain. To minimize the risk of bacterial infection, homogenates were heated at 70 °C for 10 min before inoculation. To evaluate the clinical signs appearing after inoculation, mice were observed daily and their neurological status was assessed twice a week. The presence of three signs of neurological dysfunction (using 10 different items) was required for a mouse to score positive for prion disease [3]. Clinical parameters examined were waddling gait, rough coat, dullness about head, very jumpy, incontinence, flattened back, sticky eye discharge, weight loss and hunching. Animals were sacrificed at 60 (n = 4), 150 (n = 3), 210 (n = 3) and 270 (n = 4) days post-inoculation (dpi). The brains were rapidly removed from the skulls and immediately prepared for neuropathological and biochemical studies.

Brains were prepared as follows: tissue sections containing medulla oblongata at the level of the obex and the pontine area, cerebellum, diencephalon including thalamus, hippocampus and cerebral cortex, were processed for routine histological methods and immunohistochemistry. The avidin-biotine-peroxidase complex (ABC) method was used for the immunohistochemical detection of PrPres. Briefly, tissue sections were incubated at 4 °C overnight with the primary 2A11 mAb diluted 1:400 in phosphate buffer saline (PBS). The 2A11 mAb is a PrP specific antibody recognizing the epitope 171QVYYRPVDQ179 of the bovine PrP [3]. This was followed by incubation with a secondary anti-mouse IgG (Dako, Madrid) diluted 1:20 in PBS. The immunoreaction was visualized with 3,3′-diaminobenzidine tetrahydrochloride (Sigma, Madrid) and 0.01% hydrogen peroxide. Finally, the sections were slightly counterstained with Mayer's haematoxylin, dehydrated and mounted on glass slides. The specific primary antibody was replaced by PBS or by non-immune mouse serum in some tissue sections used as negative controls. In addition, frozen brain samples were used for the determination of PrPres by gel electrophoresis and Western blotting [3]. The main characteristics of BSE-infected bovine-PrP transgenic mice are summarized in Table 1.

For the study of mGluR1/PLCβ1/PKCδ pathway 30 μg of protein was mixed with loading buffer containing 0.125 M Tris

Table 1
Main characteristics of BSE-infected bovine-PrP transgenic mice: dpi: days post-inoculation

	Controls				BSE			
	1	2	3	4	1	2	3	4
60 dpi								
WB	–	–	–	–	–	–	–	–
IHC	–	–	–	–	–	–	–	–
HP	–	–	–	–	–	–	–	–
CS	–	–	–	–	–	–	–	–

	Controls			BSE		
	1	2	3	1	2	3
150 dpi						
WB	–	–	–	–	–	–
IHC	–	–	–	–	–	–
HP	–	–	–	–	–	–
CS	–	–	–	–	–	–

	Controls			BSE		
	1	2	3	1	2	3
210 dpi						
WB	–	–	–	–	–	–
IHC	–	–	–	–	+	–
HP	–	–	–	–	+	–
CS	–	–	–	–	–	–

	Controls				BSE			
	1	2	3	4	1	2	3	4
270 dpi								
WB	–	–	–	–	+	+	+	+
IHC	–	–	–	–	+	+	+	+
HP	–	–	–	–	+	+	+	+
CS	–	–	–	–	+	+	+	+

Brain samples were analyzed by Western blot after proteinase-K treatment for PrPres detection (WB), by histopathology (HP), or by immunohistochemistry (IHC). Diseased mice were scored by clinical signs (CS) before euthanasia. HP changes are characterized by spongiform change and mild astrocytic gliosis. IHC indicates positive PrPres immunoreactivity.

(pH 6.8), 20% glycerol, 10% β-mercaptoethanol, 4% SDS and 0.002% bromophenol blue, and heated at 95 °C for 5 min. Sodium dodecylsulphate-polyacrylamide gel electrophoresis (10% SDS-PAGE) was carried out using a mini-protean system (Bio-Rad) with molecular weight standards (Bio-Rad, Madrid). Proteins were then transferred to nitrocellulose membranes using an electrophoretic transfer system (Semi-dry, Bio-Rad). The membranes were washed with TTBS containing 10 mM Tris–HCl pH 7.4, 140 mM NaCl and 0.1% Tween-20. Nonspecific blocking was performed by incubating the membranes in TTBS containing 5% skimmed milk for 20 min. Membranes were incubated with the primary antibodies at 4 °C overnight. The rabbit polyclonal antibody to mGluR1 (Upstate, Reactiva, Madrid) was used at a dilution of 1:1000; the rabbit polyclonal anti-PLCβ1 (Santa Cruz Biotechnology) antibody was used at a dilution of 1:500; and the rabbit polyclonal anti-nPKCδ (Santa Cruz Biotechnology) was used at a dilution of 1:1000. After rinsing, the membranes were incubated with the corresponding anti-rabbit secondary antibody (Dako, Madrid) at a dilution of 1:1000 for 1 h at room temperature. The membranes were then washed and developed with the chemiluminescence ECL system (Amersham, Madrid) followed by exposure of the membranes to autoradiographic films at 4 °C. The monoclonal anti-β-actin antibody (Sigma, Barcelona) was used at a dilution of 1:5000 as a control of protein loading. Protein expression levels were determined by densitometry of the bands using Total Laboratory v2.01 software. This software detects the bands obtained in Western blots and gives individual values which are dependent on the light quantification of the corresponding band. Measurements are expressed as arbitrary units. The results were normalized for β-actin. The numerical data obtained from Western blotting were statistically analyzed using Student's *t*-test with Prism 4 program (GraphPad Software, San Diego). Differences were considered statistically significant with the following *p*-values: $^{*}p<0.05$ and $^{**}p<0.01$.

Histological lesions were characterized by neuron loss, astrocytic gliosis, spongiform degeneration and punctate PrPres deposition (Fig. 1). Positive western blots were recognized by the presence of strongly immunoreactive PrPres bands appearing as smears of 28–36 kDa (Fig. 2).

As seen in Table 1, only one mouse showed focal histological changes and PrPres accumulation as revealed by immunohistochemistry, not accompanied by apparent neurological deficits. Western blot for PrPres was negative in this case and in the remaining cases at 210 dpi. In contrast, all the animals had clinical symptoms, neuropathological lesions, PrPres deposition and positive western blots to PrPres at 270 dpi.

Western blots to mGluR1 disclosed one band of 142 kDa in control and inoculated mice. The density of the band was not modified at different dpi up to 270 days (Fig. 3).

Yet, reduced PLCβ1, recognized as single band of 150 kDa in western blots, was found at 270 dpi (Fig. 4), and this was accom-

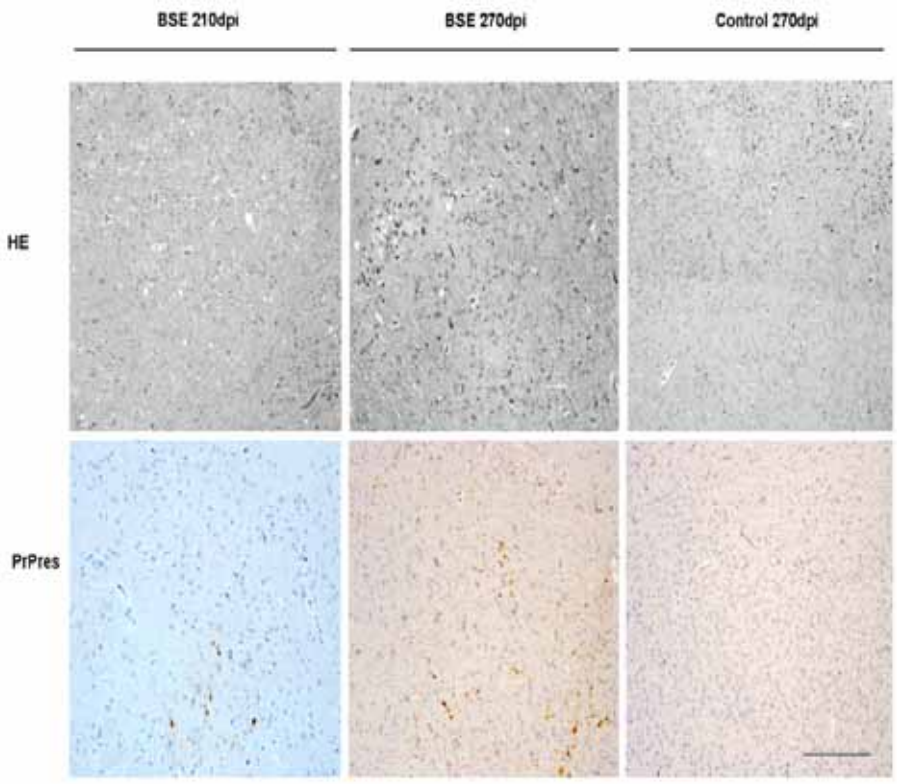

Fig. 1. Histological sections stained with haematoxylin and eosin (upper panel) and PrPres immunohistochemistry (inner panel) in infected mice at 210 and 270 days post-injection (BSE210 and BSE270 dpi, respectively) compared with age-matched controls at 270 dpi. Neuron loss, astrocytic gliosis and spongiform deposition is seen at 270 dpi. Punctate PrPres immunoreactivity is abundant in BSE-infected bovine PrP transgenic mice at 270 dpi. Mild positive staining is also observed in one mouse at 219 dpi. Cerebral cortex, paraffin sections, bar = 100 μm.

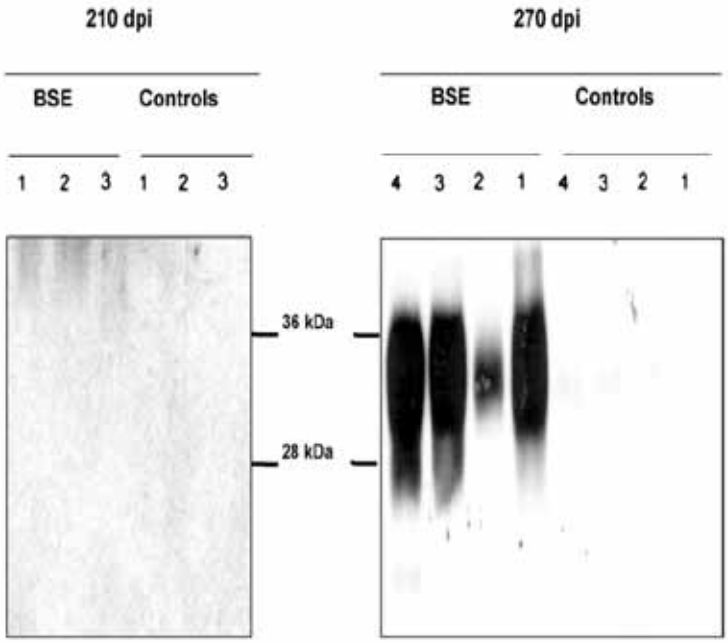

Fig. 2. Western blots to PrPres in BSE-infected bovine PrP transgenic mice at 210 and 270 dpi and corresponding age-matched controls. Positive bands are observed in the four mice at 270 dpi.

panied by reduced nPKCδ expression levels, characterized as a unique band of 85 kDa, at the same time post-infection (Fig. 5).

These abnormalities are selective to certain proteins, and probably not dependent on mere neuron loss, as could be suggested in case of generalized reduction levels of all the proteins analyzed.

Although no functional studies have been carried out in this series, several implications may be inferred from the present results. Decreased expression levels of PLCβ1 may reduce cytoplasmic calcium (Ca^{2+}) concentrations and DAG levels. cPKCα requires DAG and calcium for activation, whereas nPKCδ is sensitive only to DAG [10,11,13,14]. Since DAG must be provided for PKCδ phosphorylation [15], it is feasible that the reduced levels of PKCδ in CJD may be related to decreased PLCβ1 expression levels and the concomitantly low DAG production rate.

Together, the present findings demonstrate for the first time impairment of the mGluR1/PLCβ1/PKCδ pathway signaling with disease-progression in a murine model of BSE. Abnormal neurotransmitter receptor signaling is coincidental with PrPres deposition, histological changes and abnormal clinical score. This observation may help to increase understanding about the abnormal synaptic function in prion diseases in relation with PrP deposition and with clinical impairment.

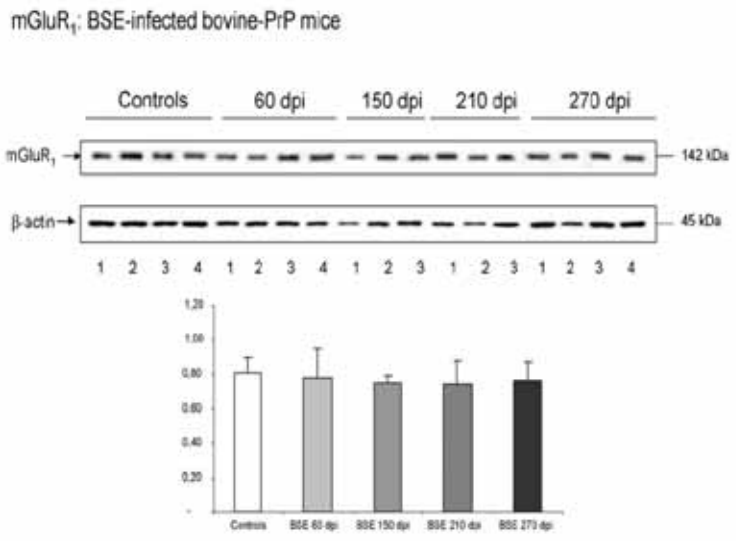

Fig. 3. No modifications in the expression levels of mGluR1 are seen in BSE-infected bovine-PrP transgenic mice (BoPrP-Tg110) at 60, 150, 210 and 270 days post-inoculation (dpi) compared with controls. β-Actin is used as a control of protein loading. Numbers in the graph are arbitrary units.

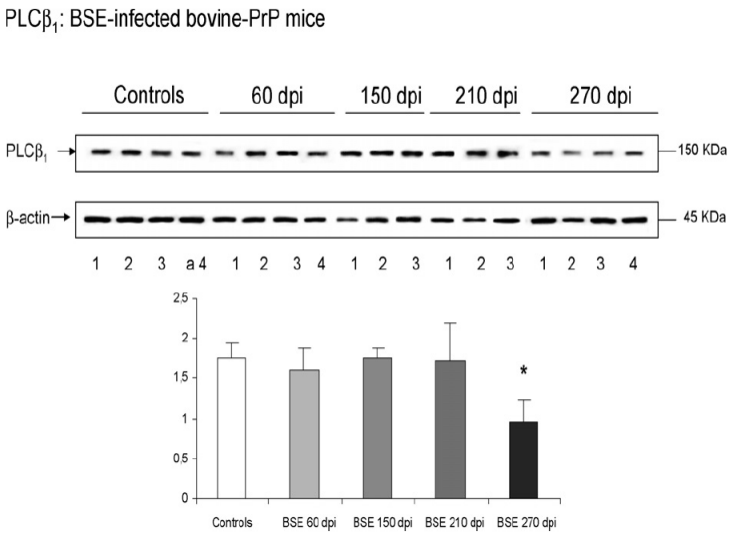

Fig. 4. PLCβ1 expression levels in BSE-infected bovine-PrP transgenic mice (BoPrPTg110) at 60, 150, 210 and 270 days post-inoculation (dpi) compared with controls. Significant differences between infected mice and controls are seen at 270 dpi. Numbers in the graph are arbitrary units. Data are mean ± S.D. Student's *t*-test, $p < 0.05$.

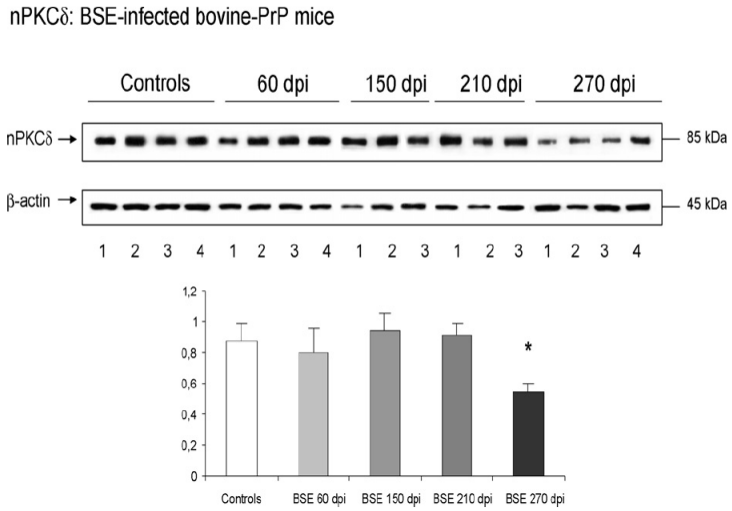

Fig. 5. PKCδ expression levels in BSE-infected bovine-PrP transgenic mice (BoPrPTg110) at 60, 150, 210 and 270 days post-inoculation (dpi) compared with controls. Significant differences between infected mice and controls are seen at 270 dpi. Numbers in the graph are arbitrary units. Data are mean ± S.D. Student's *t*-test, $p < 0.05$.

Acknowledgements

Supported by the Ministerio de Ciencia y Tecnología: EET 2001-3724 and EET2002-05168, and CAL01-018 NoE Neuroprion CT-2004-506579; Ministerio de Sanidad: FIS grants G03/167, 05/1631, and grants 04/301-01 and 04/301-02 from Fundació "La Caixa". We wish to thank T. Yohannan for editorial assistance.

References

[1] A. Aguzzi, F. Montrasio, P.S. Kaeser, Prions: health scare and biological challenge, Nat. Rev. Mol. Cell. Biol. 2 (2001) 118–126.
[2] H. Budka, M.W. Head, J.W. Ironside, P. Gambetti, P. Parchi, M. Zeidler, F. Tagliavini, Sporadic Creutzfeldt-Jakob disease, in: D. Dickson (Ed.), Neurodegeneration: The Molecular Pathology of Dementia and Movement Disorders, ISN Neuropath Press, Basel, 2003, pp. 287–297.
[3] J. Castilla, A. Gutierrez-Adan, A. Brun, B. Pintado, F.J. Salguero, B. Parra, F.D. Segundo, M.A. Ramirez, A. Rabano, M.J. Cano, J.M. Torres, Early detection of PrP(res) in BSE-infected bovine PrP transgenic mice, Arch. Virol. 148 (2003) 677–691.
[4] J. Collinge, Prion diseases of human and animals: their causes and molecular basis, Annu. Rev. Neurosci. 24 (2001) 519–550.
[5] P.J. Conn, Physiological roles and therapeutic potential of metabotropic glutamate receptors, Ann. N. Y. Acad. Sci. 1003 (2003) 12–21.
[6] P. Conn, J.P. Pin, Pharmacology and functions of metabotropic glutamate receptors, Ann. Rev. Pharmacol. Toxicol. 37 (1997) 205–237.
[7] A. Giese, H.A. Kretzschmar, Prion-induced neuronal damage—the mechanisms of neuronal destruction in the subacute spongiform encephalopathies, Curr. Top. Microbiol. Immunol. 253 (2001) 203–217.
[8] H.E. Hamm, The many faces of G protein signaling, J. Biol. Chem. 273 (1998) 669–672.
[9] C. Hammond, The metabotropic glutamate receptors, in: Cellular and Molecular Neurobiology, Academic Press, Amsterdam, Boston, Heidelberg, London, New York, Oxford, Paris, San Diego, San Francisco, Singapore, Sydney, Tokyo, 2003, Chapter 14, pp. 314–326.

[10] S. Jaken, Protein kinase C isozymes and substrates, Curr. Opin. Cell. Biol. 8 (1996) 168–173.
[11] H. Mellor, P.J. Parker, The extended protein kinase C superfamily, Biochem. J. 332 (1998) 281–292.
[12] E.K. Michaelis, Molecular biology of glutamate receptors in the central nervous system and their role in excitoxicity, oxidative stress and aging, Prog. Neurobiol. 54 (1998) 369–415.
[13] A.C. Newton, Protein kinase C: structural and spatial regulation by phosphorylation, cofactors and macromolecular interactions, Chem. Rev. 101 (2001) 2353–2364.
[14] Y. Nishizuka, Intracellular signaling by hydrolysis of phospholipids and activation of protein kinase C, Science 258 (1992) 607–614.
[15] K. Ogita, S.I. Miyamoto, K. Yamaguchi, H. Koide, N. Fujisawa, U. Kikkawa, S. Sahara, Y. Fukami, Y. Nishizuka, Isolation and characterization of δ-subspecies of protein kinase C from rat brain, Proc. Natl. Acad. Sci. U.S.A. 89 (1992) 1592–1596.
[16] S. Ozawa, H. Kamiya, K. Tsuzuki, Glutamate receptors in the mammalian central nervous system, Prog. Neurobiol. 54 (1998) 518–618.
[17] J.W. Phillis, M.H. O'Regan, A potential critical role of phospholipases in central nervous system ischemic, traumatic, and neurodegenerative disorders, Brain Res. Rev. 44 (2004) 13–47.
[18] J.P. Pin, F. Acher, The metabotropic glutamate receptors: structure, activation, mechanisms and pharmacology, Curr. Drug Target CNS Neural. Disord. 1 (2002) 297–317.
[19] S.B. Prusiner, The prion diseases of humans and animals, in: R.N. Rosenber, S.B. Prusiner, S. DiMauro, R.L. Barchi (Eds.), The Molecular and Genetic Basis of Neurological Diseases, Butterworth-Heinemann, Boston, 1997, pp. 165–186.
[20] M.J. Rebecchi, S.N. Pentyala, Structure, function, and control of phosphoinositide specific phospholipase C, Physiol. Rev. 80 (2000) 1291–1335.
[21] S.G. Rhee, Regulation of phosphoinositide-specific phospholipase C, Annu. Rev. Biochem. 70 (2001) 281–312.
[22] A. Rodríguez, M. Freixes, E. Dalfó, M. Martín, B. Puig, I. Ferrer, Metabotropic glutamate receptor/phospholipase C pathway: a vulnerable target to Creutzfeldt-Jakob disease in the cerebral cortex, Neuroscience 131 (2005) 825–832.
[23] A.C. Scallet, X. Ye, Excitotoxic mechanisms of neurodegeneration in transmissible spongiform encephalopathies, Ann. N. Y. Acad. Sci. 825 (1997) 194–205.

5.5- *Expression of transcription factors CREB and c-Fos in the brains of terminal Creutzfeldt-Jakob disease cases*

A. Rodríguez, I. Ferrer

Neuroscience letters 2007 (en prensa)

Los niveles de expresión y localización de los factores de transcripción CREB1, CREB2 y c-Fos, así como los niveles de las MAPKs/ERK (ERK-1 y ERK-2) y p38, han sido examinados en el cerebro (corteza frontal) de once casos con ECJ y en cinco muestras control. Se han observado niveles de expresión preservados de ERK-1-P, ERK-2-P y p38-P. Paralelamente, se han encontrado niveles reducidos de CREB, CREB-P, c-Fos y c-Fos-P por SDS-PAGE y WB y una disminución en el número de núcleos reactivos, tal y como se ve por inmunohistoquímica. Estas observaciones indican una disiminución de las respuestas mediadas por CREB y c-Fos, en contraste con una preservación de las kinasas, lo cual favorece la muerte celular en estadíos terminales de ECJ.

+Model
NSL-24054; No. of Pages 6
ARTICLE IN PRESS

Available online at www.sciencedirect.com
ScienceDirect

ELSEVIER

Neuroscience Letters xxx (2007) xxx–xxx

Neuroscience Letters

www.elsevier.com/locate/neulet

Expression of transcription factors CREB and c-Fos in the brains of terminal Creutzfeldt-Jakob disease cases

A. Rodríguez, I. Ferrer *

Institut de Neuropatologia, Servei Anatomia Patològica, IDIBELL-Hospital Universitari de Bellvitge, Universitat de Barcelona, Feixa Llarga sn, 08907 Hospitalet de Llobregat, Spain

Received 8 January 2007; received in revised form 22 March 2007; accepted 6 April 2007

Abstract

Expression levels and localization of transcription factors cAMP response element binding protein ($CREB_1$ and $CREB_2$) and c-Fos, as well as levels of up-stream mitogen-activated protein kinases/extracellular signal-regulated kinases (ERK-1 and ERK-2) and p38 kinase, were examined in the brains (frontal cortex) of eleven cases with Creutzfeldt-Jakob disease (CJD) and five age-matched controls. Preserved expression levels of ERK-1-P, ERK-2-P and p38-P were observed in CJD. However, significantly reduced levels, as revealed by gel electrophoresis and Western blotting, and reduced numbers of immunoreactive nuclei, as seen by immunohistochemistry, to CREB, CREB-P, c-Fos and c-Fos-P were found in CJD when compared with controls. These observations point to exhausted CREB and c-Fos brain responses, in spite of preserved up-stream signaling kinases, thus favoring cell death in terminal stages of CJD.

Keywords: Creutzfeldt-Jakob; Mitogen activated kinase; p38; CREB; c-Fos; Cell death

Transmissible spongiform encephalopathies or prion diseases are a group of neurodegenerative diseases which, according to the 'protein only' hypothesis, are caused by the presence of an infectious protein called prion [3,17]. These include bovine spongiform encephalopathy and scrapie in animals, and Creutzfeldt-Jakob disease (CJD), fatal familial insomnia, kuru and Gerstmann-Straüssler-Scheinker disease in humans. Prion diseases are characterized pathologically by neuronal loss, astrocytic gliosis and microgliosis, spongiform change and abnormal prion protein (PrP) aggregation and deposition [2,11]. CJD occurs as an inherited, sporadic or infectious disease, with the sporadic form being the most frequent type, accounting for about 85% of cases. The abnormal prion protein, also called PrP^{Sc}, is an abnormally folded isoform of the cellular prion protein PrP^{C}, which is an anchored cell membrane glycoprotein widely expressed but enriched in the central nervous system. Constitutive PrP^{C} has an α-helical structure, while pathological PrP^{Sc} has a β-sheet structure and is resistant to proteinase K digestion. A cardinal point in prion diseases is the ability of PrP^{Sc} to induce conformational changes to PrP^{C} thus leading to the propagation of the pathogenic conformation of the protein [3,17]. Cell death in prion diseases appears to be mediated by necrosis and apoptosis [7], yet the involvement of up-stream pathways which trigger the collapse of nerve cells remains unclear.

Distinct mitogen-activated protein kinases (MAPKs) regulate diverse cellular functions through the activation of signal responsive transcription factors which, in turn, modulate gene expression. The MAPK family includes three well-characterized subfamilies which become active by phosphorylation: extracellular signal-regulated kinases (ERK-1 and ERK-2), c-Jun N-terminal kinases (JNKs) and p38 [18]. The cAMP response element binding protein family includes $CREB_1$ and $CREB_2$; phosphorylation of CREB at Ser133 facilitates its interaction with the 265-kDa CREB-binding protein (CBP) and activates the basal transcription complex. CREB can be also activated by various signaling pathways including MAPKs [22]. CREB is widely expressed in numerous tissues but it plays a largely regulatory role in the nervous system, where it is believed to promote neuronal survival, precursor proliferation, neurite outgrowth and neuronal differentiation in certain neuronal populations. c-Fos encodes a 62 kDa nuclear phospho-protein that is rapidly induced by a variety of agents, and it functions as a transcriptional regulator for several genes [14].

* Corresponding author. Tel.: +34 93 4035808; fax: +34 93 2607503.
E-mail address: 8082ifa@comb.es (I. Ferrer).

0304-3940/$ – see front matter © 2007 Elsevier Ireland Ltd. All rights reserved.
doi:10.1016/j.neulet.2007.04.045

Please cite this article in press as: A. Rodríguez, I. Ferrer, Expression of transcription factors CREB and c-Fos in the brains of terminal Creutzfeldt-Jakob disease cases, Neurosci. Lett. (2007), doi:10.1016/j.neulet.2007.04.045

+Model
NSL-24054; No. of Pages 6
ARTICLE IN PRESS

The involvement of CREB and c-Fos in human degenerative diseases is little understood. Total CREB levels are unchanged but phosphorylation of CREB is decreased in Alzheimer disease (AD) [23]. c-Fos immunoreactivity is apparently increased in certain areas of the hippocampus in patients with AD [12,13]. Increased c-Fos expression has been associated with β-amyloid-induced toxicity in a mouse hippocampal cell line [9]. Yet these observations have not been replicated in a transgenic model of AD [6]. Recent immunohistochemical studies have described abnormal expression of transcription factors in PiD [15]. Since increased CREB-P and c-Fos was observed in the nuclei of neurons in vulnerable regions (frontal cortex) and in resistant regions (dentate gyrus) in PiD, it was suggested that increased expression of transcription factors is only barely a determining factor in cell death [15].

The present study examines the expression levels and cellular localization of constitutive and phosphorylated ERKs and p38, and transcription factors CREB and c-Fos, and their active phosphorylated forms in CJD frontal cortex, in an attempt to gain understanding of the implication of these factors in cell death signaling in prion diseases.

The brains of 11 patients with sporadic CJD and 5 age-matched controls were obtained from 3 to 8 h after death and were immediately prepared for morphological and biochemical studies. The main clinical characteristics are summarized in Table 1. Criteria for the neuropathological diagnosis of CJD used in the present series are those currently accepted [2,11]. Molecular and phenotypic classification is found elsewhere [2]. For biochemical studies, samples of the frontal cortex (area 8) were frozen in liquid nitrogen and stored at −80 °C until use. Specific immunohistochemical studies were carried out in sections fixed in 4% paraformaldehyde in phosphate buffer for 24 h, cryoprotected and frozen. Neuron loss, spongiform degeneration, astrocytic gliosis and microgliosis involving the cerebral neocortex, striatum and cerebellum were observed in every case. Synaptic-like PrPres deposits were found in the cerebral cortex and striatum in every case. In addition, PrPres plaques were common in the two VV2 cases (cases 5 and 8). For Western blot studies, about 0.1 g of frontal cortex was homogenized in a glass tissue grinder in 10 volumes (w/v) of cold buffer containing PBS, 0.5%, NP-40, 0.5% deoxycholic acid sodium salt, 0.1 mM phenylmethylsufonyl fluoride, 5 μg/ml aprotinin, 10 μg/ml leupeptin, 5 μg/ml pepstatin and 1 mM sodium orthovanadate, pH 7.5. After centrifugation at 2000 × *g* (Eppendorf) for 5 min, protein concentration of total homogenate was determined with the BCA Protein Assay Kit (Pierce). Thirty microgram of protein was mixed with loading buffer containing 0.125 M Tris (pH 6.8), 20% glycerol, 10% β-mercaptoethanol, 4% SDS and 0.002% bromophenol blue, and heated at 95 °C for 5 min. Sodium dodecylsulphatepolyacrylamide gel electrophoresis (10% SDS-PAGE) was carried out using a miniprotean system (Bio-Rad) with molecular weight standards (Bio-Rad). Proteins were then transferred to nitrocellulose membranes using an electrophoretic transfer system (Semi-dry, Bio-Rad). The membranes were washed with TTBS containing 10 mM Tris–HCl pH 7.4, 140 mM NaCl and 0.1% Tween-20. Nonspecific blocking was carried out by incubating the membranes in TTBS containing 5% skimmed milk for 30 min. Membranes were incubated with one of the primary antibodies at 4 °C overnight. The polyclonal rabbit anti-phospho-p38Thr180/Tyr182 (p38-P) (Calbiochem) was used at a dilution of 1:500; the polyclonal rabbit anti-MAPK/ERKThr202/Tyr204 (ERK-1-P and ERK-2-P) (Calbiochem) was used at a dilution of 1:1000; the anti-$CREB_1$ and anti-$CREB_2$ antibodies (Santa Cruz Biotech) were used at a dilution of 1:500; the rabbit polyclonal anti-phospho-CREBSer133 (CREB-P, which recognizes $CREB_1$-P) (Cell signaling) was used at a dilution of 1:500; the rabbit polyclonal anti-c-Fos (4) antibody (Santa Cruz Biotech) was used at a dilution of 1:500. After rinsing, the membranes were incubated with the secondary antibody (Dako) at a dilution of 1:1000 for 1 h at room temperature. The membranes were then washed and developed with the chemiluminescence ECL system

Table 1
Main clinical characteristics of CJD and control cases in the present series

Case number	Age	Gender	Codon 129	14-3-3	EEG	First symptom	Survival, in months	PrP type
CJD1	60	M	MM	+	+	Dementia	3	1
CJD2	60	F	MM	+	+	Dementia	6	1
CJD3	55	M	MM	+	+	Ataxia	3	1
CJD4	74	M	?	+	+	Dementia	5	1
CJD5	66	M	VV	+	Rare	Ataxia	4	2
CJD6	53	F	MM	+	+	Dementia	2	1
CJD7	85	F	MV	+	+	Dementia	14	1
CJD8	71	M	VV	+	0	Ataxia	3	2
CJD9	70	F	MM	+	+	Dementia	3	1
CJD10	59	M	MM	?	+	Dementia	8	1
CJD 11	60	M	MM	+	−	Ataxia	8	2
C1	62	M						
C2	72	F						
C3	73	M						
C4	58	F						
C5	68	M						

F: female; M: male; EEG: typical generalized triphasic pseudo-periodic complexes. M: methionine; V: valine; PrP type: PrP^{res} type 1: lower band of non-glycosylated PrP^{res} of 21 kDa; type 2: lower band of non-glycosylated PrP^{res} of 19 kDa.

Please cite this article in press as: A. Rodríguez, I. Ferrer, Expression of transcription factors CREB and c-Fos in the brains of terminal Creutzfeldt-Jakob disease cases, Neurosci. Lett. (2007), doi:10.1016/j.neulet.2007.04.045

+Model
NSL-24054; No. of Pages 6
ARTICLE IN PRESS

(Amersham) followed by exposure of the membranes to autoradiographic films at 4 °C. The monoclonal anti-β-actin antibody (Sigma), at a dilution of 1:5000, was used as a control of protein loading.

Protein expression levels were determined by densitometry of the bands using the Total Laboratory v2.01 software application. This software detects the bands obtained in Western blots and gives individual values which are dependent on the light quantification of the corresponding band. Measurements are expressed as arbitrary units. The results were normalized for β-actin. The numerical data obtained from CJD and the corresponding controls were statistically analyzed using STATGRAPHICS plus 5.0 software from ANOVA and the LSD statistical tests. Asterisks indicate the following p-values: (*) $p<0.05$ (95% confidence level); (**) $p<0.01$ (99% confidence level); and (***) $p<0.001$ (99.9% confidence level).

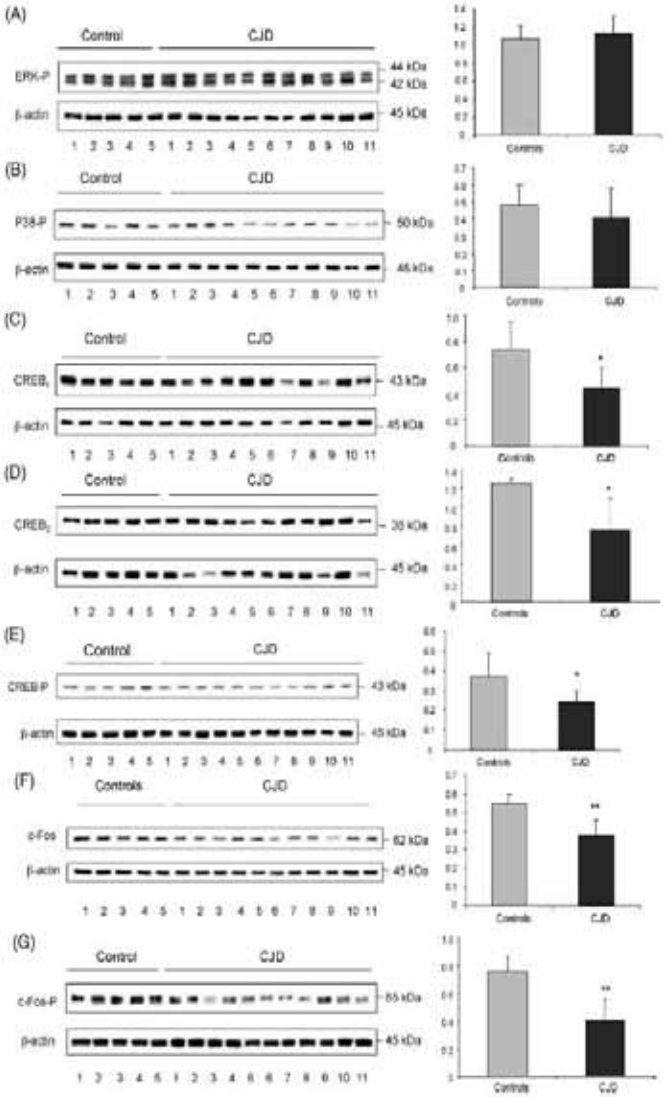

Fig. 1. Western blots to mitogen-activated protein kinases (MAPKs) and transcription factors CREB and c-Fos in the frontal cortex (area 8) of 11 cases (1–11) with Creutzfeldt-Jakob disease (CJD) and 5 (1–5) age-matched controls. Densitometric analysis is normalized for β-actin. Numbers in graphs represent arbitrary units. (A) WB to phospho-MAPK/ERK (ERK-P) shows a double band of 44 kDa and 42 kDa consistent with ERK1-P and ERK-2-P, respectively. (B) WB to phospho-p38 (p38-P). No significant differences in the expression levels of MAPK/ERK-P and p38-P are found between CJD cases and controls. (C) WB to $CREB_1$ shows a band of 43 kDa. (D) WB to $CREB_2$ shows a band of 38 kDa. (E) WB to phospho-CREB (CREB-P) shows a band of 43 kDa corresponding to phosphorylated $CREB_1$. There is a significant decrease ($p<0.05$) in the expression levels of $CREB_1$, $CREB_2$ and CREB-P in diseased brains when compared with controls. (F) WB to c-Fos shows a band of 62 kDa. A significant decrease ($p<0.01$) in the expression levels of c-Fos is observed in CJD when compared with controls. (G) WB to c-Fos-P shows a band of about 65 kDa. A significant decrease ($p<0.01$) in the levels of c-Fos-P is found in CJD when compared with controls.

Please cite this article in press as: A. Rodríguez, I. Ferrer, Expression of transcription factors CREB and c-Fos in the brains of terminal Creutzfeldt-Jakob disease cases, Neurosci. Lett. (2007), doi:10.1016/j.neulet.2007.04.045

+Model
NSL-24054; No. of Pages 6
ARTICLE IN PRESS

Previous to the study of control and diseased brains, additional samples of the frontal cortex from one control individual were obtained at 3 h post-mortem and immediately frozen, or stored at 4 °C for 3, 6, 24 and 48 h, and then frozen to mimic variable postmortem delay in tissue processing and its effect on protein preservation. Western blotting, using all the mentioned antibodies, disclosed no differences in the expression levels of samples of 3, 6 and 9 h storage. All control and CJD brains in the present study were within this range of post-mortem delay.

Densitometric studies of Western blots revealed no modifications in the expression levels of ERK-1-P and ERK-2-P, and p38-P in CJD when compared with age-matched controls (μ. 1A and B). In contrast, reduced expression levels of total $CREB_1$ ($p < 0.005$) and $CREB_2$ ($p < 0.05$) were observed in CJD (Fig. 1C and D). CREB-P was also reduced ($p < 0.05$) in diseased brains (Fig. 1E). c-Fos levels were significantly reduced ($p < 0.01$) in CJD when compared with controls (Fig. 1F). Finally, c-Fos-P levels were significantly reduced ($p < 0.01$) in diseased brain when compared with controls (Fig. 1G).

For immunohistochemical studies, paraformaldehyde-fixed, cryoprotected sections of the frontal cortex were processed free-floating. The sections, 40 μ thick, were incubated with 2% hydrogen peroxide and 10% methanol for 30 min at room temperature, followed by 5% normal serum for 2 h, and then incubated overnight with one of the primary antibodies. The polyclonal rabbit anti-$CREB_1$ antibody (Santa Cruz Biotech) was used at a dilution of 1:100; the rabbit polyclonal anti-CREB-P^{Ser133} (Cell Signaling) was used at a dilution of 1:50; the rabbit polyclonal anti-c-Fos (4) (Santa Cruz Biotech) was used at a dilution of 1:100, the anti-c-Fos (AB2) antibody raised against the amino acids 4–17 of c-Fos (Oncogene, Calbiochem) at a dilution of 1:500, and the mouse anti-c-Fos-P^{Ser374}, which only recognizes c-Fos-P (Calbiochem), was used at a dilution of 1:100. After washing, the sections were processed with the labelled streptavidin–biotin method (Dako LSAB + kit, Dako) following the instructions of the supplier. The peroxidase reaction was visualized as a dark blue precipitate with NH_4NiSO_4 (0.05 M) in phosphate buffer (0.1 M), 0.05% diaminobenzidine, NH_4Cl and 0.01% hydrogen peroxide. Some sections were stained without the primary antibody to rule out non-specific immunoreactivity. Nio immunoreasctivity was found in sections incubated with secondary antibody alone.

All these antibodies decorated the nuclei of selected cells in control and diseased cases (Fig. 2). In consonance with Western blot observations, immunohistochemistry revealed decreased numbers of cells with nuclear $CREB_1$ immunoreactivity in CJD when compared with the control cases (Fig. 3A and B). Similarly, the number of CREB-P-immunoreactive nuclei was markedly reduced in CJD (Fig. 3C and D).

Decreased numbers of c-Fos-immunoreactive nuclei was seen in CJD when compared with controls (Fig. 3E and F). The same results were observed with the two different antibodies used. Finally, decreased numbers of c-Fos-P-immunoreactive nuclei were found in CJD when compared with controls (Fig. 3G and H).

In summary, the present combined biochemical and immunohistochemical study shows decreased CREB, CREB-P,

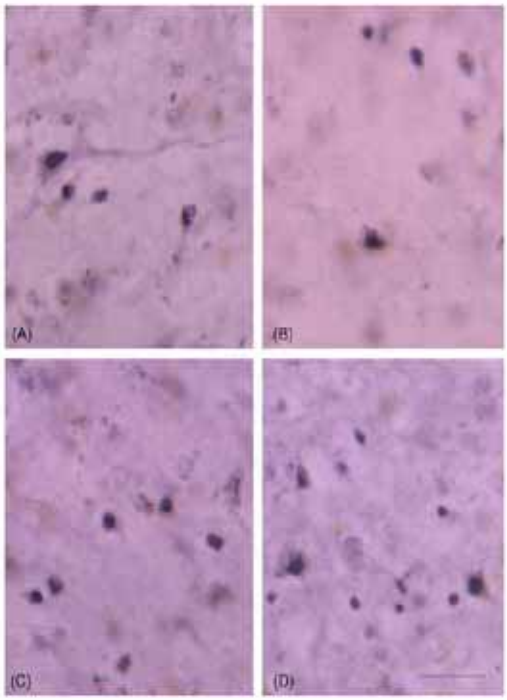

Fig. 2. Immunohistochemistry to CREB (Santa Cruz) (A), CREB-P (Cell Signaling) (B), c-Fos (AB2; Oncogene, Calbiochem) (C) and c-Fos-P (Calbiochem) (D) in the frontal cortex (area 8) in control braia. Immunoreactyivity to these antibodies is restricted to the nuclei. All these antibodies decorate the nuclei. Cryostat sections processed free-floating without counterstaining. Bar = 25 μ.

c-Fos and c-Fos-P in the frontal cortex of CJD cases at terminal stages of the disease. This is not a mere reflection of cell loss, as kinases involved in phosphorylation of these factors are preserved. Therefore, reduced expression of CREB-P is not the result of impaired upstream active kinases (i.e. ERK1-P, ERK-2-P and p-38-P), but rather the consequence of reduced CREB constitutive levels.

The functional meaning of these changes can be learned from observations of similar modifications in experimental models. CREB-P is associated with cell survival in resistant regions of the hippocampus after hypoxic insult [21], whereas continuous decrease of CREB is seen in populations that die following axotomy [1]. Similarly, CREB is reduced in cells committed to die at the time that CREB-P is increased in surviving cells in two different models of excitotoxicity following systemic kainic acid administration to adult rats [4]. Similar results have been observed following focal cerebral ischemia [5]. A crucial point here is the observation that adenoviral expression of CREB protects neurons from apoptotic and excitotoxic stress [8].

The role of c-Fos in cell death and cell survival is not clear, in that different paradigms point to one or the other of these opposite roles. Strong and maintained c-Fos expression may be associated with cell death [20]. Yet this is probably not as simple in complex settings [10]. Previous c-Fos mRNA and protein studies have shown variable gradients of induction and expression of c-Fos following excitotoxic or ischemic damage. c-Fos

Please cite this article in press as: A. Rodríguez, I. Ferrer, Expression of transcription factors CREB and c-Fos in the brains of terminal Creutzfeldt-Jakob disease cases, Neurosci. Lett. (2007), doi:10.1016/j.neulet.2007.04.045

+Model
NSL-24054; No. of Pages 6
ARTICLE IN PRESS

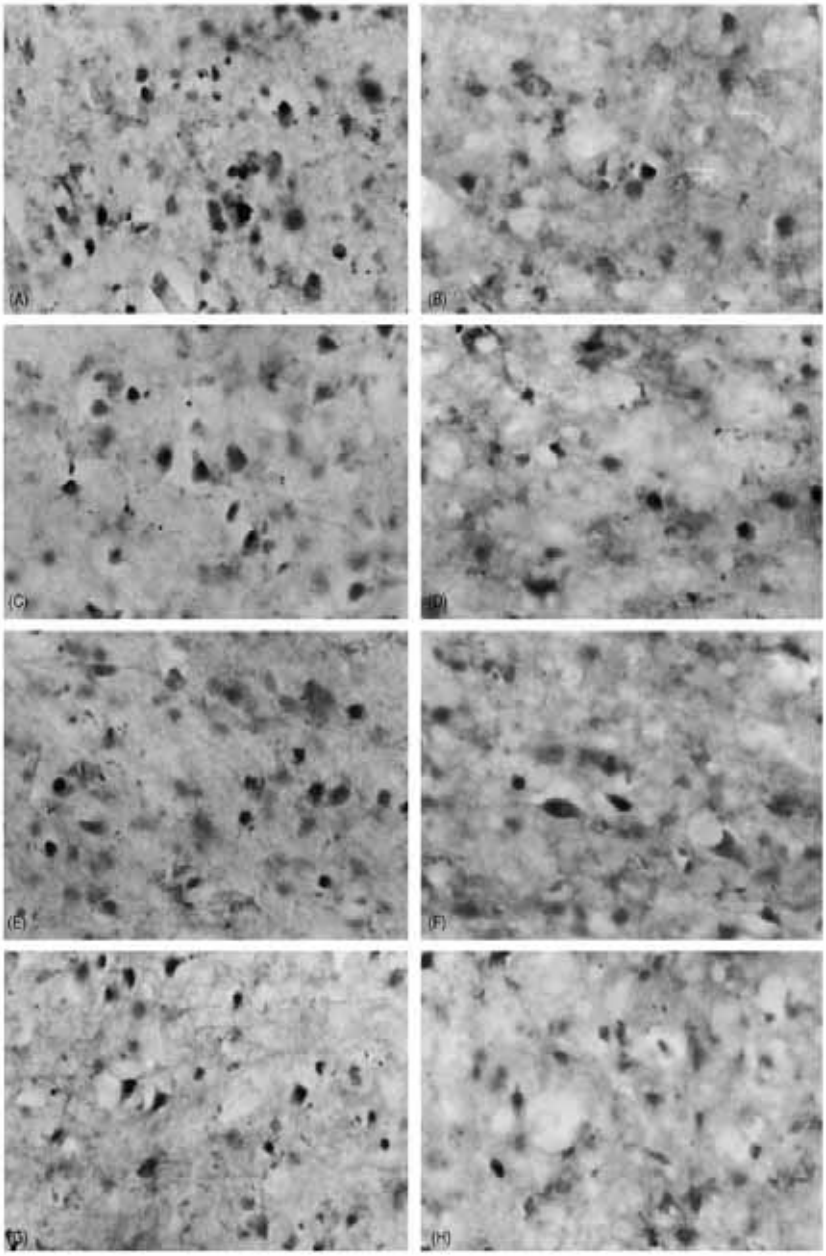

Fig. 3. Immunohistochemistry to CREB (Santa Cruz) (A, B), CREB-P (Cell Signaling) (C, D), c-Fos (AB2; Oncogene, Calbiochem) (E, F) and c-Fos-P (Calbiochem) (G, H) in the frontal cortex (area 8) of CJD (B, D, F, H) and age-matched controls (A, C, E, G). CREB, CREB-P, c-Fos and c-Fos-P immunoreactivity is localized in the nuclei of selected cells. Decreased numbers of CREB-, CREB-P-, c-Fos and c-Fos-P-immunoreactive nuclei are observed in CJD when compared with controls. Cryostat sections processed free-floating without counterstaining. Bar = 25 μ.

is expressed in neurons destined to survive in these paradigms [16,19]. Based on these findings, reduced c-Fos expression in CJD is consistent with c-Fos exhausted responses in advanced stages of CJD.

Previous immunohistochemical studies in the brains of scrapie-infected mice have shown increased c-Fos in neurons and astrocytes [24]. This appears to be a consistent finding; similar results were obtained with four different mice strains. Since there is no indication of the disease stage in infected mice, we cannot ascertain whether the animals were examined at middle or terminal stages of the disease. Yet maintained c-Fos expression in scrapie-infected mice leads to the

Please cite this article in press as: A. Rodríguez, I. Ferrer, Expression of transcription factors CREB and c-Fos in the brains of terminal Creutzfeldt-Jakob disease cases, Neurosci. Lett. (2007), doi:10.1016/j.neulet.2007.04.045

+Model
NSL-24054; No. of Pages 6
ARTICLE IN PRESS

assumption that positive cells are eventually committed to die [24].

Taken together, the present findings are consistent with the failure of CREB and c-Fos signaling pathways, in spite of the preservation of up-stream signaling kinase pathways, to maintain neuron survival in the cerebral cortex in terminal stages of CJD. Since these findings do not occur in the cerebral cortex in terminal stages of other degenerative diseases of the central nervous system such as Alzheimer's disease or Pick's disease [6,15] in tissue samples processed in the same way, it may be concluded that CREB and c-Fos exhaustion is a characteristic feature of terminal CJD.

Acknowledgements

This work was supported in part by grants EET2001-3724 and EET2002-05168 from the Ministerio de Ciencia y Tecnología. We thank T. Yohannan for editorial assistance.

References

[1] S. Brecht, P. Gass, F. Anton, R. Bravo, M. Zimmermann, T. Herdegen, Induction of c-Jun and suppression of CREB transcription factors in axotomized neurons of substantia nigra, and covariation with tyrosine-hydroxylase, Mol. Cell. Neurosci. 5 (1994) 431–441.
[2] H. Budka, M.W. Head, J.W. Ironside, P. Gambetti, P. Parchi, M. Zeidler, F. Tagliavini, Sporadic Creutzfeldt-Jakob disease, in: D. Dickson (Ed.), Neurodegeneration: The Molecular Pathology of Dementia and Movement Disorders, ISN Neuropath Press, Basel, 2003, pp. 287–297.
[3] J. Collinge, Prion diseases of human and animals. Their causes and molecular basis, Annu. Rev. Neurosci. 24 (2001) 519–550.
[4] I. Ferrer, R. Blanco, M. Carmona, B. Puig, I. Domínguez, F. Viñals, Active, phosphorylation-dependent MAP kinases, MAPK/ERK, SAPK/JNK and p38, and specific transcription factor substrates are differentially expressed following systemic administration of kainic acid to the adult rat, Acta Neuropathol. 103 (2002) 391–407.
[5] I. Ferrer, B. Friguls, E. Dalfo, A.M. Planas, Early modifications in the expression of mitogen-activated protein kinase (MAPK/ERK), stress-activated kinases SAPKJNK and p38, and their phosphorylated substrates following focal cerebral ischemia, Acta Neuropathol. 105 (2003) 425–437.
[6] I. Ferrer, G. Santpere, B. Puig, Immediate early genes, inducible transcription factors, and stress kinases in Alzheimer's disease, in: R. Pinaud, L.A. Tremere (Eds.), Immediate Early Genes in Sensory Processing, Cognitive Performance and Neurological Disorders, Springer Science/Business Media, New York, 2006, pp. 243–260.
[7] A. Giese, H.A. Kretzschmar, Prion-induced neuronal damage. The mechanisms of neuronal destruction in the subacute spongiform encephalopathies, Curr. Top. Microbiol. Immunol. 253 (2001) 203–217.
[8] C.P. Glover, D.J. Heywood, A.S. Bienemann, U. Deuschle, J.N. Kew, J.B. Uney, Adenoviral expression of CREB protects neurons from apoptotic and excitotoxic stress, Neuroreport 15 (2004) 1171–1175.
[9] F. Guillardon, T. Skutella, E. Uhlmann, F. Holsboer, M. Zimmermann, C. Behl, Activation of c-Fos contributes to β-amyloid peptide-induced neurotoxicity, Brain Res. 706 (1996) 268–286.
[10] T. Herdegen, V. Waetzig, AP-1 proteins in the adult brain: facts and fictions about effectors of neuroprotection and neurodegeneration, Oncogene 20 (2001) 2424–2437.
[11] J.W. Ironside, Review: Creutzfeldt-Jakob disease, Brain Pathol. 6 (1996) 379–388.
[12] G.A. MacGibbon, P.A. Lawlor, M. Walton, E. Sirimanne, R.L. Faull, B. Synek, E. Mee, B. Connor, M. Dragunow, Expression of Fos, Jun, and Krox family proteins in Alzheimer's disease, Exp. Neurol. 147 (1997) 316–332.
[13] D.L. Marcus, J.A. Strafaci, D.C. Miller, S. Masia, C.G. Thomas, J. Rosman, S. Hussain, M.L. Freedman, Quantitative neuronal c-fos and c-jun expression in Alzheimer's disease, Neurobiol. Aging 19 (1998) 393–400.
[14] J.I. Morgan, T. Curran, Stimulus-transcription coupling in the nervous system. Involvement of the inducible proto-oncogenes fos and jun, Ann. Rev. Neurosci. 14 (1991) 421–451.
[15] M. Nieto-Bodelón, G. Santpere, B. Torrejón-Escribano, B. Puig, I. Ferrer, Expression of transcription factors c-Fos, c-Jun, CREB-1 and ATF-2, and caspase-3 in relation with abnormal tau deposits in Pick's disease, Acta Neuropathol. 111 (2006) 341–350.
[16] E. Pozas, J. Ballabriga, A.M. Planas, I. Ferrer, Kainic acid-induced excitotoxicity is associated with a complex c-Fos and c-Jun response which does not preclude either cell death or survival, J. Neurobiol. 33 (1997) 232–246.
[17] S.B. Prusiner, The prion diseases of humans and animals, in: R.N. Rosenber, S.B. Prusiner, S. DiMauro, R.L. Carchi (Eds.), The Molecular and Genetic Basis of Neurological Diseases, McGraw-Hill, Boston, 1997, pp. 165–186.
[18] M.J. Robinson, M.H. Cobb, Mitogen-activated protein kinase pathways, Curr. Opin. Cell Biol. 9 (1997) 180–186.
[19] O. Sanz, A. Estrada, I. Ferrer, A.M. Planas, Differential cellular distribution and dynamics of HSP70, cyclooxygenase-2, and c-Fos in the rat brain after transient focal ischemia or kainic acid, Neuroscience 80 (1997) 221–232.
[20] R.J. Smeyne, M. Vendrell, M. Hayward, S.J. Baker, C.G. Miao, K. Schilling, L.M. Robertson, T. Currant, J.I. Morgan, Continuous c-fos expression precedes programmed cell death in vivo, Nature 363 (1993) 166–169.
[21] M.R. Walton, I. Dragunow, Is CREB a key to neuronal survival? Trends Neurosci. 23 (2000) 48–53.
[22] K.K. Yamamoto, G.A. Gonzalez, W.H. Biggs, M.R. Montminy, Phosphorylation-induced binding and transcriptional efficacy of nuclear factor CREB, Nature 334 (1998) 494–498.
[23] M. Yamamoto-Sasaki, H. Ozawa, T. Saito, M. Rosier, P. Riederer, Impaired phosphorylation of cyclic AMP response element binding protein in the hippocampus of dementia of the Alzheimer type, Brain Res. 824 (1999) 300–303.
[24] X. Ye, H.C. Meeker, P. Kozlowski, R.I. Carp, Increased c-Fos protein in the brains of scrapie-infected SAMP8, SAMR1, AKR and C57BL mice, Neuropathol. Appl. Neurobiol. 28 (2002) 358–366.

Please cite this article in press as: A. Rodríguez, I. Ferrer, Expression of transcription factors CREB and c-Fos in the brains of terminal Creutzfeldt-Jakob disease cases, Neurosci. Lett. (2007), doi:10.1016/j.neulet.2007.04.045